

DEVELOPMENT OF EMBEDDED ATOM
METHOD INTERATOMIC POTENTIALS
FOR GE-SN-SI TERNARY AND
CONSTITUENT BINARY ALLOYS FOR
MODELING MATERIAL
CRYSTALLIZATION

A thesis submitted in partial fulfillment of the
requirements for the degree of
Master of Science

By
SUDIP ACHARYA
B.S., Tribhuvan University, Nepal, 2017

2020
Wright State University

WRIGHT STATE UNIVERSITY
GRADUATE SCHOOL

July 30, 2020

I HEREBY RECOMMEND THAT THE THESIS PREPARED UNDER MY SUPERVISION BY Sudip Acharya ENTITLED “Development of Embedded Atom Method Interatomic Potentials for Ge-Sn-Si Ternary and Constituent Binary Alloys for Modeling Material Crystallization” BE ACCEPTED IMPARTIAL FULFILLMENT OF THE REQUIREMENTS FOR THE DEGREE OF Master of Science.

Amit Sharma, Ph. D.
Thesis Advisor

Jason Deibel, Ph.D.
Chair, Department of Physics

Final Examination Committee

Amit Sharma, Ph. D.

Brent D. Foy, Ph. D.

Sarah F. Tebbens, Ph. D.

Barry Milligan, Ph. D.
Interim Dean of the Graduate School

Abstract

Acharya, Sudip. M.S. Department of Physics, Wright State University, 2020. Development of Embedded Atom Method Interatomic Potentials for Ge-Sn-Si Ternary and Constituent Binary Alloys for Modeling Material Crystallization.

Group IV elements based nanoelectronics devices (mainly Si and Ge based devices) have been developed and improved over a long period of time and are the most influencing materials of semiconductor electronics, but due to their indirect bandgap their use in optoelectronics is limited. Alternatively, new Group IV alloys comprised of Ge, Si, and Sn semiconductor materials have emerged as attractive options for various electronic and optoelectronic applications. The binary and ternary alloys provide strain and energy bandgap engineering by controlling element content, a route for realizing direct-transition semiconductors, improvement in interface and defect properties, and a reduction of the process temperature related to the crystal growth. However, there are many obstacles and challenges for the crystal growth of Ge-Sn alloy on the Silicon or Germanium substrate. One of the problems in Ge-Sn growth is Sn precipitation from Ge-Sn.

Theoretical calculation predicts that Ge transitions from an indirect semiconductor to a direct semiconductor by incorporation of Sn on Ge matrix. For tensile strained Ge-Sn alloys, the transition is predicted at 6.3% Sn concentration. This is the main driving force for the growth of epitaxial Ge-Sn crystals on Si substrates. The epitaxial growth of Ge-Sn is very challenging because of huge lattice mismatch between Ge and Sn and, the strong surface segregation of Sn on Ge and extremely low equilibrium solubility of

Sn on Ge. In the recent past, a lot of progress has been made for the development of epitaxial growth techniques. Besides other techniques like MBE for the deposition of Ge-Sn on the substrate of Si, chemical vapor deposition has been achieved. Similarly, pulsed laser-induced epitaxy is also another technique for the deposition. Besides the experimental efforts to study the Ge-Sn-Si elemental binary and ternary alloys, Molecular Dynamics (MD) modeling provides insight into atomic configurations and structural dynamics, which requires the accurate inter-atomic potential for Ge-Sn-Si binary and ternary system. Present work is an effort to generate Embedded Atom Method (EAM) potential for this system, which can then be used with the MD method to study epitaxial growth.

The work presented here uses classical molecular dynamics approach and EAM potential fitting code to develop the EAM potential, which can be used to study the properties of Ge-Sn, Ge-Si, Si-Sn, and Ternary Ge-Sn-Si system. Density Functional Theory (DFT) calculations are performed for each binary pair - Ge-Sn, Ge-Si and Si-Sn using Vienna Ab initio Simulation Package, better known as VASP for a range of temperatures in the range of 1200K- 1500K.

The interatomic potential fitting code, MEAMfit, is used to fit EAM potentials to energies and atomic forces generated from DFT calculations. The data to be fitted are directly read from “vasprun.xml” files from VASP.

Three different methods were used to test the accuracy of developed potentials, namely, testing the fit for its predictability of DFT energies in the testing set; computing elastic properties, and crystal properties such as phonon band-structure with fitted potential and comparing those with direct DFT calculations.

TABLE OF CONTENTS

CHAPTER 1.INTRODUCTION	1
1.1 Modeling growth	3
1.2 Thesis Outline	5
CHAPTER 2.THEORY	7
2.1 MEAM fit	8
2.2 Molecular Dynamics	8
2.3 Velocity Verlet Algorithm	9
2.4 Ensemble	11
2.4.1 NVE	12
2.4.2 NVT	12
2.4.3 NPT	13
2.4.4 TV μ	13
2.5 Interatomic potential	14
2.6 Density Functional Theory	14
2.6.1 The Born Oppenheimer approximation	15
2.6.2 Hohenberg and Kohn	16
2.6.3 The Kohn Sham Scheme	17
2.7 Embedded Atom Model Method	18
2.8 VASP	20
2.8.1 INCAR	20
2.8.2 POSCAR	20
2.8.3 POTCAR	20
2.8.4 KPOINTS	21
2.8.5 CONTCAR	21
2.8.6 OSZICAR	21
2.8.7 OUTCAR	21
2.8.8 CHGCAR	21
2.9 LAMMPS	21
CHAPTER 3. STUDY OF GERMANIUM-TIN	23
3.1 Simulation method	23
3.2 Result and Discussion	26
3.2.1 Testing using testing set	26
3.2.2 Reproduction of Force by the developed potential	27

3.2.3	Cohesive energy test	28
3.2.4	Free-Energy Fitted EAM Parameters	32
3.2.5	Stress-Tensor Fitted EAM Parameters	33
CHAPTER 4.STUDY OF GERMANIUM-SILICON		45
4.1	Simulation method	45
4.2	Result and Discussions	47
4.2.1	Testing using testing set	47
4.2.2	Reproduction of Force by the developed potential	48
4.2.3	Cohesive energy test	49
4.2.4	Free-Energy Fitted EAM Parameters	53
4.2.5	Stress-Tensor Fitted EAM Parameters	54
CHAPTER 5.STUDY OF TIN-SILICON		65
5.1	Simulation method	66
5.2	Result and discussion	67
5.2.1	Testing using testing sets	67
5.2.2	Reproduction of Force by the developed potential	69
5.2.3	Cohesive energy test	70
5.2.4	Free-Energy Fitted EAM Parameters	74
5.2.5	Stress-Tensor fitted EAM parameters	75
CHAPTER 6.STUDY OF GERMANIUM-TIN SILICON		84
6.1	Simulation method	85
6.2	Result and Discussion	86
6.2.1	Testing using testing sets	86
6.2.2	Reproduction of Force by the developed potential	87
6.2.3	Cohesive energy test	88
6.2.4	Free-Energy Fitted EAM Parameters	91
6.2.5	Stress-Tensor fitted EAM parameters	93
CHAPTER 7.DISCUSSION AND CONCLUSION		97
REFERENCES		98

LIST OF FIGURES

Figure 1 – Schematic Diagram of Molecular dynamics algorithm	11
Figure 2 – Interatomic interaction potential	14
Figure 3 – Ground state and excited states and change in energy ΔE	16
Figure 4 – Snapshot of movement of 64 atoms of Germanium(32) and Tin(32) in the box of dimension 11.3148 Å * 11.3148 Å * 11.3148 Å at temperature 1200K	24
Figure 5 – Plot of K-points versus Energy for Ge-Sn system MD input in VASP	25
Figure 6 – Histogram of interatomic separation for Ge-Sn MD-run at 1200K	25
Figure 7 – (a, b)Plot of Cohesive energy vs distance of Sn atom from its lattice point for Free energy fitted EAM1, DFT and EAM2, DFT. (c, d) Plot of difference in change of Cohesive energy in plot a and b with respect to distance in Angstrom.	28
Figure 8 – (a, b):Plot of Cohesive energy vs distance of Sn atom from its lattice point for Stress tensor fitted EAM1, DFT and EAM2, DFT. (c, d) :Plot of difference in change of Cohesive energy in plot a and b with respect to distance in Angstrom.	31
Figure 9 – Plot of Ge-Ge interatomic distance versus pair-interaction energy by Free-energy fitted EAM1 potential	35

Figure 10 – Plot of Sn-Sn pair interaction distance versus interaction energy by free energy fitted EAM1 potential	35
Figure 11 – Plot of Ge-Sn pair interaction distance versus interaction energy by free energy fitted EAM2 potential	36
Figure 12 – (a, b) plot of Embedding energy function of Ge and Sn respectively by free energy fitted EAM1. (c, d) plot of Density function versus distance of Ge and Sn using free energy fitted EAM1	39
Figure 13 – (a)The variation of Total energy with lattice constant for Ge-Sn by stress fitted EAM1 potential .(b) The Variation of Total energy with lattice constant in for Ge-Sn by DFT(LDA).	40
Figure 14 – Plot of phonon Band structure of Ge-Sn using Free-energy fitted EAM1	43
Figure 15 – Plot of Total Phonon density of States of Ge-Sn using Stress-fitted EAM	44
Figure 16 – Snapshot of movement of 64 atoms of Germanium(32 atoms) and Silicon(32 atoms) in the box of dimension 11.3148 A * 11.3148 A * 11.3148 A at temperature 1200K.	46
Figure 17 –(a, b):Plot of Change of Cohesive energy vs distance of Si atom from its lattice point for Free energy fitted EAM1, DFT and EAM2, DFT. (c, d) :Plot of difference in change of Cohesive energy in the plot a and b with respect to distance in Angstrom.	49
Figure 18 – (a, b):Plot of Change of Cohesive energy vs distance of Si atom from its lattice point for Stress tensor fitted EAM1, DFT and EAM2, DFT. (c, d) :Plot of	

difference in change of Cohesive energy in plot a and b with respective to distance in Angstrom.	51
Figure 19 – Plot of Ge-Ge interatomic distance versus pair-interaction energy using Stress Tensor fitted EAM1 potential	56
Figure 20 – Plot of Ge-Ge interatomic distance versus pair-interaction energy using Stress Tensor fitted EAM1 potential	56
Figure 21 – Plot of Ge-Si interatomic distance versus pair-interaction energy using Stress Tensor fitted EAM1 potential	57
Figure 22 – (a, b) plot of Embedding energy function of Ge and Si respectively by free energy fitted EAM2. (c, d) plot of Density function versus distance of Ge and Si using free energy fitted EAM2	60
Figure 23 – (a)The variation of Total energy with lattice constant for Ge-Si by free energy fitted EAM1 potential . (b) The Variation of Total energy with lattice constant i for Ge-Si by DFT(LDA).	61
Figure 24 – Plot of phonon Band structure of Ge-Si using Free-energy fitted EAM1	63
Figure 25 – Plot of Total Phonon density of States of Ge-Si using free energy fitted EAM1	64
Figure 26 – Snapshot of movement of 64 atoms of Tin(32 atoms) and Silicon(32 atoms) in the box of dimension 11.3148 A * 11.3148 A * 11.3148 A at temperature 1200K.	67

- Figure 27 – (a, b):Plot of Change of Cohesive energy vs distance of Si atom from its lattice point or Free energy fitted EAM1, DFT and EAM2,DFT. (c, d) :Plot of difference in change of Cohesive energy in plot a and b with respective to distance in Angstrom 70
- Figure 28 – (a, b):Plot of Change of Cohesive energy vs distance of Si atom from its lattice point for Stress tensor fitted EAM1, DFT and EAM2,DFT. (c, d) :Plot of difference in change of Cohesive energy in plot a and b with respective to distance in Angstrom. 72
- Figure 29 – Plot of Si-Si interatomic distance versus pair-interaction energy by Free energy fitted EAM2 potential. 77
- Figure 30 – Plot of Si-Sn interatomic distance versus pair-interaction energy by Free energy fitted EAM1 potential. 77
- Figure 31 – Plot of Sn-Sn interatomic distance versus pair-interaction energy by Free energy fitted EAM1 potential 78
- Figure 32 – (a, b) plot of Embedding energy function of Si and Sn respectively by free energy fitted EAM1. (c, d) plot of Density function versus distance of Si and Sn using free energy fitted EAM1. 80
- Figure 33 –(a)The variation of Total energy with lattice constant for Ge-Si by free energy fitted EAM1 potential .(b) The Variation of Total energy with lattice constant in for Ge-Si by DFT(LDA). 81
- Figure 34 – Plot of phonon Band structure of Si-Sn using Free-energy fitted EAM1 83

Figure 35 – Plot of Total Phonon density of States of Si-Sn using Free energy -fitted

EAM1 83

Figure 36 – Snapshot of movement of 64 atoms of Germanium, Silicon, and Tin in the

box of dimension 11.3148 A * 11.3148 A * 11.3148 A at temperature 1200K. 85

Figure 37 – Plot of Change of Cohesive energy vs distance of Ge atom from its lattice

point for Free energy fitted EAM1, DFT and EAM2,DFT. (c, d) :Plot of difference

in change of Cohesive energy in plot a and b with respective to distance in

Angstrom 88

Figure 38 – Plot of Change of Cohesive energy vs distance of Ge atom from its lattice

point for Free energy fitted EAM1, DFT and EAM2, DFT. (c, d) :Plot of difference

in change of Cohesive energy in plot a and b with respective to distance in

Angstrom 90

Figure 39 – Plot of interatomic distance versus pair-interaction energy by(a) Free energy

fitted EAM1 potential and (b) Stress fitted EAM2 potential for each pair of atoms 95

LIST OF TABLES

Table 1 –: Embedding function parameters for free energy fitted EAM1 and EAM2 potentials	32
Table 2 –: Electron density parameters for free energy fitted EAM1 and EAM2 potentials	32
Table 3 –: Pairwise interaction potential parameters for free energy fitted EAM1 and EAM2 potentials	33
Table 4 –: Embedding function parameters for stress fitted EAM1 and EAM2 potentials	33
Table 5 –: Electron density parameters for Stress fitted EAM1 and EAM2 potentials	34
Table 6 –: Pairwise interaction potential parameters for free energy fitted EAM1 and EAM2 potentials	34
Table 7 – Calculated Elastic properties of Ge-Sn alloy	42
Table 8 –: Embedding function parameters for free energy fitted EAM1 and EAM2 potentials	53
Table 9 –: Electron density parameters for free energy fitted EAM1 and EAM2 potentials	53

Table 10 –: Pairwise interaction potential parameters for free energy fitted EAM1 and EAM2 potentials	54
Table 11 –: Embedding function parameters for free energy fitted EAM1 and EAM2 potentials	54
Table 12 –: Electron density parameters for free energy fitted EAM1 and EAM2 potentials	55
Table 13 –: Pairwise interaction potential parameters for free energy fitted EAM1 and EAM2 potentials	55
Table 14 – Calculated Elastic properties of Ge-Si alloy by EAM potentials	62
Table 15 –: Embedding function parameters for free energy fitted EAM1 and EAM2 potentials	74
Table 16 –: Electron density parameters for free energy fitted EAM1 and EAM2 potentials	74
Table 17 –: Pairwise interaction potential parameters for free energy fitted EAM1 and EAM2 potentials	75
Table 18 –: Embedding function parameters for free energy fitted EAM1 and EAM2 potentials	75
Table 19 –: Electron density parameters for free energy fitted EAM1 and EAM2 potentials	76
Table 20 –: Pairwise interaction potential parameters for free energy fitted EAM1 and EAM2 potentials	76
Table 21 – Calculated Elastic properties of Si-Sn alloy by EAM potentials	82

Table 22 –: Embedding function parameters for free energy fitted EAM1 and EAM2 potentials	91
Table 23 –: Electron density parameters for free energy fitted EAM1 and EAM2 potentials	91
Table 24 –: Pairwise interaction potential parameters for free energy fitted EAM1 and EAM2 potentials	92
Table 25 –: Embedding function parameters for free energy fitted EAM1 and EAM2 potentials	93
Table 26 –: Electron density parameters for free energy fitted EAM1 and EAM2 potentials	93
Table 27 –: Pairwise interaction potential parameters for free energy fitted EAM1 and EAM2 potentials	94

ACKNOWLEDGEMENT

I would like to express my deepest gratitude to my supervisor Dr. Amit Raj Sharma. This work would not be possible without his help and support. I am also thankful to my committee members, Dr. Brent D Foy and Dr. Sarah F. Tebbens, for their invaluable suggestion and comments regarding my thesis work. I highly acknowledge the support from the physics department and Chair, Dr. Jason Deibel for their guidance and help throughout this thesis work. Huge thanks to my friends at Wright State University for their relentless support and courage during entire project. Finally, I thank to my family for their care, love, support and best wishes.

CHAPTER 1. INTRODUCTION

Over the past 20 years, Group-IV semiconductor alloys such as Si-Sn, Ge-Sn, Ge-Si are of great scientific and technological interest due to their desirable chemical and physical properties, such as, high melting point, high thermal conductivity, large bulk modulus, as well as, large band gap and low dielectric constant [3] for device applications. Germanium (Ge) remains a promising material candidate for the next generation of semiconductor devices and Germanium-Tin (Ge-Sn) alloys have potential applications in photonics and microelectronics [2]. In conjunction with other group IV materials such as Silicon (Si), Silicon-Germanium alloy (Si-Ge) has shown to deliver high-speed transistors. The discovery of Germanium-Tin alloys has paved the way for photonics with higher carrier mobilities than either Silicon or Germanium[6], and it has been proposed that they can be used as a channel material in high speed metal-oxide-semiconductor field effect transistors. Tin concentration in Ge is a critical factor and a challenge. The solubility of Sn in Ge is very low (less than 0.5%) with a large lattice mismatch between Ge and Sn, where higher concentration of Sn in Ge is desired. At a Sn content beyond approximately 9%, Germanium-Tin alloys become direct bandgap semiconductor, having efficient light emission which are deemed suitable for the fabrication of Lasers [6].

Since the diamond lattice of Sn is unstable above 13-degree Celsius the growth of Ge-Sn layers on Si substrate must be done under non-equilibrium conditions. The primary challenge being the precipitation of Sn in the crystal growth of Ge-Sn alloy, where it is difficult to increase the Sn concentration in Ge-Sn alloy because during crystal growth and after crystal growth Sn precipitates easily from Ge-Sn alloy at lower temperature.

Group-IV ternary alloys, $\text{Si}_{1-x-y}\text{Ge}_x\text{Sn}_y$, have only been experimentally demonstrated over a narrow range of composition ($\text{Sn} < 10\%$) because of technical challenges associated with the growth process and limited scan of experimental parametric/phase space. To access desired MWIR and LWIR spectral regions an increase in the level of Sn incorporation will be required, however, at present the fundamental structural, optical, and electrical characteristics of these higher Sn containing compounds are unknown. Compositional and thickness uniformity data is measured via transmission, reflection, and absorption spectra with FTIR and IR-Variable Angle Spectroscopic Ellipsometry (IR-VASE).

Different growth methods have been demonstrated for the Ge-Sn system which is known to be thermodynamically unstable and can only be grown as metastable films. Chemical Vapor Deposition (CVD) and Molecular Beam Epitaxy (MBE) on a nearly-lattice matched substrates such as In-Sb and, other candidate substrates such as CdZnTe with (001), (011), and (111)A/B surface orientations have been demonstrated. The search for optimal substrate material and orientation is also a major and active area of research in epitaxially grown films. There are two categories of substrates (a) lattice matched substrates – for example Cd-Zn-Tn and Cd-Se-Tn where the alloy surface atom arrangement is turned to the lattice parameter of the epitaxial layer, and, (b) non-

lattice matched substrates such as GaAs, Si and Sapphire. The lattice mismatch can vary from 0.2% to up to 20% which is sufficient to increase the dislocation density thus modifying the electronic and optical property of the material from its idealized bulk lattice form.

Using Molecular Beam Epitaxy (MBE) approach complex structures can be grown atomic-layer by atomic-layer with precise control over thickness, alloy composition and doping levels. MBE has been used to grow a wide range of materials including semiconductors, superconductors, metals, oxides nitrides and organic films. Experimentally the MBE growth systems have various control parameters such as the UHV system, temperature control, rotation of substrate, control of effusion cell to control the composition, uniformity, and, doping level of the epitaxial layers. For modeling such growth at the atomic level, the surface orientation of the substrate, chemical reaction mechanism and chemical dynamics, kinetics and thermodynamics must be known.

1.1 Modeling growth

Molecular dynamics (MD) can be used to simulate the motion of atoms and molecules under predefined conditions such as temperature and pressure over a chosen orientation of the substrate. MD essentially utilizes the numerical solution of Newton's equations of motion via numerical integration by discretizing time into small intervals. The interatomic potential which describes the interaction between the atoms can either be calculated using Density Functional Theory (DFT), or, obtained in the form of fitted semi-classical or classical potentials. The force computed as the negative gradient of

the potential determines displacement of the atoms which in turn are propagated and the positions and velocities are updated toward the next time step. Standard MD simulations reproduce a microcanonical ensemble (NVE) where the number of atoms (N), the volume (V), and the total energy (E) are conserved – which represents a completely isolated system. To simulate experiments which are not isolated and allow for energy exchange (Temperature held constant) or to study temperature dependent processes (for example thermal coefficients, temperature dependent phase transition) MD simulations is performed with temperature control via use of thermostat. Because the instantaneous temperature is directly related to the atomic internal velocities in MD simulations a control on the rate of change of particle velocities is achieved by thermostat algorithms to hold temperature constant. Nose-Hoover chain thermostat NVT MD is a commonly used technique and aside from that NVT algorithms such as NVT Berendsen and Langevin dynamics are also commonly used. The latter solves Langevin equation which explicitly includes atomic friction coefficient and a stochastic collision force.

To overcome this problem many research works have been done. J Tersoff developed the interatomic potential of Germanium Silicon to model the multicomponent system interpolates between potentials for the respective elements to treat heteronuclear bonds [11]. Similarly, there are some work on Embedded atom method to develop potential of Monoatomic system. Won-Seok Ko and his research group in 2018 developed an Embedded atom method interatomic potential for pure Tin [12]. This developed potential was based on second nearest neighbor modified embedded atom method formalism. Also the Ge-Sn Structures were grown with a solid source MBE system for

6 inch wafers[13]. This current method of developing the potential is based on EAM formalism but work is still being done by Andrew Duff and his research team to improve this formalism to modified Embedded atom method (MEAM) which takes the angular contribution of electron density into account.

1.2 Thesis Outline

This thesis is divided into six chapters, starting with Introduction to the subject of Ge-Sn-Si binary and ternary alloys in this chapter, and followed by a brief background and outline of the methodologies such as Molecular Dynamics, Density functional theory, Embedded atom method, in chapter II. In the next chapter, we also describe the VASP calculation method, statistical ensembles and LAMMPS format of EAM potential.

In Chapter III, we present the results of EAM fitting for Ge-Sn system and provide Force-fitted and Stress-fitted EAM parameters for Ge-Sn binary system and interatomic pair interaction results. Elastic properties, Phonon band structure and Phonon density of states calculated using EAM potential and their comparison to those calculated using the DFT methods are presented in Chapter III.

Chapter IV outlines the EAM parameters, MD simulations details and Elastic properties of Ge-Si alloy by both EAM and DFT methods. In Chapter V, similar to the previous two chapters, we present our EAM potential for the Si-Sn binary system. Free-energy and Stress fitted EAM parameters, pair-interaction results, Embedded function, equilibrium lattice constant, and elastic properties like Bulk modulus, Youngs modulus, Shear modulus, Poisson's ratio etc. calculated using both EAM and DFT methods are presented. In Chapter VI, we present our results for Ge-Si-Sn ternary alloy

including the EAM parameters for fitted potential, Free energy and Stress fitted potential parameters and testing set results of Ge-Sn-Si ternary alloy. Chapter VII summarizes the present work and provides future direction.

CHAPTER 2. THEORY

Most of the important theoretical and experimental data on binary and ternary alloy parameter and properties can be classified into six groups (1) structural parameters; (2) mechanical, elastic and lattice Vibrionic properties (3) thermal properties; (4) energy band parameters; (5) Optical properties, and; (6) Carrier transport properties. The present work aims to develop inter-atomic potential for Ge-Si-Sn system to aid the study of some of these properties and especially provide a tool to model the epitaxial growth via Molecular dynamics (MD). MD method is the study of the motion of atoms and molecules under predefined conditions, such as temperature, pressure, stress, external forces to investigate dynamical processes at the nanoscale.

In this chapter we outline the method and software for developing Embedded Atom Method (EAM) potential, Molecular dynamics, Velocity Verlet Algorithm, Ensemble, Density functional theory, Embedded atom method, VASP, inter atomic potential and LAMMPS.

2.1 MEAM fit

The Embedded Atom Method (EAM) potential is the description of interatomic potential wherein the energy is expressed as the sum of functions of separation between an atom and its neighbors. This many-body potential formulation was first developed by Daw Murray S and Michael I Bakes; in which the potential energy of an atom is written as the sum of two terms, namely, the embedding function that represents the energy required to place an atom into the electron cloud due to other atoms, and, pair-wise potential function. For a binary alloy (AB for example), the EAM potential requires seven functions: three pair-wise interactions (A-A, A-B, B-B), two embedding functions, and two electron cloud contribution functions. This method of potential description is particularly appropriate for metallic system and is widely used for MD simulations.

MEAMfit is an interatomic potential fitting code developed by Andrew Duff and co-workers that capable of fitting embedded atom method (EAM) and reference-free modified embedded atom method (RF-MEAM) potentials to energies and/or atomic forces produced by the VASP density functional theory (DFT) package. Data for MEAMfit is read in directly from vasprun.xml files, requiring minimal user input. Potentials produced by the code are directly usable with the LAMMPS [8] or Camelion [9] molecular-dynamics packages.

2.2 Molecular Dynamics

Molecular dynamics simulation has evolved into a mature technique that can be used effectively to understand macromolecular structure-to-function relationships [2]. It is a

computer simulation technique which allows one to predict the time evolution of system of interacting particles. First, one has to specify the initial position and velocities of all the particles in the system and specify the interaction potential to derive the forces among all the particles of the system. After setting the initial conditions the evolution of the system with time is performed by solving the classical equation of motions for each particle in the system. In classical mechanics, the equation of motion for classical particles is derived from Newton's Second law:

$$m_i a_i = F_i$$

$$m_i \frac{dv_i}{dt} = F_i$$

$$m_i \frac{d^2 r_i}{dt^2} = F_i$$

where, the force acting on i^{th} atom is obtained from the interatomic potential, $U(r_1, r_2, r_3, \dots, r_N)$,

$$F_i = -\Delta U(r_1, r_2, r_3, \dots, r_N)$$

The position and velocities are updated over a pre-selected time step using Euler method or more refined approach such as Velocity-Verlet Algorithm. The equations of motion are solved for each atom in the system and the cycle is repeated as shown in Figure 2.1.1

2.3 Velocity Verlet Algorithm

Velocity Verlet integration method is a numerical method to integrate Newtonian equation of motion. This method is used to evolve the velocities and position over time

thus tracing the trajectory of the atoms during the simulation. The advantage of using this algorithm is the stability of the solver due to its time-reversibility and symplectic property. The following scheme represents the implementation of Velocity Verlet Algorithm in MD calculation[11]:

a) It starts with following equations:

$$r(t + \Delta t) = r(t) + \Delta t * v(t) + \frac{1}{2} * \Delta t^2 * a(t) + \dots\dots,$$

$$v(t + \Delta t) = v(t) + \frac{1}{2} * \Delta t * [a(t) + a(t + \Delta t)]$$

b) Let's choose time step Δt

c) Calculate the velocities at mid-step using:

$$v\left(t + \frac{\Delta t}{2}\right) = v(t) + \frac{1}{2} * \Delta t * a(t);$$

d) Calculate $r(t + \Delta t) = r(t) + v\left(t + \frac{\Delta t}{2}\right) * \Delta t$

e) Calculate $a(t + \Delta t)$ from potential

f) Apply suitable boundary condition such as constant temperature and pressure as needed

g) Update the velocity on using the new acceleration:

$$v(t + \Delta t) = v\left(t + \frac{\Delta t}{2}\right) + \frac{1}{2} a(t + \Delta t) * \Delta t$$

h) Repeat the same process for next time step and increasing number of iteration as we desired to get final output of MD calculation.

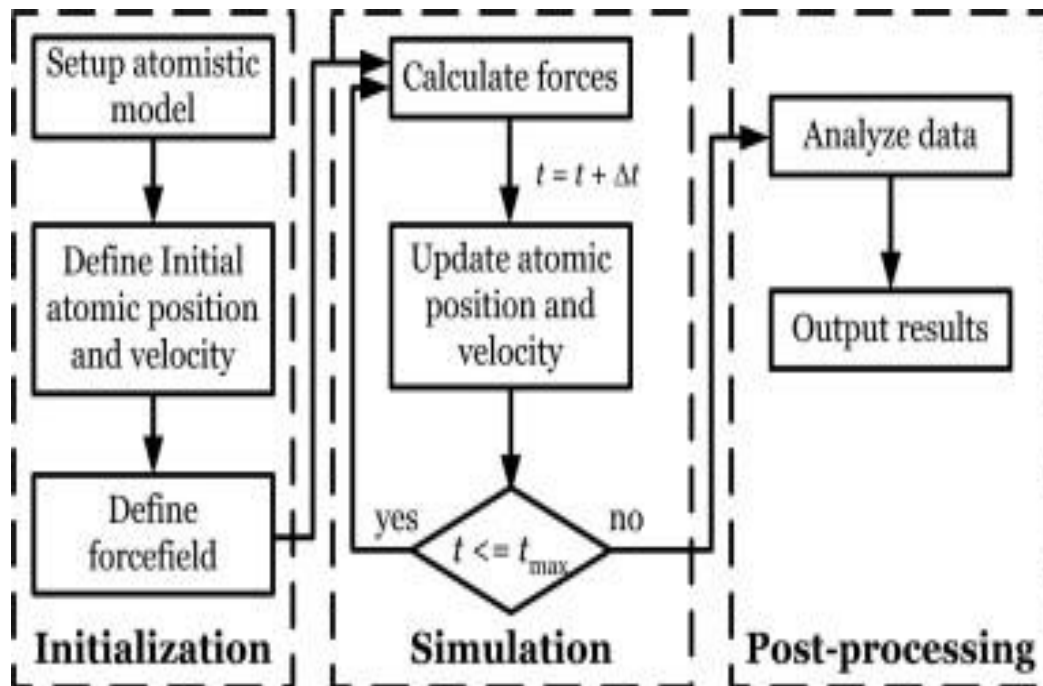


Figure 1 – Schematic Diagram of Molecular dynamics algorithm [3]

2.4 Ensemble

In complex systems like statistical systems it is impossible to know all the parameters which is needed to understand the system completely. But it is not necessary for us to know all the details of the system to know some properties like Pressure, Volume and Temperature. Suppose we have many particles in a box and consider one of the particles as our system. The small collections of other particles in the box are called assembles and the collection of all the assembles is called ensemble. For the Molecular Dynamics simulation, we mainly need to know about Thermodynamic state, Mechanical or microscopic state and Ensemble of the system. Thermodynamic state of the system is defined as the Temperature(T),Pressure(P) and number of particles(N).Mechanical state is defined as the atomic position(q) and momenta(p) which is considered as coordinate in the multi-dimensional space which is also called as phase space.

Ensemble is the collection of points in phase space satisfying the condition of a particular thermodynamic state or we can also define ensemble as the collection all possible systems which have different microscopic state but have identical macroscopic or thermodynamic state.

There are mainly three kinds of ensembles: NVE, NVT and $TV\mu$ which are explained below:

2.4.1 NVE

It is one of the types of ensembles which is also known as microcanonical ensemble in which the Number of particles in the system(N), Volume of system(V) and the total energy of the system ϵ remains fixed. For NVE ensemble the walls of the container or the box should be rigid, Impermeable and Isolated. But in real practice is it very difficult to make the system isolated from the surrounding so NVE ensemble is not highly preferred In MD simulation.

2.4.2 NVT

Also known as canonical ensemble, it is the one in which we keep Number of particles(N), Volume of box(V) and Temperature(T) constant. For this ensemble, the container should be rigid, permeable and the walls should be diathermic. In work NVT ensemble used was for MD simulation. In VASP, for NVT simulation, three kinds of thermostat available

2.4.2.1 Andersen Thermostat:

This is the thermostat which correctly sample the NVT ensemble. It couples the system to the heat bath imposing the desired temperature. If we want to find the dynamical

Properties of any system, then this thermostat is not a good choice because it decorrelated the velocities.

2.4.2.2 Nose-Hoover thermostat:

In NVT ensemble, at constant temperature the energy of the system keeps on changing and to introduce the fluctuation in energies we need mechanism.

2.4.2.3 Langevin thermostat:

In this thermostat Langevin equation is solved which includes friction as well as stochastic collision to imitate the interaction of particles in heat bath.

2.4.3 NPT

NPT ensemble is also called isobaric-isothermal ensemble. It describes the system in contact with thermostat at temperature T and at barostat pressure P . The system exchanges both the heat as well as volume with thermostat and barostat respectively. In this ensemble the total number of particles, remains constant. However, the total energy and Volume changes at thermal equilibrium.

2.4.4 $TV\mu$

It is made up of large number of assemblies having same number of particles, same volume and same chemical potential. Here each assemblies are separated by permeable walls as a result of which particles can move through all the assemblies. Hence there is the exchange of Temperature, number of molecules. But since the system are always in equilibrium, the chemical potential of the system always remains constant.

2.5 Interatomic potential

The interatomic potential describes the interaction between a pair of atoms or an interaction of an atom with group of atoms. The potential should have both the attractive and repulsive component if binding is to occur.

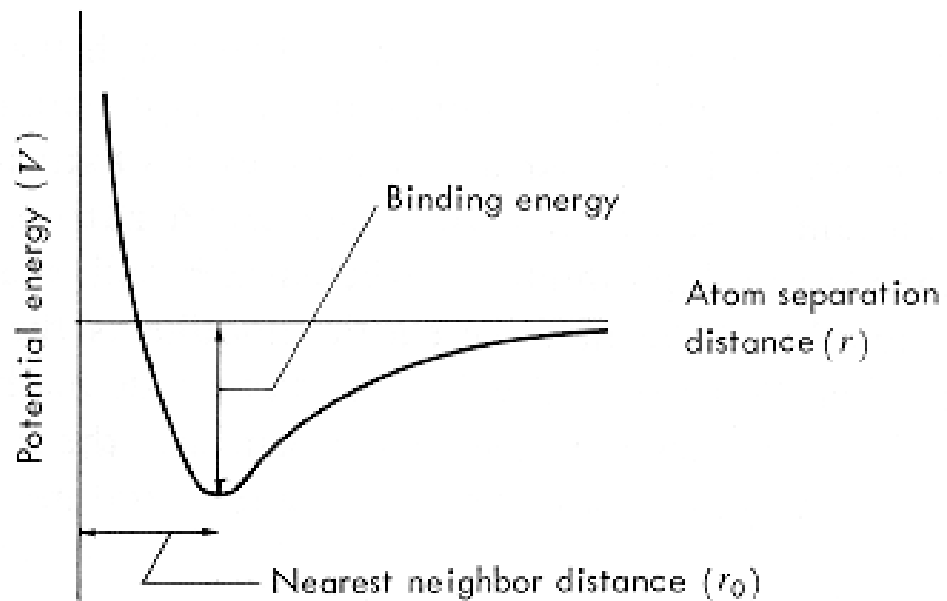


Figure 2 – Interatomic interaction potential

The binding energy of the atom in the solid is the depth of the potential well at its minimum. The location of this minimum determines the nearest neighbor distance, r_0 , for atoms in the solid.

2.6 Density Functional Theory

Density functional theory (DFT) calculates the ground state energy of systems using various exchange correlation functions incorporated in the Hamiltonian part of the corresponding Schrodinger's wave equation. The calculations are more accurate for ground states rather than for excited states. It is used extensively in calculating defect

formation energies in solids, formation enthalpy of compounds and materials as well as surface energies of various crystallographic planes of crystals. DFT deals with the electrons in the given system and as a consequence the number of degrees of freedom involved is much higher. Various approximations such as local density and generalized gradient approximations are used to model exchange-correlation functions. Computationally it is more expensive.

2.6.1 The Born Oppenheimer approximation

According to this approximation the nuclei are big, heavier and they are slow while electrons are small and fast. So, it is possible to decouple the dynamics of nuclei and electrons.

$$\Psi(\{\mathbf{r}_i\}, \{\mathbf{R}_i\}) \rightarrow \Psi_N(\{\mathbf{R}_i\}) * \Psi_e(\{\mathbf{r}_i\})$$

The Schrodinger equation for many body systems is given by

$$H\Psi(\mathbf{r}_1, \mathbf{r}_2, \mathbf{r}_3, \dots, \mathbf{r}_N) = E \Psi(\mathbf{r}_1, \mathbf{r}_2, \mathbf{r}_3, \dots, \mathbf{r}_N)$$

The electronic Hamiltonian consists of three terms:

$$\hat{H} = \frac{\hbar^2}{2m} \sum \tilde{\nabla}^2 + \sum V_{\text{ext}}(\mathbf{r}_i) + \sum \sum U(\mathbf{r}_i, \mathbf{r}_j)$$

The electron density is defined as follows:

$$n(\mathbf{r}) = \Psi^*(\mathbf{r}_1, \mathbf{r}_2, \mathbf{r}_3, \dots, \mathbf{r}_N) \Psi(\mathbf{r}_1, \mathbf{r}_2, \mathbf{r}_3, \dots, \mathbf{r}_N)$$

Here the 3N dimension decreases to 3 dimensions

The j^{th} electron is treated as a point charge in the field of all the other electrons. This simplifies the many-electron problem to many one electron problem.

$$n(\mathbf{r}) = 2 \sum \Psi^*(\mathbf{r})\Psi(\mathbf{r})$$

2.6.2 Hohenberg and Kohn

a. Theorem 1: The ground State energy is the unique functional of the electron density

$$E = E[n(\mathbf{r})]$$

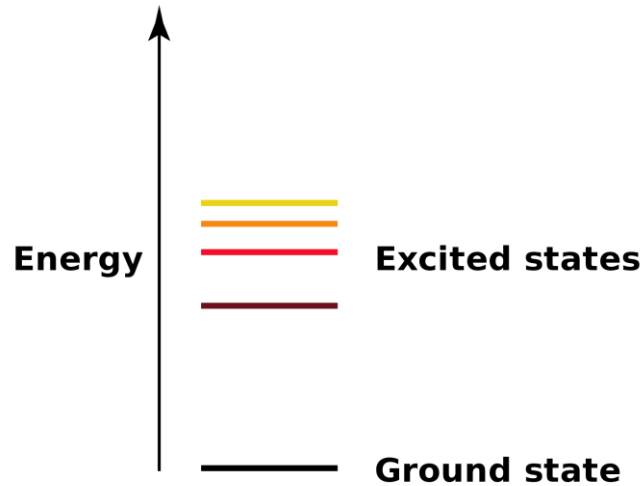


Figure 3 – Ground state and excited states and change in energy ΔE

b. Theorem 2: The electron density that minimizes the energy of overall functional is the true ground state electron density

$$E[n(\mathbf{r})] > E_0[n_0(\mathbf{r})]$$

The energy functional can be divided into two main parts, Known part and unknown part

$$E[\{\Psi_i\}] = E_{\text{known}}[\{\Psi_i\}] + E_{\text{xc}}[\{\Psi_i\}]$$

$$E_{\text{known}}[\{\Psi_i\}] = -\frac{\hbar}{2m_e} \sum_i \int \Psi_i^* \nabla^2 \Psi_i d^3r + \int V(r)n(r)d^3r + \frac{e^2}{2} \iint \frac{n(r)n(r')}{r-r'} d^3r d^3r' + E_{\text{ion}}$$

$$E_{\text{xc}}[\{\Psi_i\}] = \text{Exchange correlation functional}$$

The exchange correlation functional includes all the quantum mechanical terms. It is not known, and it needs to be approximated while doing DFT calculation. The Simplest XC-functional are:

1. LDA: Local density approximation
 2. GGA: Generalized gradient approximation.
- In this work GGA as exchange correlation was used.

2.6.3 The Kohn Sham Scheme

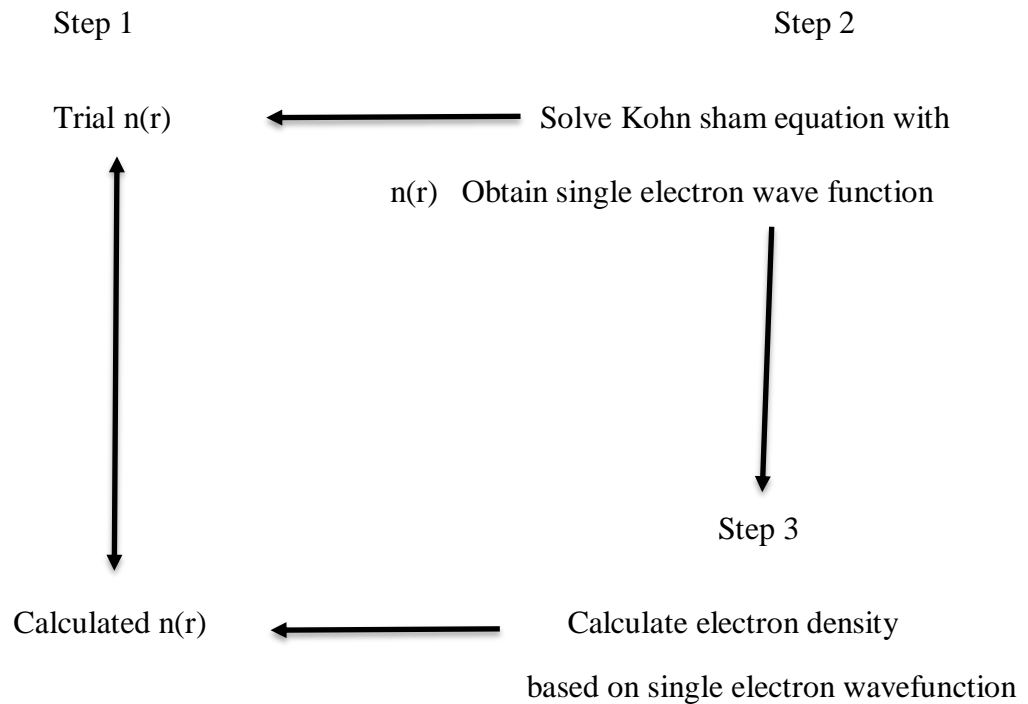
The Kohn Sham equation to find the ground state electron density is given as:

$$-\frac{\hbar}{2m} \nabla^2 + V(r) + V_H(r) + V_{\text{xc}}(r)]\psi_i(r) = \epsilon_i(r)\psi_i$$

In this scheme we first consider a single set of electrons wavefunction which are not interacting. Here $V_H(r)$ is the Hartree potential, which is electron interacting with electron density, $V_{\text{xc}}(r)$ is the exchange-correlation potential which we have to approximate. This is self-consistency scheme is the one that we do in the calculation.

Here the first work is to guess some electron density, which we just make a trial electron density. Then we put this trial electron density into the Hamiltonian above and solve the Kohn Sham equation. After solving, one can obtain a set of single electrons wavefunctions. After that the electron density is re-calculated based on single-electron

wavefunctions. If the electron density is the same as the one guessed before (trial electron density) then there is self-consistency in the loop which means true ground state energy is obtained. If the obtained electron density is not same as before then the trial electron density is replaced with new electron density and run the loop.



2.7 Embedded Atom Model Method

Interatomic potential is used in describing the interaction of atoms in the matter [4]. It is one of the approximations which describe the energy between the atoms in the system.

The total energy of a system of N atoms is given by [1]:

$$\sum_{i=1}^N E_{\alpha_i}^{\text{emb}}(\rho_i) + \frac{1}{2} \sum_{i \neq j}^N \phi_{\alpha_i \alpha_j}(\mathbf{r}_{ij})$$

$$E_{\alpha}^{\text{emb}}(\rho) = a_{\alpha} \rho^{1/2} + b_{\alpha} \rho^2 + c_{\alpha} \rho^3$$

$$\rho_i = \frac{2\rho_i^{(0)}}{1 + e^{-T_i}}$$

$$T_i = \sum_{i=1}^n t_i^{(1)} \left(\frac{\rho_i^{(1)}}{\rho_i^{(0)}} \right)^2$$

where $\phi_{\alpha_i \alpha_j}(\mathbf{r}_{ij})$ is the pair potential between atom i and j with separation \mathbf{r}_{ij} , $E_{\alpha_i}^{\text{emb}}(\rho_i)$ is the embedding energy function, ρ_i is the electron density at site i . $\rho_i^{(0)}$ is the sum over electron densities.

$$\rho_i^{(0)} = \sum_{j \neq i}^N f_{\alpha_j}^{(0)}(\mathbf{r}_{ij})$$

Where $\rho_i^{(l>0)}$, are angular contribution to electron-density for MEAM approach and for zero it is EAM approach.

The expression for partial electron densities and

$$f_{\alpha_i}^{(1)}(\mathbf{r}) = \sum_{i=1}^n a_{\alpha_i}^{(n,1)} \left(r_{\alpha_i}^{(n,1)} - r \right)^3 \theta(r_{\alpha_i}^{(n,1)} - r)$$

$$\phi_{\alpha_i \alpha_j}^{(1)} = \sum_{n=1}^4 b_{\alpha_i \alpha_j}^{(n)} \left(s_{\alpha_i \alpha_j}^{(n)} - r \right)^3 \theta(s_{\alpha_i \alpha_j}^{(n)} - r)$$

where $a_{\alpha_i}^{(n,l)}$, $r_{\alpha_i}^{(n,l)}$, $b_{\alpha_i\alpha_j}^{(n)}$, $s_{\alpha_i\alpha_j}^{(n)}$ are the optimization parameters which will be determined in this work for each Ge-Sn, Ge-Si and Si-Sn binary alloys as well as Ge-Sn-Si ternary alloy and will be discussed in Chapter III, IV and V in detail.

2.8 VASP

VASP, Vienna Ab initio Simulation Package, is a simulation package used to perform ab initio calculation of quantum mechanical system. It uses periodic boundary condition. It uses pseudopotential method with a plane waves basis set. It is a commercial software package which can model system with maximum number of atoms in the range of 100-200. In this thesis work, this software was used to do DFT calculation because it is well documented, and it has a large set of pseudopotentials which are well tested. While doing the VASP calculation some input files need to be created for the system.

2.8.1 INCAR

In it the user specifies the parameters that define the calculation. For example, Energy cutoff, Ionic and geometric relaxation degree of freedom, number of steps etc. are some of the parameters that are specified in the INCAR file.

2.8.2 POSCAR

It is also called Position CAR. In this file the periodic simulation cell is defined. It mainly consists of information regarding the geometry of the system.

2.8.3 POTCAR

This file consists of Pseudopotential (PP). This is basically something that is provided by the VASP itself. It contains information about the pseudopotential and exchange correlation (XC).

2.8.4 KPOINTS

This file specifies how the k-points sampling in Brillouin zone.

After all the INPUT files are ready and calculation is finished, VASP generates OUTPUT files which are as follows:

2.8.5 CONTCAR

It contains position of the atoms in the system after the calculation has completed.

2.8.6 OSZICAR

It contains information about data of electronic steps and ionic steps.

2.8.7 OUTCAR

It contains complete output of the calculation like Total forces, charges on ions, symmetry etc.

2.8.8 CHGCAR

It contains information about the charge density of the system after calculation is completed.

2.9 LAMMPS

LAMMPS is a classical molecular dynamics simulation package. The name LAMMPS stands for **L**arge-scale **A**tomic/**M**olecular **M**assively **P**arallel **S**imulator. It is a simulator because molecular simulation with large number of atoms can be run and it is massively parallel because it can be run in supercomputers with many CPU cores to

get simulation results quicker. Also, it is an open course and free which means source code is available to all the users and it can be changed accordingly to fit needs. Molecular Dynamics simulations are computationally expensive. So, if there is only a single processor to run the simulation then only small number of atoms can be simulated and small-time scaled simulations can be done. To run a large simulation with large time scale it is necessary to have multiple processors to run simulation efficiently. However, writing codes on multiple processors is not an easy task and this is where parallel simulation package like LAMMPS comes

CHAPTER 3. STUDY OF GERMANIUM-TIN

In this Chapter MD simulations and the EAM potential developed for Ge-Sn alloy by fitting the data from VASP simulation using EAM code is discussed in detail. This chapter contains the input parameters that are used for doing simulation in VASP and it intends to explain about the fitting of EAM potentials to Energies, Forces and stress tensor generated by VASP .After generating EAM potential it will be necessary to test whether the developed potential is good or not, so the testing technique for Ge-Sn EAM potential will also be explained. Finally, after making sure that the potential that is developed is good enough properties like Band structure, Density of states, Bulk modulus, Lattice constant etc. using both the VASP generated data and developed EAM potential will be calculated.

3.1 Simulation method

The simulation was performed in a box size 11.3148 Å * 11.3148 Å * 11.3148 Å. For the simulation work to start we need INCAR, POSCAR, KPOINTS and POTCAR as input files in VASP. The POSCAR file which contains the lattice geometry and ionic position of was created using Quantum ATK. For this Ge-Sn simulation

Canonical ensemble (NVT) was applied by setting SMASS tag = 0 and the Noose-Hoover thermostat was used. Also, by adding ISIF = 2 tag in INCAR file, stress tensor was calculated. Six different simulations were performed at 800K-1200K each generating more

than 800 different configurations of energies, Forces and Stress tensor from each simulation which were used in EAM fit to develop potential. In KPOINT file Gamma centered K-point sampling of $8*8*8$ was used. Though KPOINT file was generated using quantum ATK, it was also confirmed by doing K-Point convergence test which is shown in Figure 4.

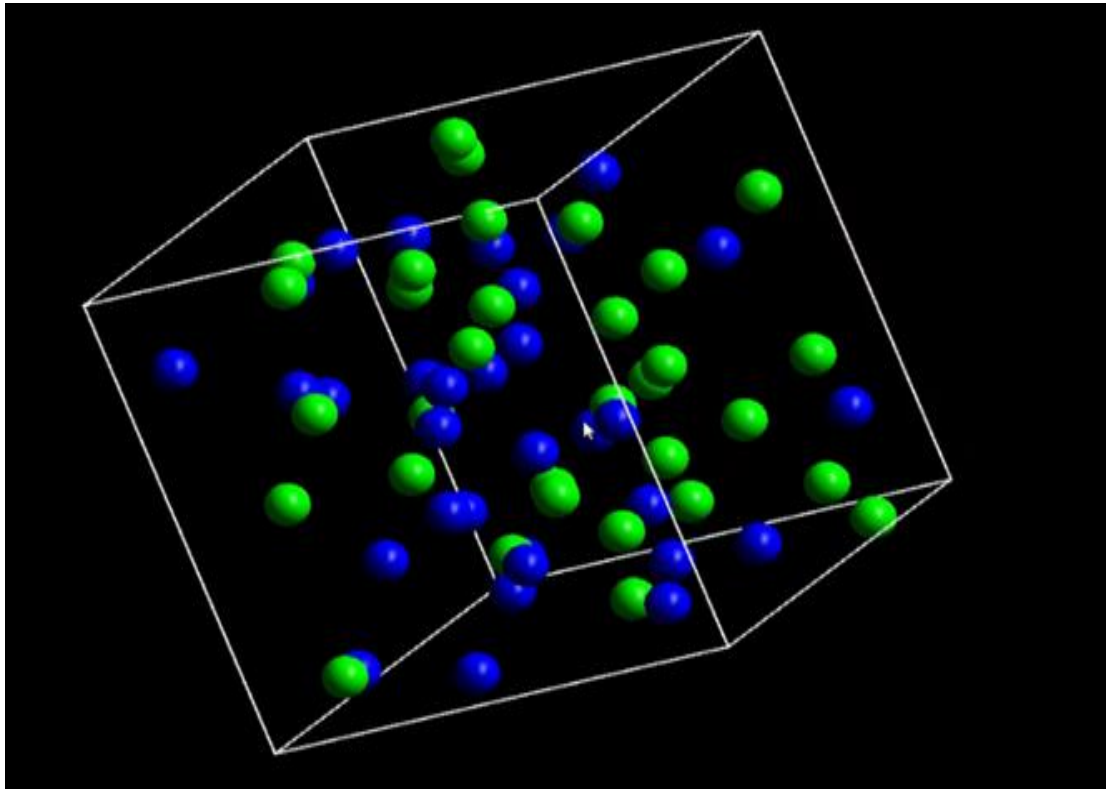


Figure 4 – Snapshot of movement of 64 atoms of Germanium(32) and Tin(32) in the box of dimension $11.3148 \text{ \AA} * 11.3148 \text{ \AA} * 11.3148 \text{ \AA}$ at temperature 1200K

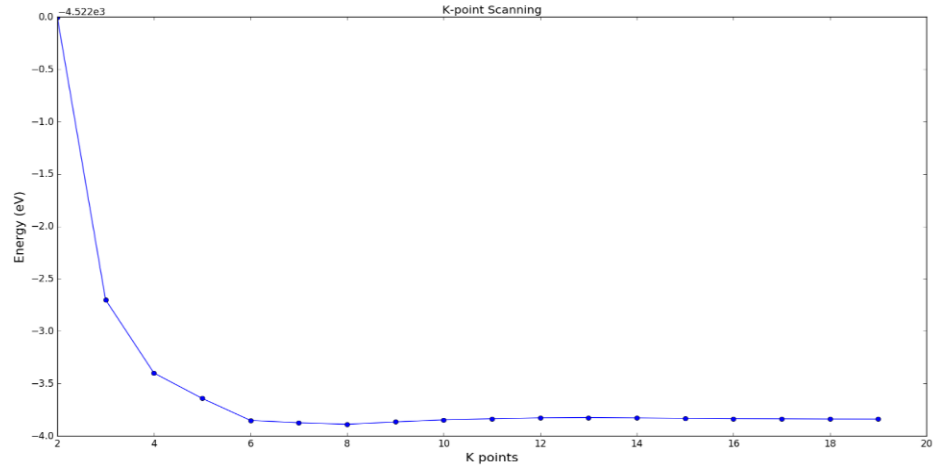


Figure 5 – Plot of K-points versus Energy for Ge-Sn system MD input in VASP

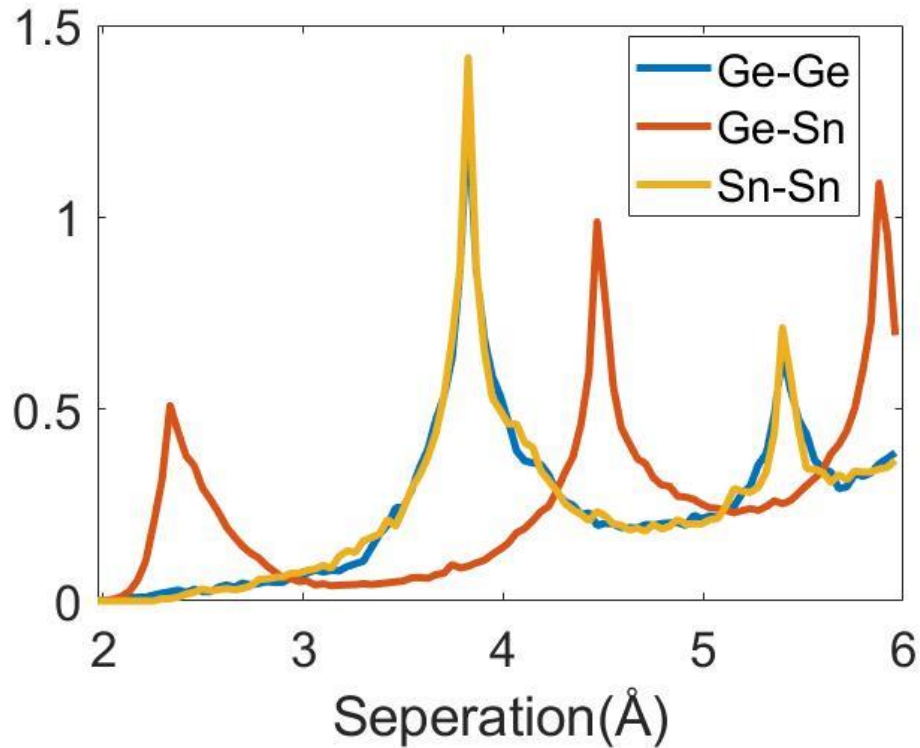


Figure 6 – Histogram of interatomic separation for Ge-Sn MD-run at 1200K

For EAM fitting it is necessary to specify the cutoff radius in the setting of INPUT files in EAM code. To find the cutoff radius initially with all the files which had data points to fit were numbered from 1 to 9 and EAM fitting was run which generated “FITDBSE” and

setting files. In setting a random number, more than 10\AA as cutoff radius was chosen and fit was run without optimization. This generated a file “SEPNHISTOGRAM.OUT” which had the data of separation of (1,1), (1,2) and (2,2) atoms and by using MATLAB these data were plotted which is figure 3.1.3 above. From above cutoff radius was chosen to be 5.6\AA to get the potential which includes up to third nearest neighbor interaction. Also, to avoid negative electron density, ‘NEGELECDENS= true ‘input was given in the setting file of EAM fitting, which was third step in fitting process.

3.2 Result and Discussion

In this section we outline the testing method of developed EAM potential of Ge-Sn alloy, potential parameters, plotting and elastic properties.

3.2.1 Testing using testing set

3.2.1.1 Free energy fitted EAM1 and EAM2

After developing the Potential, it is now necessary to test whether the developed potential is good or not. One of the methods used to test the potential was reproduction of Free energy using testing set. While doing DFT calculations in VASP, more than 1000 energies were used for fitting and more than 2000 energies, which were not used in the fitting, were used as testing set. For EAM1, the optimization function due to optimization of data points was 0.3523 and with the testing set without optimization the optimization function was 0.3901 where the error was about 7.6 % which shows that the developed potential performed nicely with the testing set as in fitting sets. Similarly, for EAM2 with the fitting sets the optimization functions was 0.3569 while with the testing set it was 0.3715.

3.2.1.2 Stress-Tensor fitted EAM1 and EAM2

For Stress-tensor fitted potential also two different sets of data were separated, fitting set and testing sets. For EAM1, by using fitting set the optimized functions was 0.3032 and with the testing set it was 1.0586. Similarly, for EAM2, the objective functions were 0.3216 and 0.7755 respectively which suggest performance of Stress fitted EAM1 and EAM2 potentials was not as good as free energy fitted potentials while testing with the testing sets. Some probable reason why stress- tensor fitted potential did not perform comparable performance with testing sets will be discussed in the Chapter VII.

3.2.2 Reproduction of Force by the developed potential

3.2.2.1 Free energy fitted EAM1 and EAM2

In this test, it was checked how well are the developed potential to reproduce force. For this, the POTPARAS files, which contain the parameters of potential, of both EAM1 and EAM2 were taken separately and ran the EAM fitting without optimizations. And while doing this, the data were taken in such a way that those were not used in fitting. By doing so the optimized function on the output were 0.3439 and 0.3401 for EAM1 and EAM2 respectively which were within 3-4 % of the data fitted optimized function as mentioned above. From this it was found that the developed potential did reproduce the force nicely.

3.2.2.2 Stress fitted EAM1 and EAM2

In this test the similar steps were followed as above but here Force was reproduced by using Stress fitted EAM1 and EAM2. I The data, which were not used during fitting, and POTPARAS

files for both EAM1 and EAM2 were taken. Then EAM fitting was run without optimization and the optimization functions were 1.599 and 1.281 for EAM1 and EAM2 respectively.

3.2.3 Cohesive energy test

3.2.3.1 Free energy fitted EAM1 and EAM2

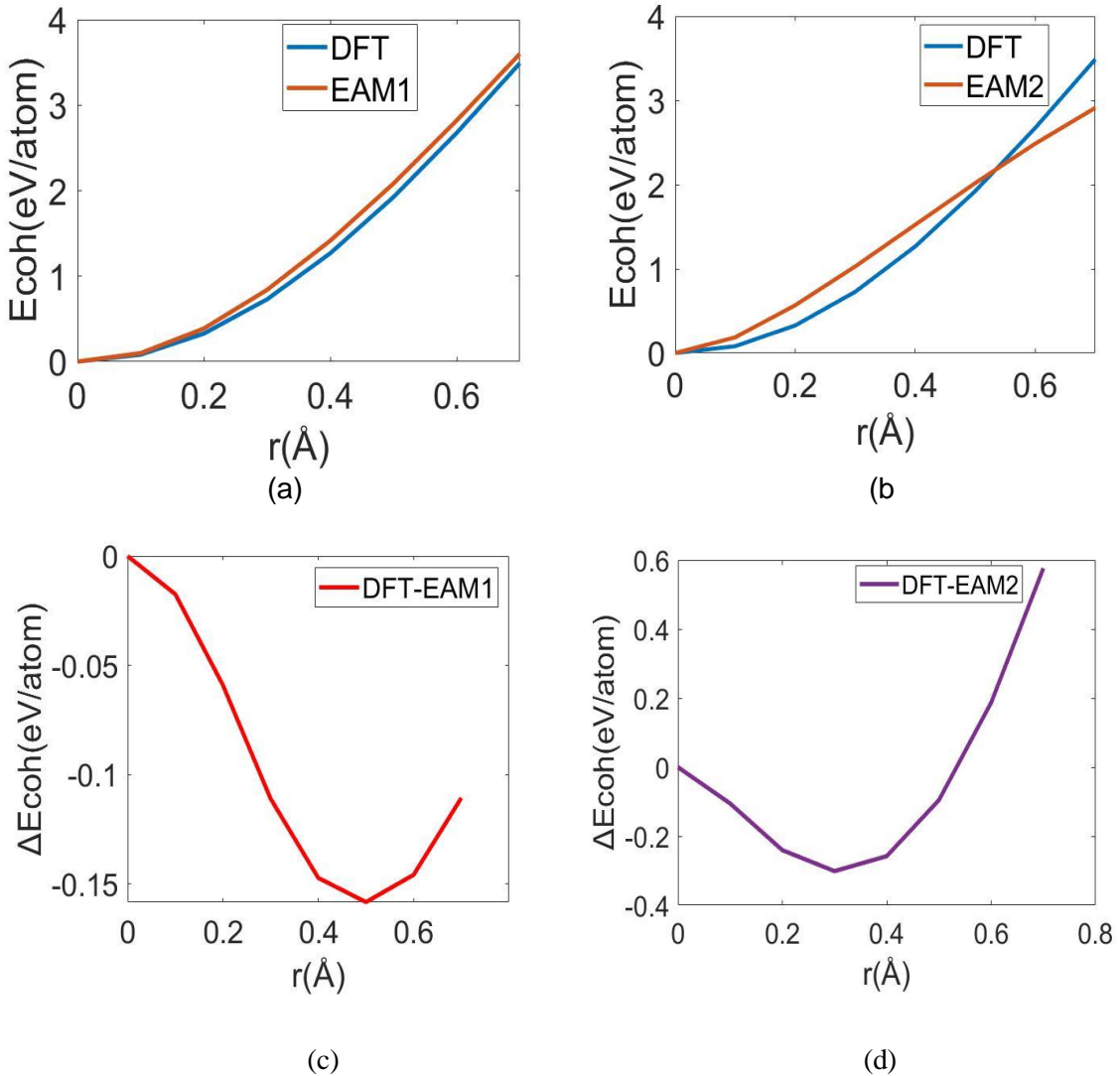


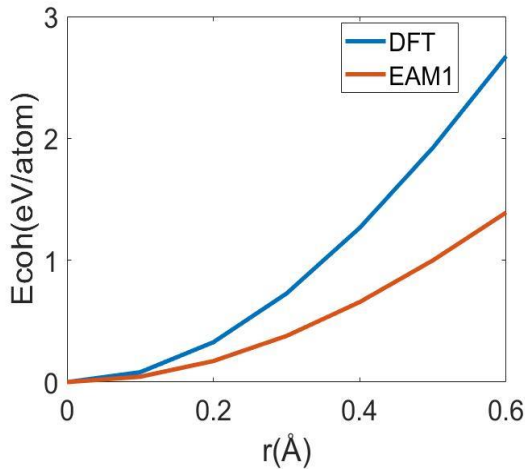
Figure 7 – (a, b) Plot of Cohesive energy vs distance of Sn atom from its lattice point for Free energy fitted EAM1, DFT and EAM2, DFT. (c, d) Plot of difference in change of Cohesive energy in plot a and b with respective to distance in Angstrom.

For this an FCC cubic structure of Ge-Sn with 4 Ge atoms and 4 Sn atoms was created by quantum ATK. Then one of the Sn atoms was selected whose z-coordinate was 3.57587Å. The aim here was to calculate the Total energy by using EAM potentials. So, in Quantum ATK the force field calculator was selected and the LAMMPS format of EAM1 file was provided to calculate the total energy of the system which came out to be 3.67704 eV. This energy was the energy when all the atoms were on equilibrium position, so this energy was taken as reference energy. After this, the position of the above selected Sn atom was changed to 3.63587Å along z-axis and the total energy was 3.77603. By following the above steps the position of same Sn atom was changed each times by 0.1Å as 3.73587Å, 3.83587Å, 3.93587Å, 4.03587Å, 4.13587Å, 4.23587Å and the corresponding values of energies were 4.06424 eV, 4.51585 eV, 5.09091 eV, 5.75930 eV, 6.49745 eV, 7.27664 eV respectively. Similarly, the same procedure was applied to find the total energy of Ge-Sn configuration with 4 atoms each by using free energy fitted EAM2 potential and the energies were -24.23255 eV, -24.04576 eV, -23.66434 eV, -23.20344 eV, -22.7080 eV, -22.21329 eV, -21.74499 eV, -21.31989 eV. Then by changing the position of Sn atom each time different POSCAR were created using quantum ATK and INCAR file was created in such a way to do Static calculation. The KPOINT and POTCAR files were same. Then for each changed positions the DFT calculation was performed in VASP. The final energies on DFT calculations were -29.406530 eV, -29.324938 eV, -29.078710 eV, -28.678670 eV, -28.139848 eV, -27.482520 eV, -26.731890 eV, -25.917574 eV. After calculation of total energies by EAM1, EAM2 potentials and DFT, each of the energies were subtracted from the energy at which the system was at equilibrium i.e. equilibrium state energy and this was called Cohesive energy which goes along Y-axis on the plot (a) and (b) above and

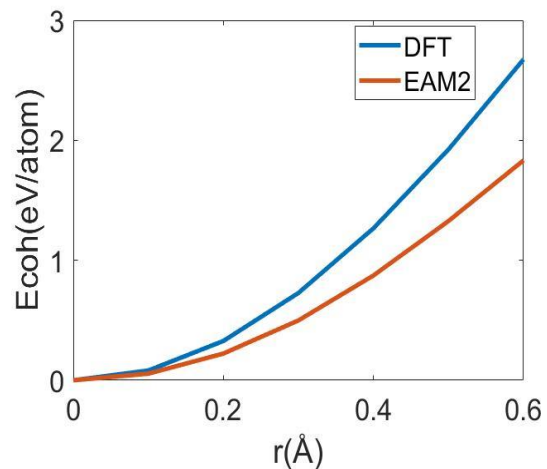
along X-axis is the change of position of Sn atom along z-axis each time by 0.1Å. From the plots (a) and (b) it is seen with EAM1 potential the cohesive energy of Sn atom to move away from its initial equilibrium position each time by 0.1Å is nearly same as that in DFT. Also, EAM2 potential is showing comparable performance as that of DFT but little less than EAM1 which is expected because EAM1 potential here is considered as the best potential. On plot c and d above the difference in cohesive energies of Sn atom by DFT and EAM potentials were calculated and plotted along Y-axis with X-axis being the change in position of Sn atom as before.

From the plot it can be seen that the difference in Cohesive energies between DFT and EAM1 decreases as Sn changes its position from equilibrium state (taken as 0Å) to 0.5Å and the difference starts to increase afterward while for EAM2 and DFT the difference in Cohesive energy decreased up to position 0.3Å and it started increasing.

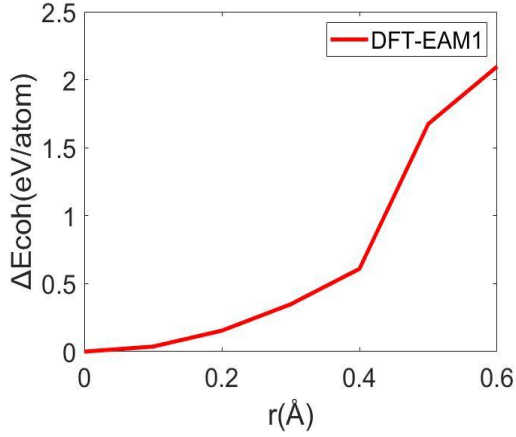
3.2.3.2 Stress Fitted EAM1 and EAM2



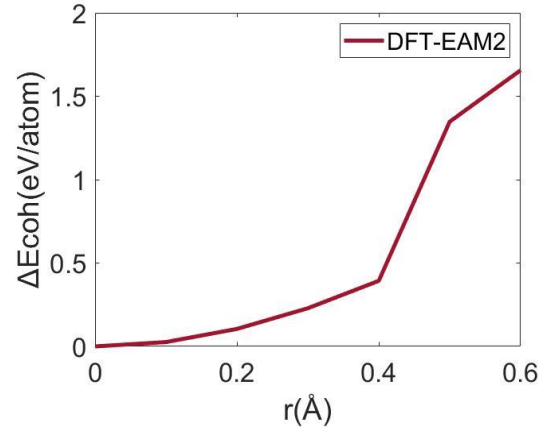
(a)



(b)



(c)



(d)

Figure 8 – (a, b):Plot of Cohesive energy vs distance of Sn atom from its lattice point for Stress tensor fitted EAM1, DFT and EAM2,DFT. (c, d) :Plot of difference in change of Cohesive energy in plot a and b with respective to distance in Angstrom.

The above plots a and b in Figure number 3.2.1.1 are the Cohesive energy plots for Changing the position of an Sn atom along z-axis on the configuration of 4 Ge and 4 Sn atoms by the EAM1 and EAM2 potentials developed by fitting Stress-tensor data points and compared with the DFT cohesive energies. For EAM1, the total energy, when all the atoms were in equilibrium state was -4.8160eV which was taken as reference energy here. Then an Sn atom was moved each time by 0.1Å along z-axis and in each time the total energy recorded were -4.77174 eV, -4.64269 eV, -4.43655 eV, -4.15854 eV, -3.81642 eV, -3.42412 eV. As before these energies were subtracted from the initial reference energies and plotted in Y-axis with respect to changed position along X-axis. Similarly, in plot ‘b’ the reference energy by stress fitted EAM2 potential was -39.03933 eV and the energies when the position of Sn was changed by 0.1Å each time were -38.98381 eV, -38.81638

eV, -38.54032 eV, -38.16588 eV, -37.71190 eV, -37.20632 eV. Then the cohesive energy was plotted against the position.

Plots ‘c’ and ‘d’ are the difference in the cohesive energies of EAM1 and EAM2 respectively with cohesive energy from DFT.

3.2.4 Free-Energy Fitted EAM Parameters

Table 1 –: Embedding function parameters for free energy fitted EAM1 and EAM2 potentials

	<i>EAM1</i>		<i>EAM2</i>	
	f_{Ge}^0	f_{Sn}^0	f_{Ge}^0	f_{Sn}^0
$a^1(ev)$	0.6029	43.3476	0.3603	33.5827
$r^1(\text{Å})$	4.4259	5.4981	4.8948	4.1378
$a^2(ev)$	41.5457	-42.9499	1.9827	-33.9737
$r^2(\text{Å})$	2.2325	5.5019	1.6692	4.1093

Table 2 –: Electron density parameters for free energy fitted EAM1 and EAM2 potentials

	<i>EAM1</i>		<i>EAM2</i>	
	E_{Ge}^{emb}	E_{Sn}^{emb}	E_{Ge}^{emb}	E_{Sn}^{emb}
$a(ev)$	$1.035 \cdot 10^{-3}$	$8.359 \cdot 10^{-3}$	0.622	1.779
$b(ev)$	$3.582 \cdot 10^{-3}$	$2.198 \cdot 10^{-5}$	$1.786 \cdot 10^{-3}$	$1.227 \cdot 10^{-2}$
$c(ev)$	$2.574 \cdot 10^{-9}$	$-4.453 \cdot 10^{-10}$	$6.412 \cdot 10^{-8}$	$1.742 \cdot 10^{-4}$

Table 3 –: Pairwise interaction potential parameters for free energy fitted EAM1 and EAM2 potentials

	<i>EAM1</i>			<i>EAM2</i>		
	ϕ_{Ge-Ge}	ϕ_{Ge-Sn}	ϕ_{Sn-Sn}	ϕ_{Ge-Ge}	ϕ_{Ge-Sn}	ϕ_{Sn-Sn}
$b^1(ev)$	3.0018	11.5467	0.1241	-4.7511	-2.7979	-0.9224
$s^1(\text{Å})$	3.1935	2.6551	4.5428	1.6133	2.4924	3.5259
$b^2(ev)$	-1.5337	-4.46*10 ⁻²	5.9520	6.5304	2.7977	4.1174
$s^2(\text{Å})$	3.6108	4.6687	2.8977	2.6066	2.4924	3.2024

3.2.5 Stress-Tensor Fitted EAM Parameters

Table 4 –: Embedding function parameters for stress fitted EAM1 and EAM2 potentials

	<i>EAM1</i>		<i>EAM2</i>	
	E_{Ge}^{emb}	E_{Sn}^{emb}	E_{Ge}^{emb}	E_{Sn}^{emb}
$a(ev)$	4.0123*10 ⁻⁶	0.83724	1.1643*10 ⁻³	5.1614
$b(ev)$	1.344*10 ⁻²	-2.8881*10 ⁻³	2.2008*10 ⁻²	2.8669*10 ⁻³
$c(ev)$	1.9062*10 ⁻⁷	5.7594*10 ⁻⁹	2.6197*10 ⁻⁸	3.6969*10 ⁻⁹

Table 5 –: Electron density parameters for Stress fitted EAM1 and EAM2 potentials

	<i>EAM1</i>		<i>EAM2</i>	
	f_{Ge}^0	f_{Sn}^0	f_{Ge}^0	f_{Sn}^0
$a^1(ev)$	0.4213	5.3772	0.2564	5.3773
$r^1(\text{\AA})$	5.0366	2.1364	5.0627	2.1364
$a^2(ev)$	0.4094	22.2956	-9.6815	17.3603
$r^2(\text{\AA})$	1.6361	2.3827	2.7835	2.4586

Table 6 –: Pairwise interaction potential parameters for free energy fitted EAM1 and EAM2 potentials

	<i>EAM1</i>			<i>EAM2</i>		
	ϕ_{Ge-Ge}	ϕ_{Ge-Sn}	ϕ_{Sn-Sn}	ϕ_{Ge-Ge}	ϕ_{Ge-Sn}	ϕ_{Sn-Sn}
$b^1(ev)$	7.4372	1.1816	6.2557	1.1237	6.8432	5.8157
$s^1(\text{\AA})$	4.3379	3.5158	4.5254	2.8129	4.8402	4.5900
$b^2(ev)$	-7.5502	4.9613	-6.2934	1.4440	5.9325	-5.7833
$s^2(\text{\AA})$	4.3455	2.5832	4.5316	2.3133	5.5003	4.6033

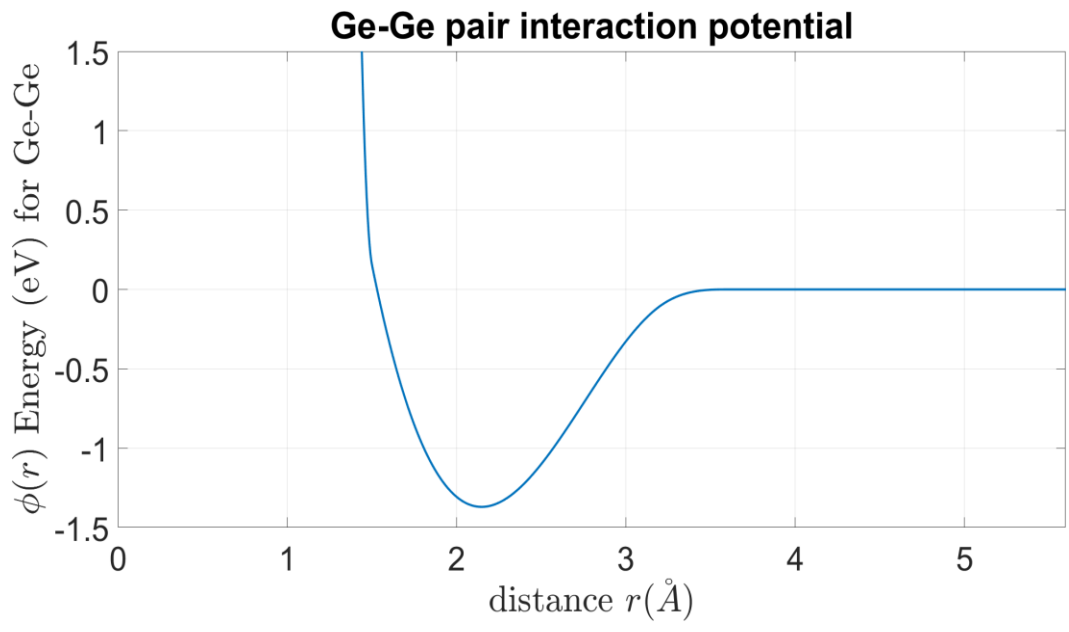


Figure 9 – Plot of Ge-Ge interatomic distance versus pair-interaction energy by Free-energy fitted EAM1 potential

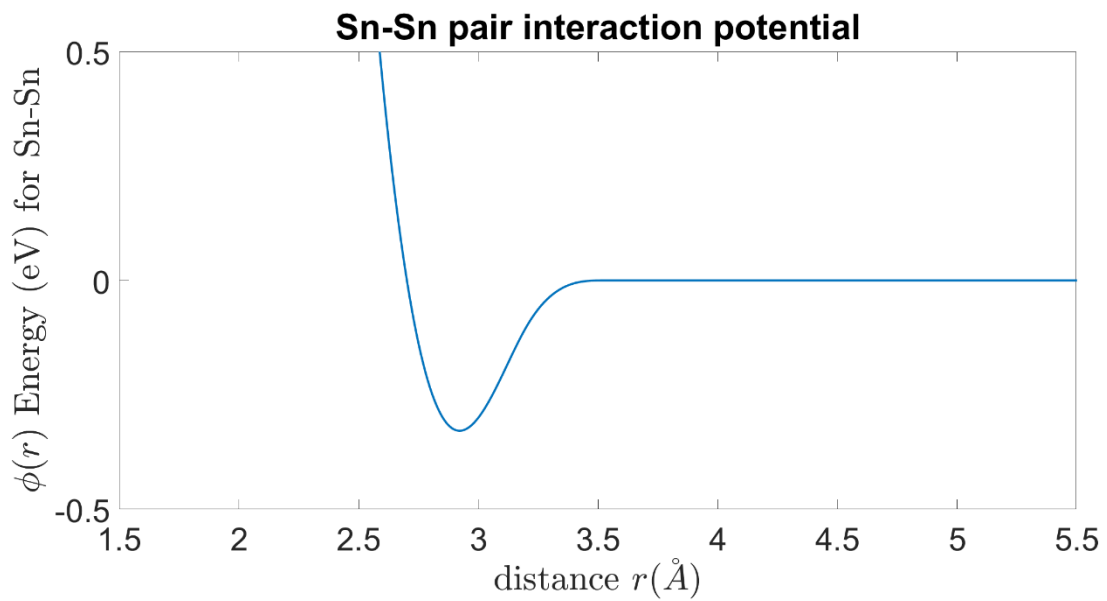


Figure 10 – Plot of Sn-Sn pair interaction distance versus interaction energy by free energy fitted EAM1 potential

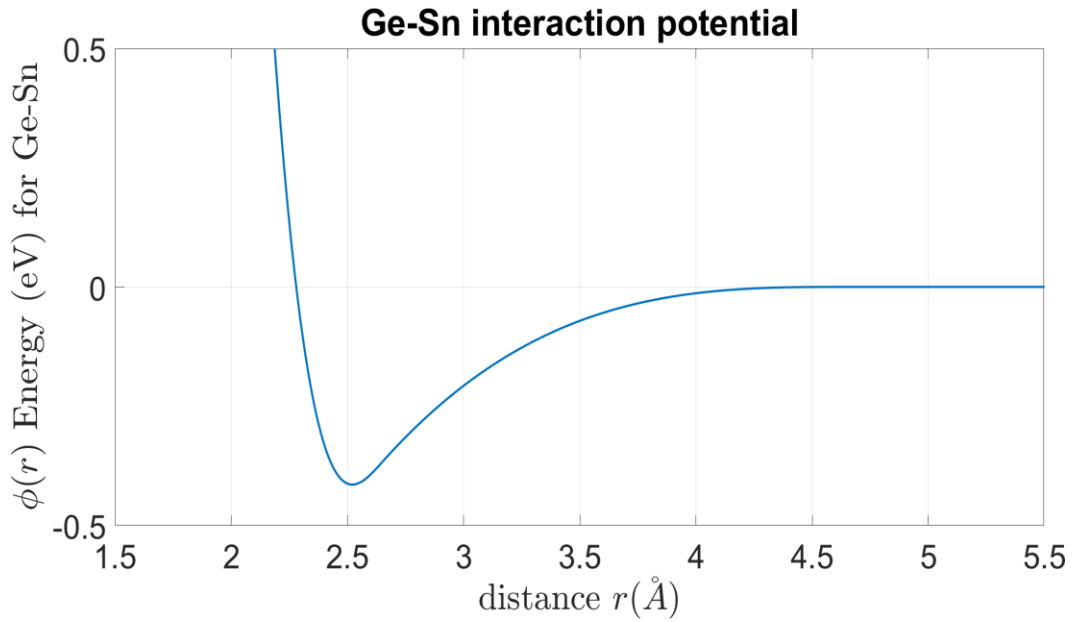


Figure 11 – Plot of Ge-Sn pair interaction distance versus interaction energy by free energy fitted EAM2 potential

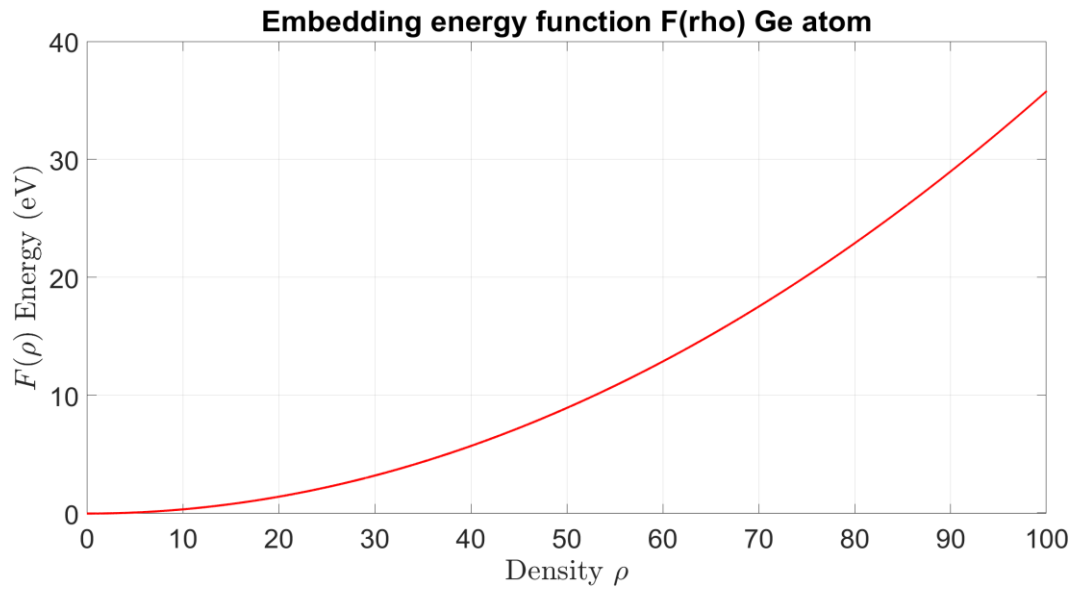
The above plots are the plots of Interaction potential energy of Ge-Ge, Sn-Sn and Ge-Sn atoms with the atom separations. The two atoms have both the attractive and repulsive force in between them. The attractive forces are between the dipoles and repulsive force occurs when the electron cloud of two atoms come closer which is enough to repel one another and when these two forces are equal then these two forces are at the equilibrium condition. These attractive and repulsive energies determine the potential energy of two atoms. The above plots are the change in Total Potential energies with the change in distance between atoms. Attractive forces correspond to negative potential energy and repulsive force correspond to positive potential energy. The tendency will be two atoms moving to a position where their potential energy is at minimum. For Ge-Ge, if the atoms are widely separated initially at around 6\AA , the attractive force is dominate and if the atoms

are moved closer to each other, the total potential energy becomes more negative and the point at which the potential is minimum is the equilibrium point which is called r_0 and in Ge-Ge the r_0 is approximately 2.2Å. If they get more closer the PE start becoming more positive as repulsive force begin to become more dominate. For Sn-Sn the equilibrium distance at which the PE between two Tin atoms become minimum is nearly 2.9Å after which the repulsive force starts getting dominate. Finally, at distance of 2.5Å between Germanium and Tin atoms, the PE become minimum.

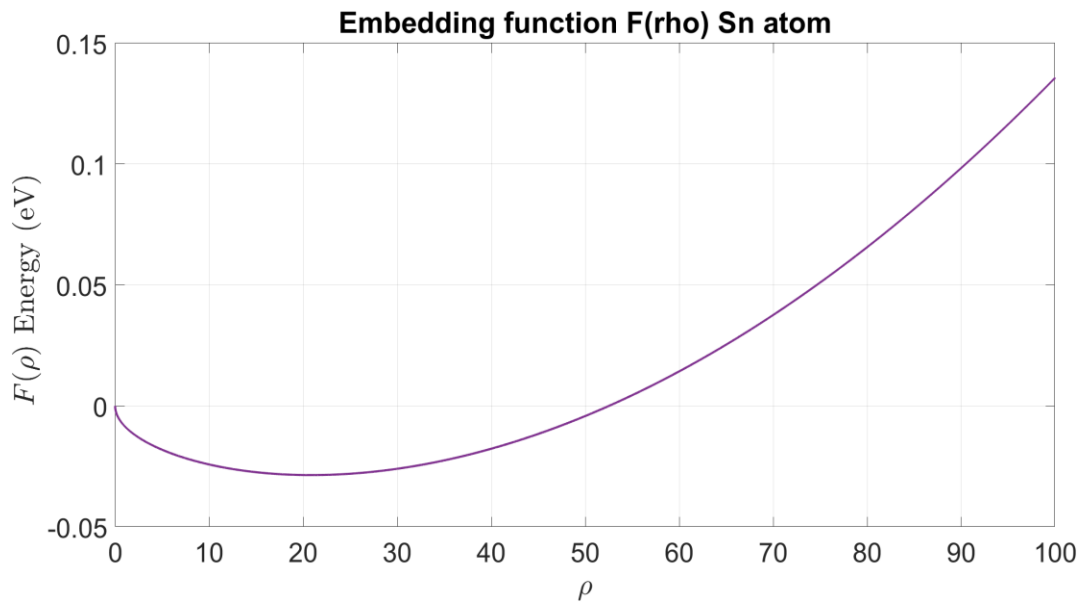
The above plots are for free-energy fitted EAM1 potential and EAM2 potentials and for Ge-Ge, Sn-Sn and Ge-Sn pair interaction, the minimum energies are approximately -1.4eV, -0.3eV and -0.4eV respectively.

The embedding function and electron density function of mono atoms Germanium and Tin are shown in figure 12. For an alloy model, an embedding function $F(\rho)$ and an atomic electron density function $f(r)$ must be specified for each atomic species and two-body potential $\phi(r)$ specified for each possible combination of atomic species. Since electron density at any location is taken as linear superposition of atomic electron densities and since the embedded energy is assumed to be independent of the source of electron density, these two functions can be taken directly from monoatomic model.

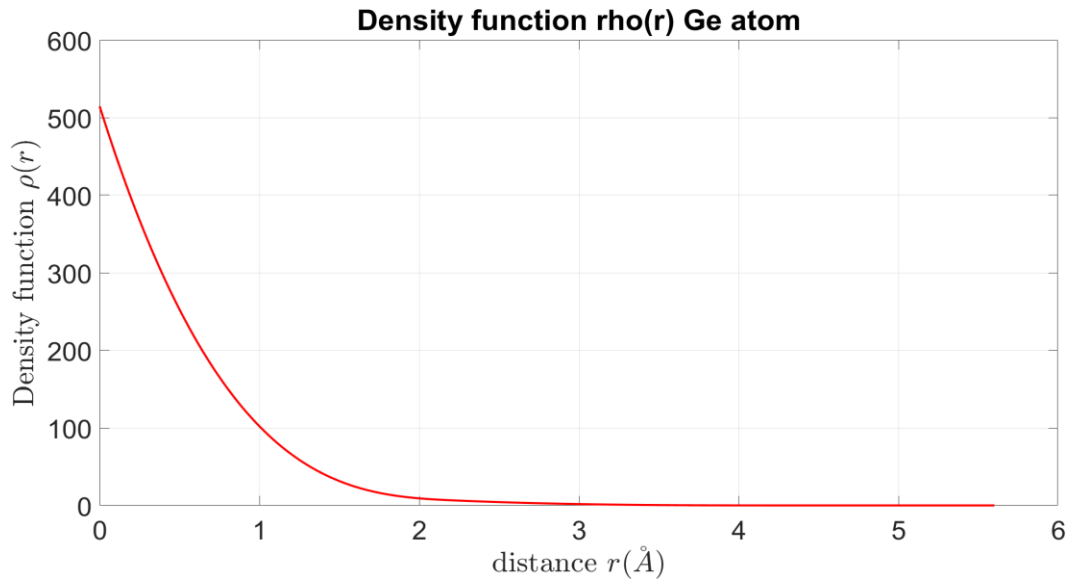
The embedding function and the electron density function plot of Mono atoms Germanium and Tin are shown in figure 12



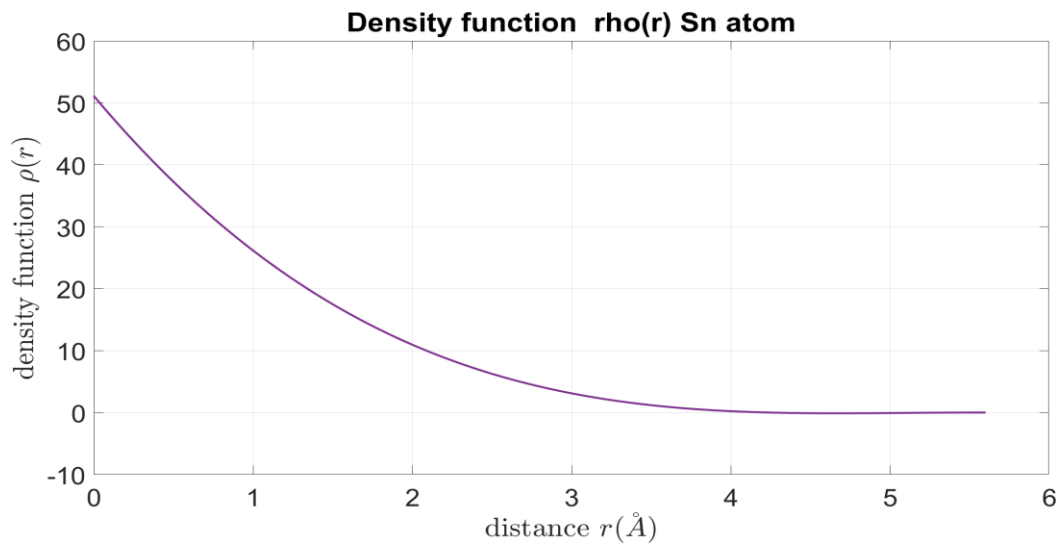
(a)



(b)

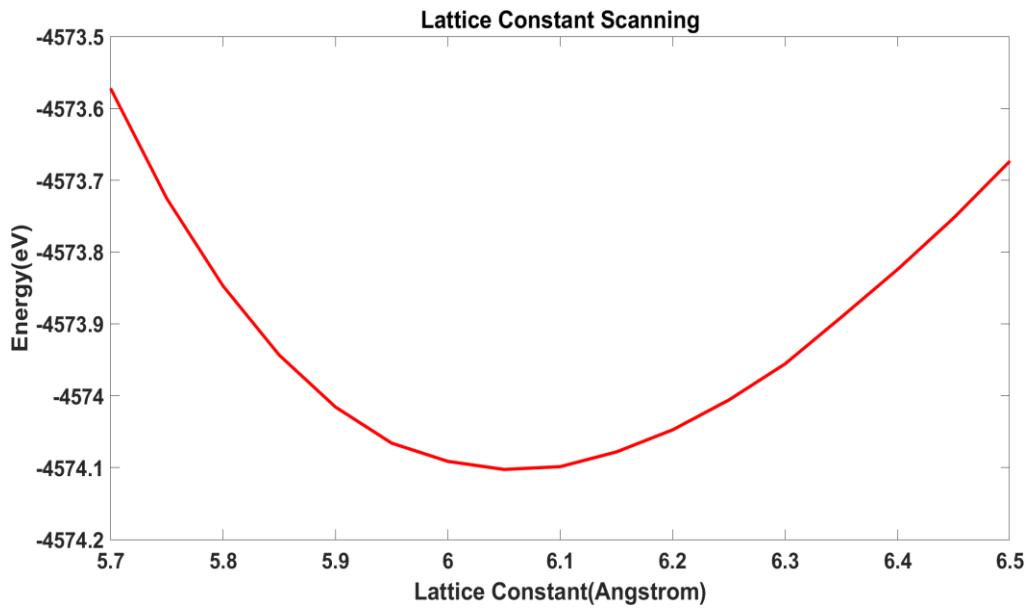
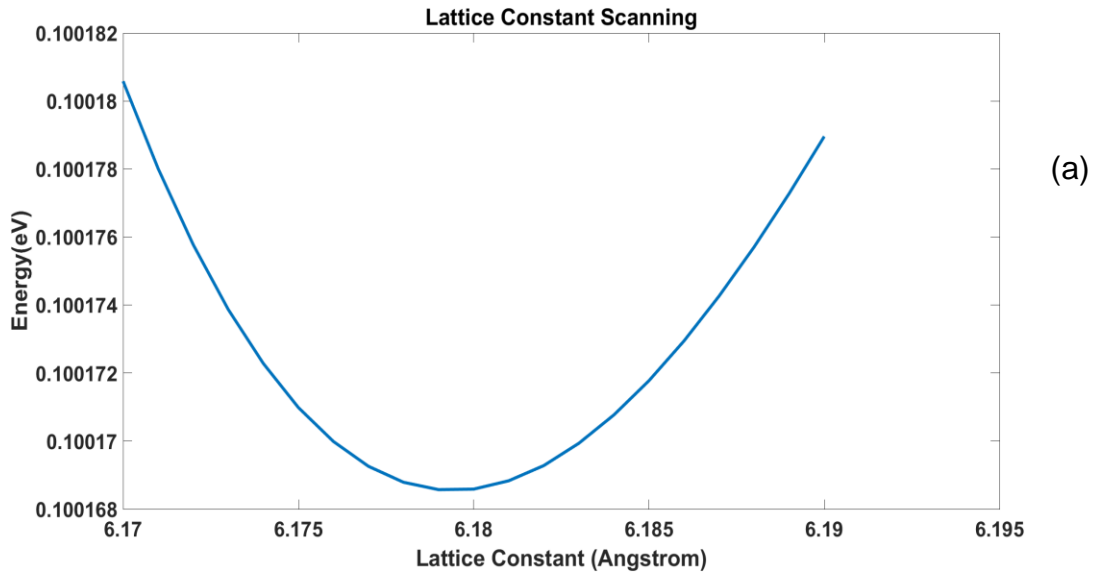


(c)



(d)

Figure 12 – (a, b) plot of Embedding energy function of Ge and Sn respectively by free energy fitted EAM1. (c, d) plot of Density function versus distance of Ge and Sn using free energy fitted EAM1



(b)

Figure 13 – (a)The variation of Total energy with lattice constant for Ge-Sn by stress fitted EAM1 potential .(b) The Variation of Total energy with lattice constant in for Ge-Sn by DFT(LDA).

Above plot is the plot of equilibrium lattice constant of Germanium-Tin configuration EAM1 potential and DFT. Though lattice constant was calculated by both the EAM1 and

EAM2 potential of stress fit as shown in the table below, the plot above is for EAM1 potential and DFT with LDA exchange correlation. To find the lattice point python code was written for quantum atk and LAMMPS format EAM1 potential was supplied which gave lattice constant with corresponding Energy of the configuration. The energies were plotted against the lattice constant and the lattice constant with lowest energy was chosen as the equilibrium lattice constant. Similar procedure was followed for DFT calculation which had LDA correlation and the lattice constant from both DFT and EAM1 potential are very close, 6.08Å and 6.15Å respectively.

Some elastic properties like Bulk Modulus, Young's Modulus, Elastic constants and so on as shown in table 7 were calculated using stress fitted EAM1 and EAM2 potential and were compared with the DFT using both GGA and LDA exchange correlation. Similarly, the calculated values by developed potentials were also compared with the experimental works that were done before but results from EAM potentials were closer to that of from DFT rather than experimental. From above table it can be seen that the bulk modulus value by LDA exchange correlation differs from EAM1 and EAM2 by approximately 28% and 21% respectively while value by GGA correlation differs from EAM1 and EAM2 by 17% and 40% respectively which are in acceptable range. These results suggest that if the DFT calculations is improved then the EAM potential developed by fitting Stress-Tensor data generated by DFT perform comparable performance with the result of DFT.

Table 7 – Calculated Elastic properties of Ge-Sn alloy

	LDA	GGA	EAM1	EAM2
Lattice constant(a)	6.08	6.09	6.15	6.18
Bulk modulus(B)	144.14	124.66	103.53	175.69
Youngs modulus(Y)	90.12	84.37	66.56	71.68
Shear Modulus	39.80	35.67	36.98	41.46
C ₁₁	187.18	165.21	76.93	145.22
C ₁₂	122.62	104.39	117.34	190.92
C ₄₄	47.13	40.32	77.68	90.69
Poisson Ratio	0.3958	0.3872	0.6071	0.5680

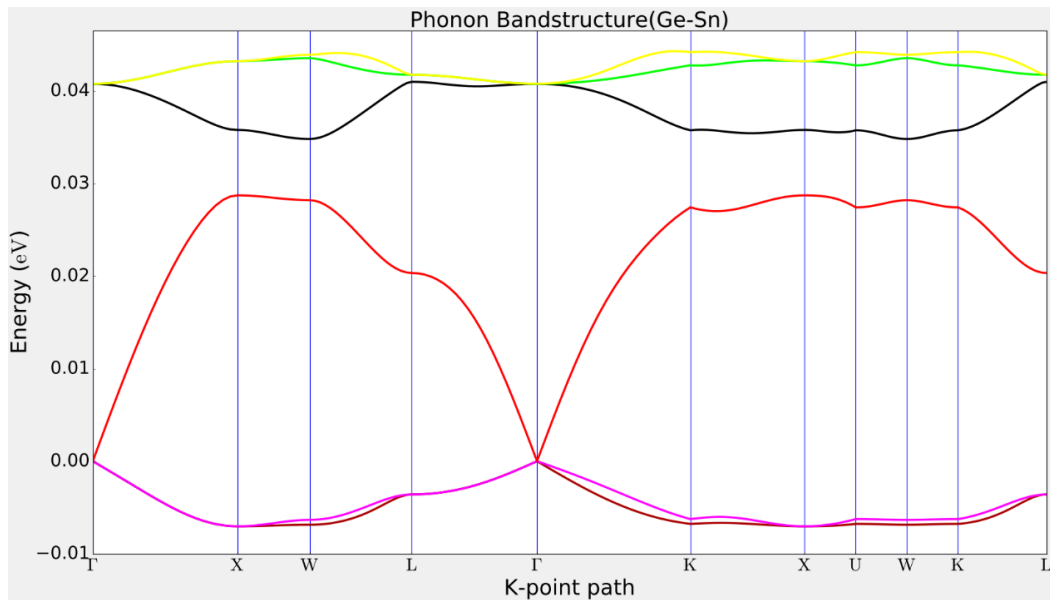


Figure 14 – Plot of phonon Band structure of Ge-Sn using Free-energy fitted EAM1

By the free energy fitted EAM1 potential the band structure of Ge-Sn alloy was calculated and plotted as shown above. It is the FCC lattice with atom basis, Germanium and Tin at $(0,0,0)$ and $(1/4,1/4,1/4)$ per unit cell. Each then Germanium and Tin have 4 valence electrons each, so total of 8 valence electrons were there per unit cell. By providing the potential in quantum ATK, Band structure was plotted. As shown above, there are three bands and there is a gap. So, all the bands below gap will be filled and the bands above gaps will be empty. The lowest band has shape like parabola as given by free electron model and how wide the parabola it gives the mass of the electron. Below gap, at the Brillouin zone edge, i.e L point, the band gap can be seen again like in nearly free electron model. Now going back to the Gamma point beneath the gap which separates occupied and unoccupied band, it can be seen that there is now bandgap at Gamma point. The highest

filled band, red, is called valence band and the highest unfilled band, black in Ge-Sn band plot, is called conduction band.

The Density of States plot of Germanium- Tin alloy is shown in figure 15

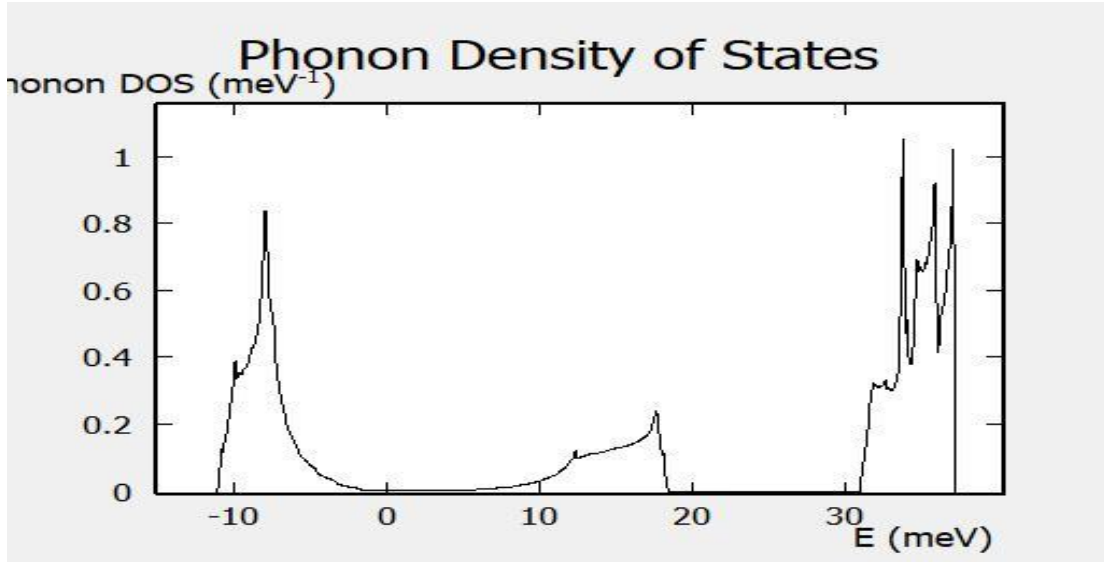


Figure 15 – Plot of Total Phonon density of States of Ge-Sn using Stress-fitted EAM

CHAPTER 4. STUDY OF GERMANIUM-SILICON

In this chapter the simulation method of Ge-Si system using VASP and fitting of VASP output Free-energy and Stress tensor using EAM fitting code to develop the EAM potential is discussed. This chapter contains EAM parameters of developed EAM potentials, both free fitted potential and Stress-tensor fitted potential. After developing the potential, it is necessary to check if the developed potential is working good or not. So, for that three tests were done which are explained in this chapter. Similarly, after confirming that the potential was working well, interatomic pair interaction with respect to distance, embedding function and Density function of Germanium and Silicon are plotted. Also, Elastic properties like Bulk modulus, Young's modulus. Shear modulus, elastic constants, equilibrium lattice constants etc. are also calculated both by DFT, using LDA and GGA, and developed EAM potentials and the values are compared. Also. This chapter contains the phonon band structure and Phonon density of states plot of Ge-Sn by using EAM potential.

4.1 Simulation method

The simulation was performed in a box size $11.3148 \text{ \AA} * 11.3148 \text{ \AA} * 11.3148 \text{ \AA}$ as in Ge-Si system above. For the simulation work to start we needed INCAR, POSCAR, KPOINTS and POTCAR as input files in VASP. The POSCAR file which contains the lattice geometry and ionic position of was created using Quantum ATK. For this Ge-Sn simulation

Canonical ensemble (NVT) was used by setting SMASS tag = 0 and the thermostat that was used is Noose-Hoover thermostat. Also, by adding ISIF = 2 tag in INCAR file, stress tensor was also calculated. Six different simulations were performed at 9500K each generating more than 800 different configurations of energies, Forces and Stress tensor from each simulation which were used in EAM fit to develop potential. In KPOINT file Gamma centered K-point sampling of 8*8*8 was used. Since the K-point convergence test was already done for Ge-Sn and ATK generated k-points were good enough so for Ge-Si testing was not done. For the energy cutoff, the default value was set on INCAR by which the was taken from POTCAR by VASP.

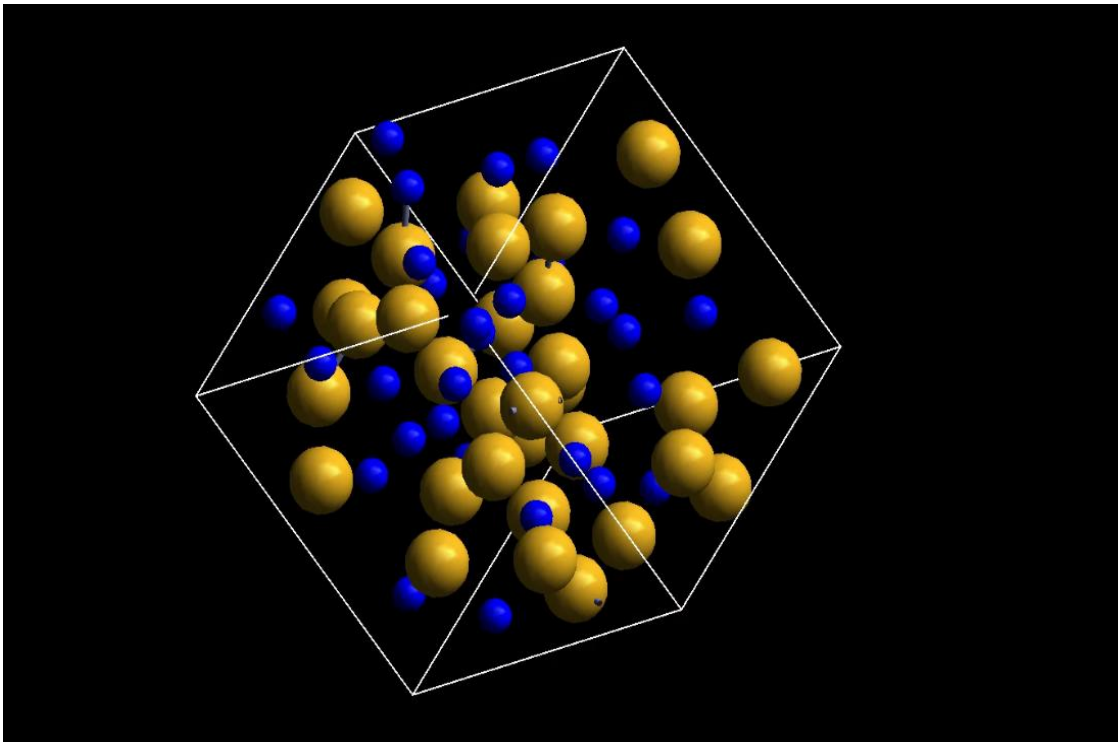


Figure 16 – Snapshot of movement of 64 atoms of Germanium(32 atoms) and Silicon(32 atoms) in the box of dimension 11.3148 Å * 11.3148 Å * 11.3148 Å at temperature 1200K.

4.2 Result and Discussions

In this section we outline the testing method of developed EAM potential of Ge-Si alloy, potential parameters, plotting's and elastic properties.

4.2.1 Testing using testing set

4.2.1.1 Free energy fitted EAM1 and EAM2

To test whether the developed potential performs well or not testing with the data sets which were not used in fitting is one of the methods. As before, for Ge-Si fitting data sets and testing data sets were separated. About 3000 energy data were used for fitting using EAM code and about 4000 data were used as testing set. None of the data in testing set were used in fitting. While fitting the Free energy optimization was done by which best two optimized functions **0.3146** and **0.3149** were chosen and corresponding to these optimized functions were EAM1 and EAM2. For EAM1, the optimization function due to optimization of data points is **0.3146** and by the testing set without optimization the optimization function is **0.3728** where the error was about 13 % which shows that the developed potential performed nicely with the testing set as in fitting sets. Similarly, for EAM2 with the fitting sets the optimization functions is **0.3149** while with the testing set it is **0.3749**.

4.2.1.2 Stress fitted EAM1 and EAM2

For Stress-tensor fitted potential also two different sets of data, fitting set and testing sets were separated. For EAM1, by using fitting set the optimized functions is **0.0268** and with

the testing set it is **0.0328**. Here Stress fitted EAM 1 is in nice agreement with the testing sets. Similarly, for EAM2, the objective functions are **0.0275** and **0.0323** respectively suggesting that stress fitted potential is performing good with testing data set.

4.2.2 Reproduction of Force by the developed potential

4.2.2.1 Free energy fitted EAM1 and EAM2

The aim of this test is to know how well the developed potential by reproduce force. For this the POTPARAS files were taken, which contain the parameters of potential, of both EAM1 and EAM2 separately and ran the EAM fitting without optimizations. And while doing this the data were taken in such a way that those were not used in fitting. By doing so the optimized function on the output were **0.3707** and **0.3802** for EAM1 and EAM2 respectively which are within 18%-20% of the optimized function by fitting free energies as mentioned above in part 'a' of testing by testing sets. From this the developed potential did reproduce the force which is the confirmation that developed potentials are performing as expected.

4.2.2.2 Stress fitted EAM1 and EAM2

In this test the similar steps were followed as above to Force by using Stress fitted EAM1 and EAM2. As above POTPARAS best files were taken along with the data points (in VASPRUN files) which were not used during fitting. Then EAM fitting was run without optimization and the optimized functions were **0.0305** and **0.0306** which is within 12% - 15% range of optimized functions by fitting stress-tensor data and this suggest that stress

fitted EAM1 and EAM2 potentials are reproducing the force and both the potentials are performing good as expected

4.2.3 Cohesive energy test

4.2.3.1 Free energy fitted EAM1 and EAM2 potential

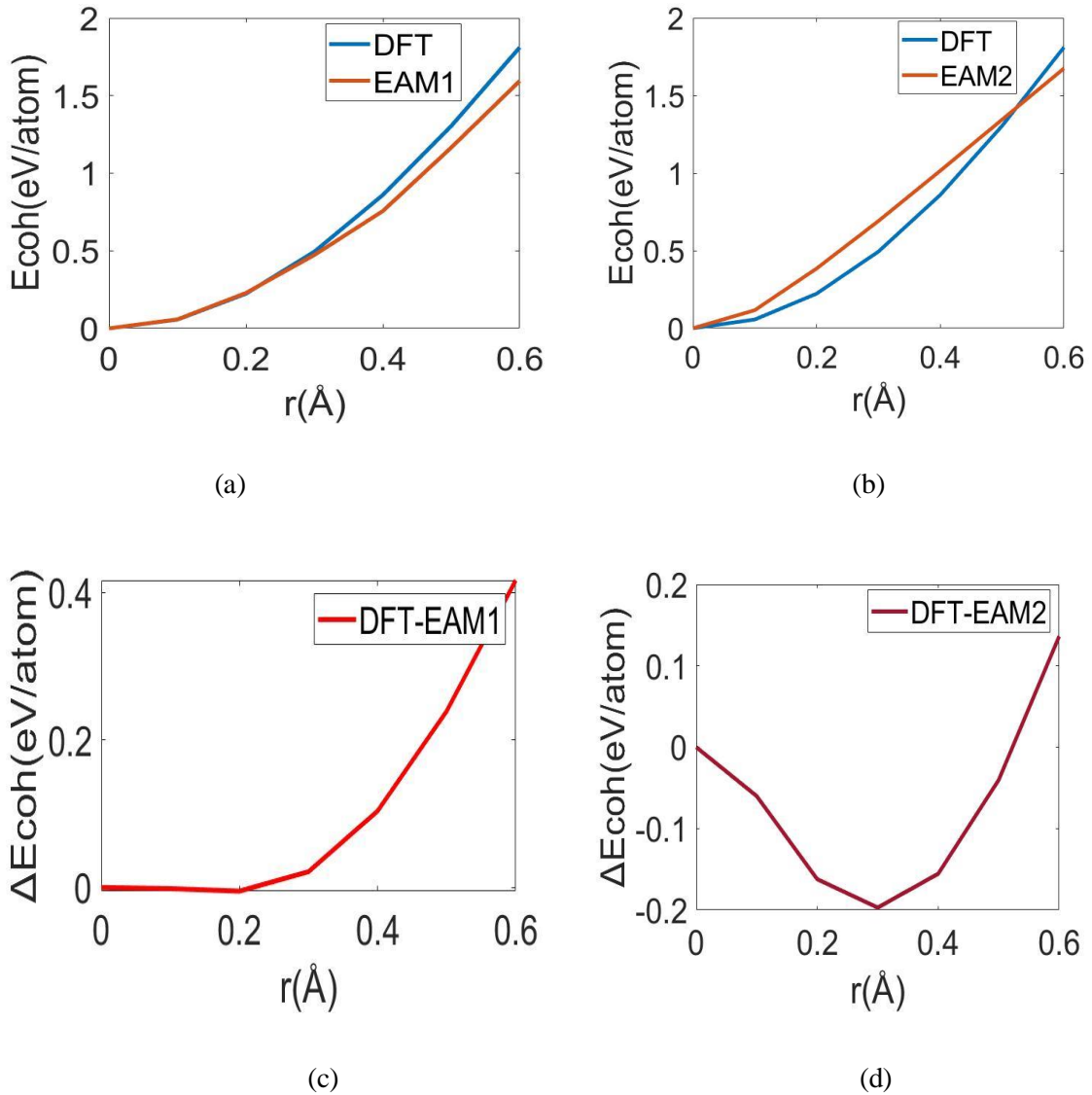


Figure 17 –(a, b):Plot of Change of Cohesive energy vs distance of Si atom from its lattice point for Free energy fitted EAM1, DFT and EAM2,DFT. (c, d) :Plot of difference in change of Cohesive energy in plot a and b with respect to distance in Angstrom.

To calculate the Cohesive energy by EAM1, EAM2 and DFT method, FCC cubic structure of Ge-Si with 4 Ge atoms and 4 Sn atoms was created by quantum ATK. By using the force field calculator and providing the LAMMPS format EAM1 potential, the total energy of the initial configuration was calculated and found to be -31.37832eV. This energy was taken as reference energy because all the atoms were in the lattice points. Now one of the Silicon (Si) atom, whose X-coordinate was 3.53587Å was selected and moved it by 0.1Å away from the lattice point along X-axis. With this configuration the energy of system was calculated as -31.32046eV. Similarly repeating the process for other five times, the energy of the system was found to be -31.15021eV, -30.90533eV, -30.6223eV, -30.31260, -29.98343eV for the positions 3.73587Å, 3.83587Å, 3.93587Å, 4.03587Å, 4.13587Å respectively. All the energy when the position of Silicon was changed were subtracted from the first reference energy and the resultant is called cohesive energy which is plotted along Y-axis against the change in position of Si atom each time by 0.1Å. Similarly, by taking all above seven configurations four input files, INCAR, POSCAR, POTCAR and KPOINTS were created and the static calculations was performed on VASP to calculate Total energy for each of the configurations. The calculated energies were -39.338794eV, -39.282498eV, -39.115648eV, -38.844424eV, -38.479130eV, -38.034137eV, -37.527708eV starting from equilibrium position configuration to the one in which Silicon atom was moved by 0.6Å. Now, by following the same procedure as for EAM1, EAM2 was supplied to quantum ATK by which energies were calculated as -33.33554eV, -33.21909eV, -32.95018eV, -32.64406eV, -32.32028eV, -31.99056eV, -31.66065eV respectively from reference structure to the structure in which the position of Silicon was

changed by 0.7\AA . Plot a and b above are the cohesive energy plots against the distance by which each time Silicon was changed for EAM1, EAM2 and DFT.

4.2.3.2 Stress fitted EAM1 and EAM2

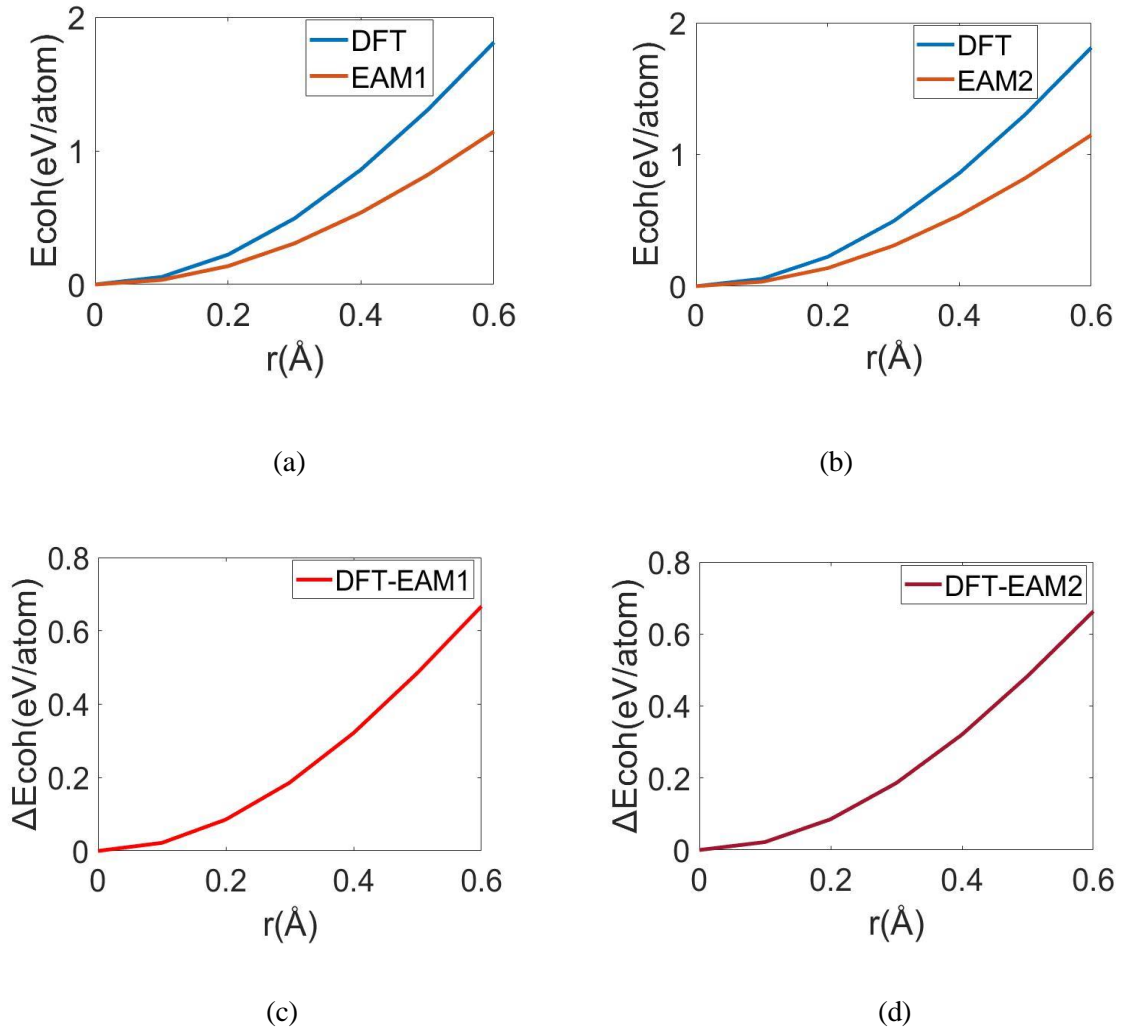


Figure 18 – (a, b):Plot of Change of Cohesive energy vs distance of Si atom from its lattice point for Stress tensor fitted EAM1, DFT and EAM2,DFT. (c, d) :Plot of difference in change of Cohesive energy in plot a and b with respect to distance in Angstrom.

Cohesive energy plots for Changing the position of an Si atom along X-axis on the configuration of 4 Ge and 4 Si atoms by the EAM1 and EAM2 potentials developed by

fitting Stress-tensor data points are shown above in figure 4.2.1.2 and compared with the DFT cohesive energies. For EAM1, the total energy, when all the atoms were in equilibrium state was -17.62837eV which is taken as reference energy here. One of the Si atoms was moved each time by 0.1Å from its equilibrium position along x-axis and in each time the total energy recorded were -17.59415eV, -17.49083eV, -17.32041eV, -17.09055eV, -16.80948eV, -16.48414eV. These energies were then subtracted from the initial reference energies and plotted along Y-axis with respect to changed position by 0.1Å each time along X-axis. Similarly in plot 'b' the reference energy by stress fitted EAM2 potential was -19.22921eV and the energies when the position of Sn was changed by 0.1Å each time were -19.19502eV, -19.09169eV, -18.92097eV, -18.69031eV, -18.40798eV, -18.08118eV. Then the cohesive energy was plotted against the distance in Angstrom.

Plots 'c' and 'd' are the difference in cohesive energies of EAM1 and EAM2 respectively with cohesive energy from DFT.

4.2.4 Free-Energy Fitted EAM Parameters

Table 8 –: Embedding function parameters for free energy fitted EAM1 and EAM2 potentials

	<i>EAM1</i>		<i>EAM2</i>	
	E_{Ge}^{emb}	E_{Si}^{emb}	E_{Ge}^{emb}	E_{Si}^{emb}
$a(ev)$	0.3502	5.1434	$1.0951 \cdot 10^{-2}$	0.9124
$b(ev)$	$4.0859 \cdot 10^{-4}$	$2.8584 \cdot 10^{-3}$	$6.9502 \cdot 10^{-4}$	$1.8704 \cdot 10^{-4}$
$c(ev)$	$2.3309 \cdot 10^{-8}$	$3.3514 \cdot 10^{-8}$	$2.7783 \cdot 10^{-7}$	$1.2194 \cdot 10^{-8}$

Table 9 –: Electron density parameters for free energy fitted EAM1 and EAM2 potentials

	<i>EAM1</i>		<i>EAM2</i>	
	f_{Ge}^0	f_{Si}^0	f_{Ge}^0	f_{Si}^0
$a^1(ev)$	1.9664	3.3862	0.4941	4.8027
$r^1(\text{Å})$	3.1402	1.8321	5.0883	2.9252
$a^2(ev)$	-1.9786	3.4947	-6.4384	11.2847
$r^2(\text{Å})$	3.4075	1.7069	1.71453	3.3028

Table 10 –: Pairwise interaction potential parameters for free energy fitted EAM1 and EAM2 potentials

	<i>EAM1</i>			<i>EAM2</i>		
	ϕ_{Ge-Ge}	ϕ_{Ge-Si}	ϕ_{Si-Si}	ϕ_{Ge-Ge}	ϕ_{Ge-Si}	ϕ_{Si-Si}
$b^1(ev)$	6.4524	7.1055	6.8226	-2.0502	-1.3973	2.9834
$s^1(\text{Å})$	3.1618	2.5352	2.5615	4.0259	2.1130	3.0355
$b^2(ev)$	-4.9505	-3.6714	-2.3509	2.3724	-4.1182	-1.1974
$s^2(\text{Å})$	3.2108	2.2781	5.1034	3.9113	1.6043	1.9479

4.2.5 Stress-Tensor Fitted EAM Parameters

Table 11 –: Embedding function parameters for free energy fitted EAM1 and EAM2 potentials

	<i>EAM1</i>		<i>EAM2</i>	
	E_{Ge}^{emb}	E_{Si}^{emb}	E_{Ge}^{emb}	E_{Si}^{emb}
$a(ev)$	$6.7564 \cdot 10^{-4}$	2.4097	$8.7967 \cdot 10^{-5}$	2.8667
$b(ev)$	$-1.0267 \cdot 10^{-2}$	$1.8496 \cdot 10^{-2}$	$-1.5355 \cdot 10^{-2}$	$-9.272 \cdot 10^{-3}$
$c(ev)$	$3.9837 \cdot 10^{-9}$	$4.6973 \cdot 10^{-9}$	$9.4242 \cdot 10^{-9}$	$3.179 \cdot 10^{-9}$

Table 12 –: Electron density parameters for free energy fitted EAM1 and EAM2 potentials

	<i>EAM1</i>		<i>EAM2</i>	
	f_{Ge}^0	f_{Si}^0	f_{Ge}^0	f_{Si}^0
$a^1(eV)$	0.8090	1.7714	0.2437	0.9531
$r^1(\text{Å})$	3.6893	4.4019	3.9337	4.4031
$a^2(eV)$	-1.5712	-1.4143	-0.8949	-0.6594
$r^2(\text{Å})$	3.3204	4.3868	3.1839	4.3905

Table 13 –: Pairwise interaction potential parameters for free energy fitted EAM1 and EAM2 potentials

	<i>EAM1</i>			<i>EAM2</i>		
	ϕ_{Ge-Ge}	ϕ_{Ge-Si}	ϕ_{Si-Si}	ϕ_{Ge-Ge}	ϕ_{Ge-Si}	ϕ_{Si-Si}
$b^1(eV)$	0.3423	2.9935	$-3.7015 \cdot 10^{-2}$	0.4798	3.1204	0.3126
$s^1(\text{Å})$	4.4624	2.4228	2.2272	4.9997	2.4220	4.3730
$b^2(eV)$	-0.2719	2.8150	0.5858	-0.3776	2.7711	0.2637
$s^2(\text{Å})$	4.3416	2.6601	4.5507	5.1052	2.6628	4.7203

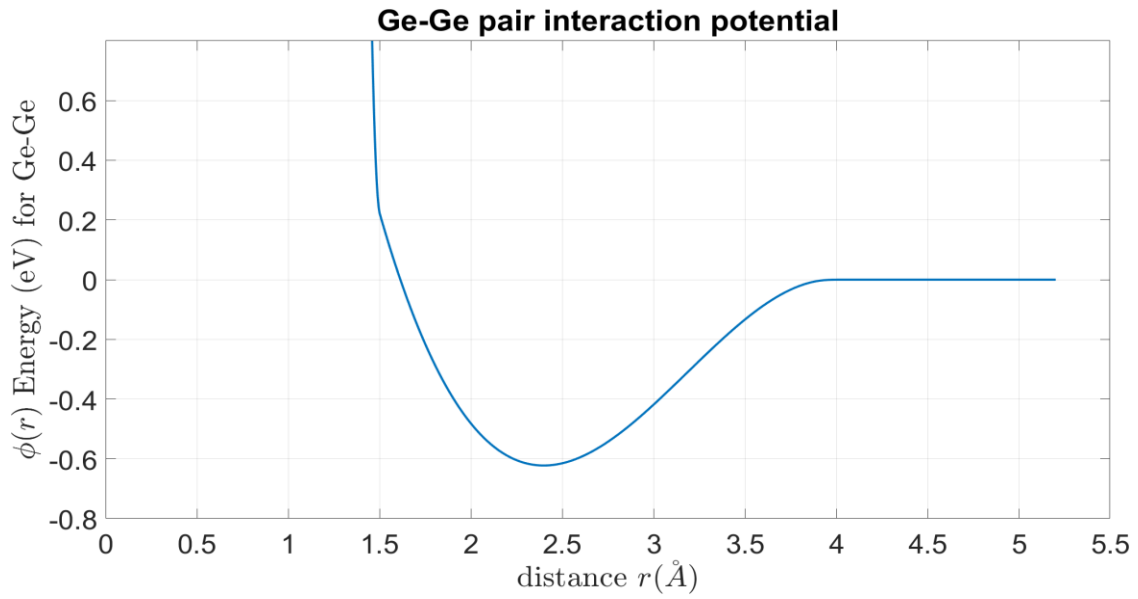


Figure 19 – Plot of Ge-Ge interatomic distance versus pair-interaction energy using Stress Tensor fitted EAM1 potential

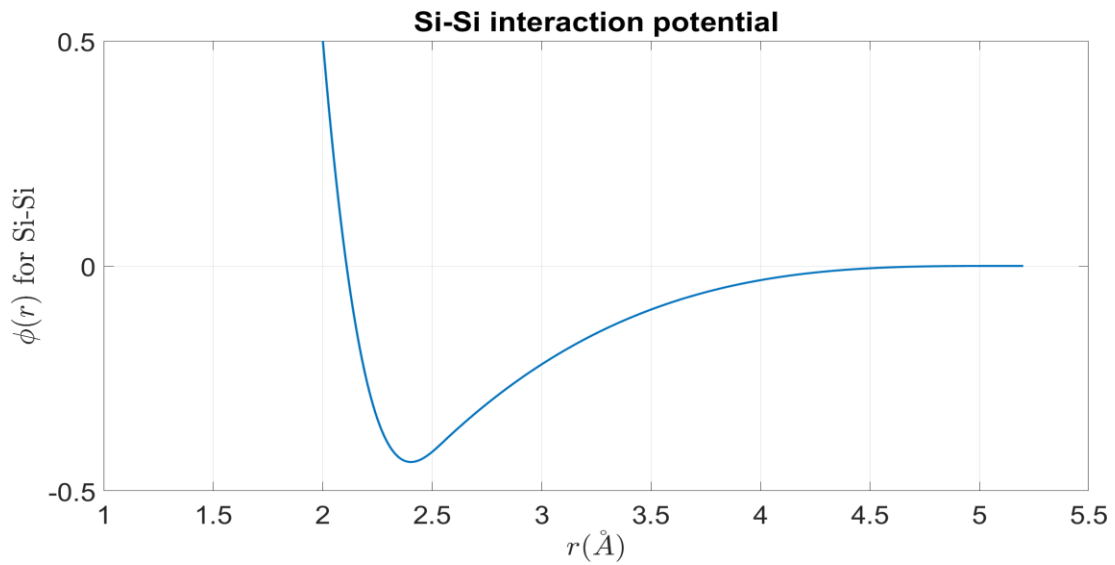


Figure 20 – Plot of Ge-Ge interatomic distance versus pair-interaction energy using Stress Tensor fitted EAM1 potential

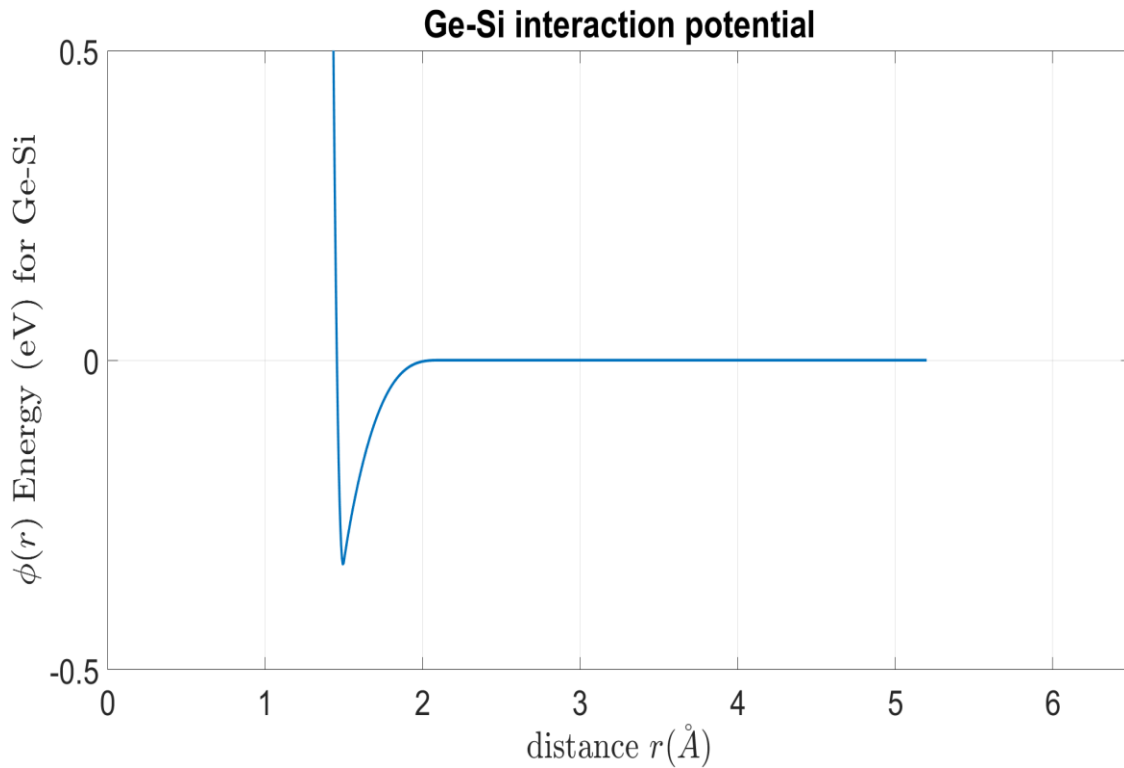


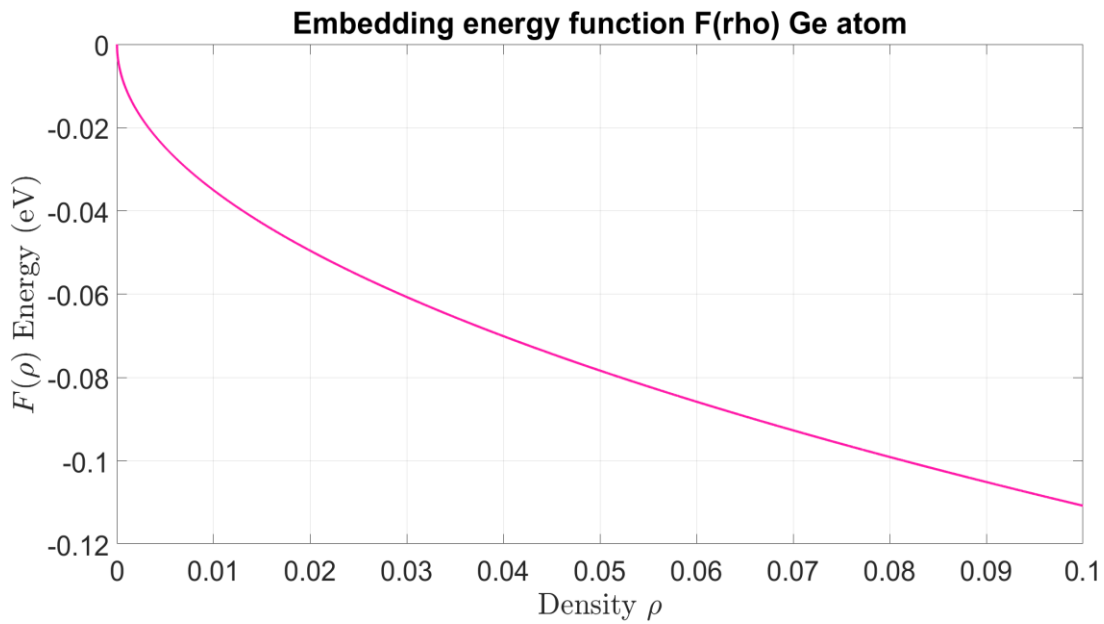
Figure 21 – Plot of Ge-Si interatomic distance versus pair-interaction energy using Stress Tensor fitted EAM1 potential

The plots of di-atomic Interaction potential energy of Ge-Ge, Sn-Sn and Ge-Sn alloy with the atom separations is show above in above three figures respectively. These attractive and repulsive energies determine the potential energy of two atoms. The above plots are the change in Total Potential energies with the change in distance between atoms. Attractive forces correspond to negative potential energy and repulsive force correspond to positive potential energy. For Ge-Ge , if the atoms are separated by very large distance of around 5.3 \AA initially , the attractive force is dominate and if the atoms are moved closer to each other, the total potential energy becomes more negative and the point at which the

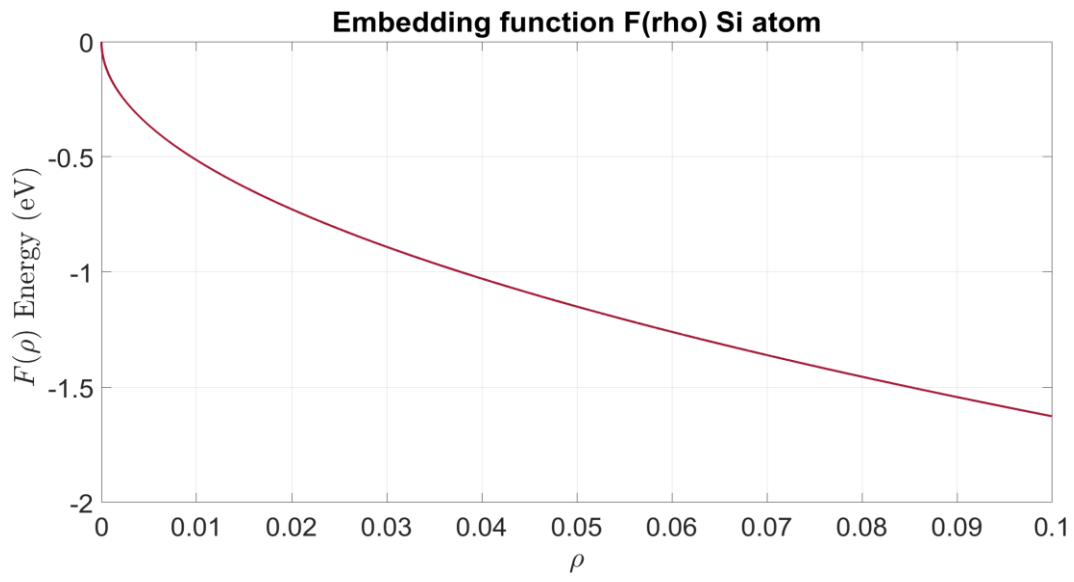
potential is minimum is the equilibrium point which is called r_0 and for Ge-Ge the r_0 is approximately 2.2Å. If they get more closer the PE start becoming more positive as repulsive force begin to become more dominate. Similarly, for two Silicon atoms the equilibrium distance at which the PE between two Silicon atoms become minimum is nearly 2.3Å after which the repulsive force starts getter dominate. The final plot is the Change in interaction potential energy of Germanium and Silicon atoms which shows that the distance between Ge-Si at which the interaction PE is minimum is approximately 1.5Å

From Ge-Ge, Si-Si and Ge-Si pair interaction, the minimum energies are approximately -0.6eV, -0.4eV and -0.3eV respectively.

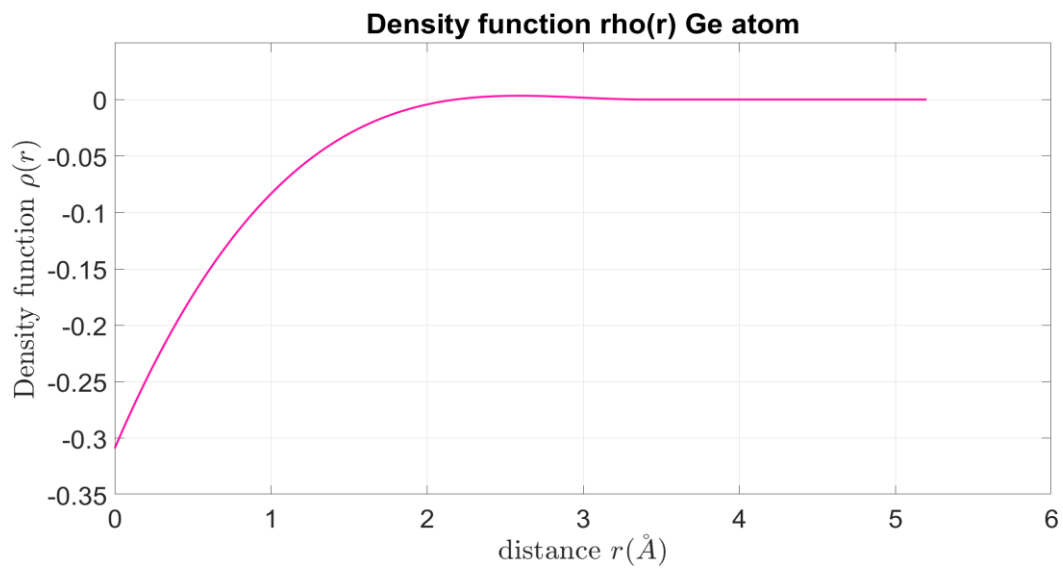
The embedding function and electron density function of mono atoms Germanium and Silicon are shown in figure 22.



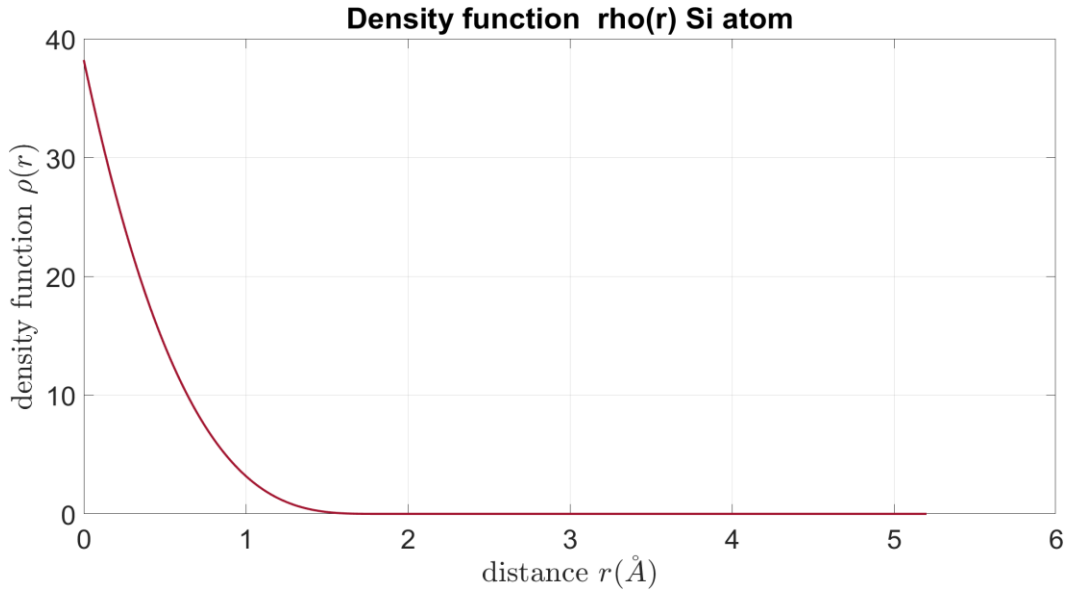
(a)



(b)

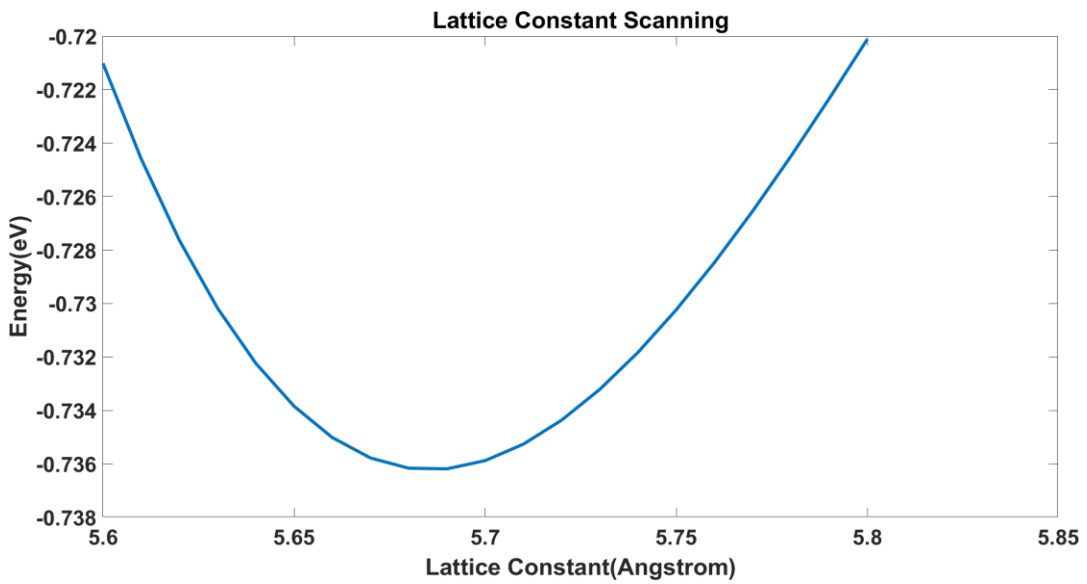


(c)

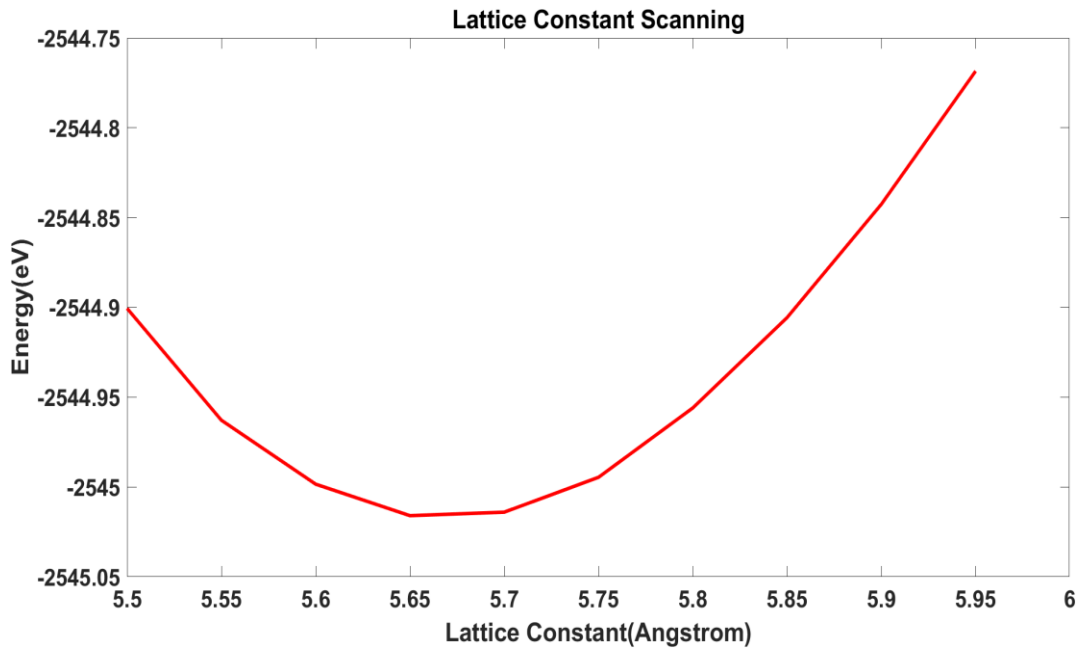


(d)

Figure 22 – (a, b) plot of Embedding energy function of Ge and Si respectively by free energy fitted EAM2. (c, d) plot of Density function versus distance of Ge and Si using free energy fitted EAM2



(a)



(b)

Figure 23 – (a)The variation of Total energy with lattice constant for Ge-Si by free energy fitted EAM1 potential .(b) The Variation of Total energy with lattice constant in for Ge-Si by DFT(LDA).

Plot of scanning the lattice constant of Germanium- Silicon alloy by the developed EAM1 potential and DFT to get the equilibrium lattice constant is shown in figure 22. The procedure here was same as done for Germanium-Tin alloy in which the LAMMPS format EAM1 potential file was provided to quantum atk and by setting the input parameters, lattics constant was calculated which came out to be 5.69Å. Similarly, the lattice constant was also calculated by DFT using LDA correlation and found to be 5.65Å

Table 14 – Calculated Elastic properties of Ge-Si alloy by EAM potentials

	LDA	GGA	EAM1	EAM2	REFERENCE
Lattice constant(a)	5.62	5.58	5.72	5.69	5.46
Bulk modulus(B)	68.18	73.28	75.10	84.88	88.6, 89.4
Youngs modulus	81.9	89.5	24.52	28.17	150
Shear Modulus	41.77	44.87	17.47	15.33	
C ₁₁	110.21	119.36	86.41	97.88	110.21
C ₁₂	47.17	50.24	69.45	78.38	47.17
C ₄₄	53.34	56.03	23.47	24.82	

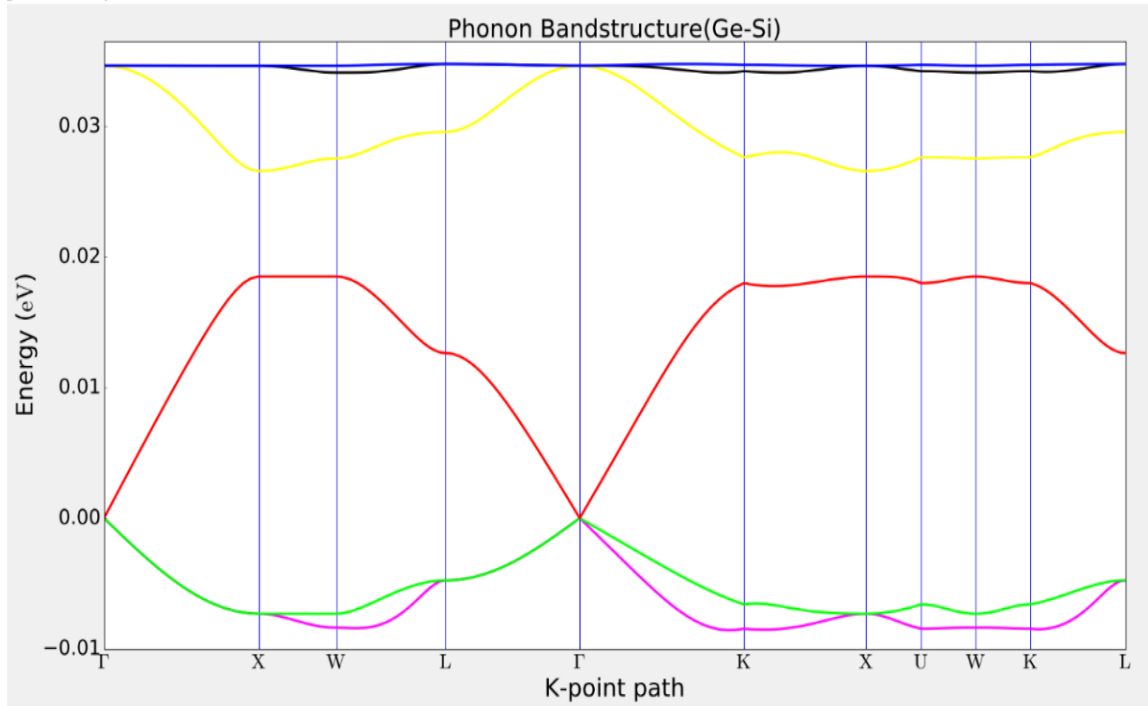


Figure 24 – Plot of phonon Band structure of Ge-Si using Free-energy fitted EAM1

The band structure of Ge-Si by using free energy fitted EAM potential is shown above. The yellow line and the red line in above plots are conduction band and Valence band respectively. The energy difference between the top of valence band and the bottom of Conduction band is called band gap. The bandgap for Ge-Si is found to be approximately 0.01 eV. This plot above shows how the actual electron states are equally spaced in k-space. Which means that the density of states depends on the slope of the E-k curve.

The Density of states plot of Germanium – Silicon alloy is shown in figure 25.

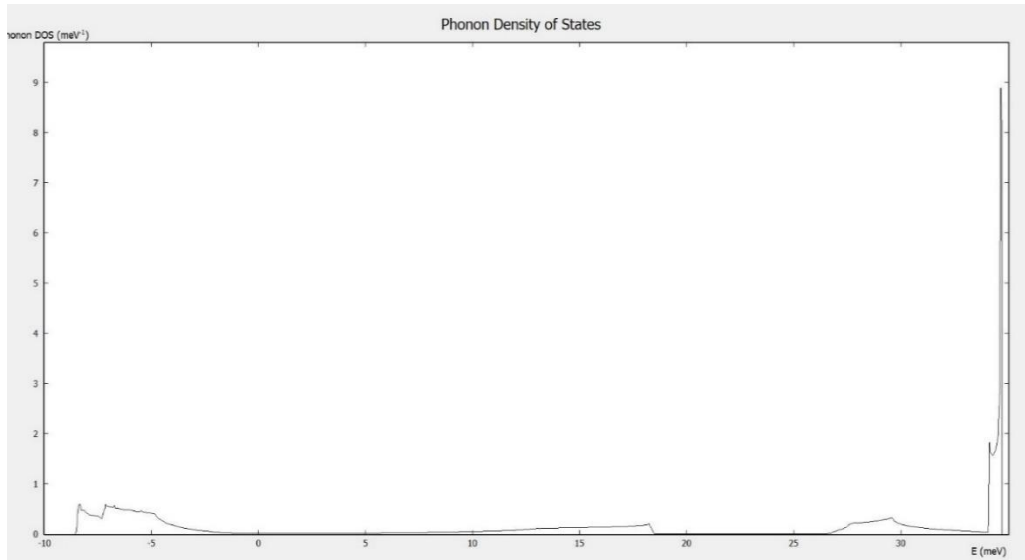


Figure 25 – Plot of Total Phonon density of States of Ge-Si using free energy fitted EAM1

CHAPTER 5. STUDY OF TIN-SILICON

This chapter explains on detail about the simulation method of Silicon-Tin binary alloy system using VASP and fitting of VASP output Free-energy and Stress tensor using EAM fitting code to develop the EAM potential. EAM parameters of developed EAM potentials, both free fitted potential and Stress-tensor fitted potential are presented in this chapter. After developing the potential as before three tests are performed, testing using data sets which were not used in fitting, reproduction of Free energy, Force and Tensor, and change in cohesive energy when a single atom is moved away from its lattice point and its comparison with DFT output. Detail explanation about these testing processes is explained in this chapter. Similarly, after confirming that the potential is working well, interatomic pair interaction with respective to distance, embedding function and Density function of Germanium and Silicon separately are plotted. Similarly, Elastic properties like Bulk modulus, Young's modulus. Shear modulus, elastic constants, equilibrium lattice constants etc. are also calculated both by DFT, using LDA and GGA, and developed EAM potentials and the values are compared. Also. This chapter has the phonon band structure and Phonon density of states plot of Sn-Si by using EAM potential.

5.1 Simulation method

The simulation was performed in a box size 11.3148 Å * 11.3148 Å * 11.3148 Å as in Ge-Sn system above. For the simulation work to start we need INCAR, POSCAR, KPOINTS and POTCAR as input files in VASP. The POSCAR file which contains the lattice geometry and ionic position of was created using Quantum ATK. For this Sn-Si simulation Canonical ensemble (NVT) by setting SMASS tag = 0 and the thermostat that was used is Noose-Hoover thermostat. Also, by adding ISIF = 2 tag in INCAR file, stress tensor was also calculated. Six different simulations were performed at 9500K each generating more than 800 different configurations of energies, Forces and Stress tensor from each simulation which were used in EAM fit to develop potential. In KPOINT file Gamma centered K-point sampling of 8*8*8 was used. Since the K-point convergence test was already done for Ge-Sn and ATK generated k-points were good enough so for Ge-Si testing was not done. For the energy cutoff, the default value was set on INCAR by which the was taken from POTCAR by VASP.

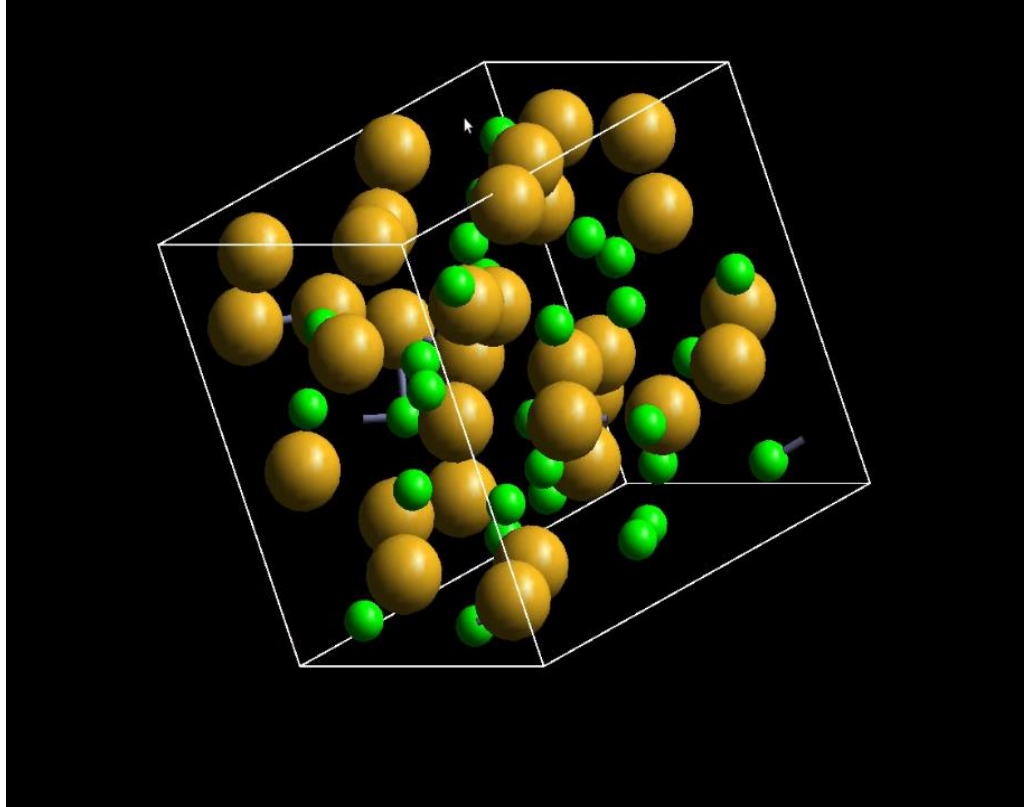


Figure 26 – Snapshot of movement of 64 atoms of Tin(32 atoms) and Silicon(32 atoms) in the box of dimension 11.3148 Å * 11.3148 Å * 11.3148 Å at temperature 1200K.

5.2 Result and discussion

In this section we outline the testing method of developed EAM potential of Sn-Si alloy, potential parameters, plotting and elastic properties.

5.2.1 Testing using testing sets

5.2.1.1 Free energy fitted EAM1 and EAM2

Testing the developed potential using the completely different data sets other than those which were used in fitting is one of the ways to confirm that developed potential is performing well. Here, the aim was to see how well the developed potential reproduce the Energy with the testing sets of data. By taking 6000 data points the free energy fitting was done and the data points used for testing the potentials were 3500. During the Free energy fitting, optimization was done and the best two optimized functions **0.1995** and 0.1996 were chosen and EAM1 and EAM2 were the corresponding potentials. For EAM1, the optimization function due to optimization of data points was 0.1995 and by the testing set without optimization the optimization function was 0.2379 where the error was about 19 % which shows that the developed potential performed nicely with the testing set as in fitting sets. Similarly, for EAM2 with the fitting sets the optimization functions is 0.1996 while with the testing set it is 0.2379 with an error of 19% again.

5.2.1.2 Stress fitted EAM1 and EAM2

For Stress-tensor fitted potential two different sets of data, fitting set and testing sets were separated as before. For EAM1, the optimization function due to optimization of data points was 0.02329 and with the testing set it was 0.02699. Here Stress fitted EAM 1 is in nice agreement with the testing sets because the percent error between these two values is approximately 16%. Similarly, for EAM2, the optimization functions were 0.02359 and 0.02707 respectively with the percent error of 15% suggesting that stress fitted potential is performing good with testing data set.

5.2.2 Reproduction of Force by the developed potential

5.2.2.1 Free energy fitted EAM1 and EAM2

After testing the EAM potentials with the testing sets, the second way to test the developed potential was to see whether the EAM1 and EAM2 potentials can reproduce the force or not. For this the same testing data sets were taken and the weighting factor in EAM fitting was changes in such a way that Force was calculated. Then the EAM fitting was run without optimization by which the optimized function came out to be 0.2264, which is within 15% of optimization function,0.1996, which was by fitting the data as talked earlier. This shows that Free energy fitted EAM1 potential did reproduced the force and is performing well. Similarly, For EAM2, the optimization function for reproduction of force without optimization was 0.2262 and as discussed before the optimization function by fitting data was 0.1995.

5.2.2.2 Stress fitted EAM1 and EAM2

By following the similar procedures as in b(i) , the force was calculated here by stress fitted EAM1 and EAM2 potentials. As before the weighting factor was changed from 0 to 1 to calculate the Force in EAM fitting. The data sets used were the testing set to make sure that none of the data which were used while fitting be used to reproduce the force. Then EAM fitting was run without optimization and the optimized functions for EAM1 and EAM2 were **0.0192** and **0.0198** which are within 12% - 15% range of optimized functions by fitting stress-tensor data and this suggest that stress fitted EAM1 and EAM2 potentials are reproducing the force and both the potentials are preforming good as expected

5.2.3 Cohesive energy test

5.2.3.1 Free energy fitted EAM1 and EAM2 potential

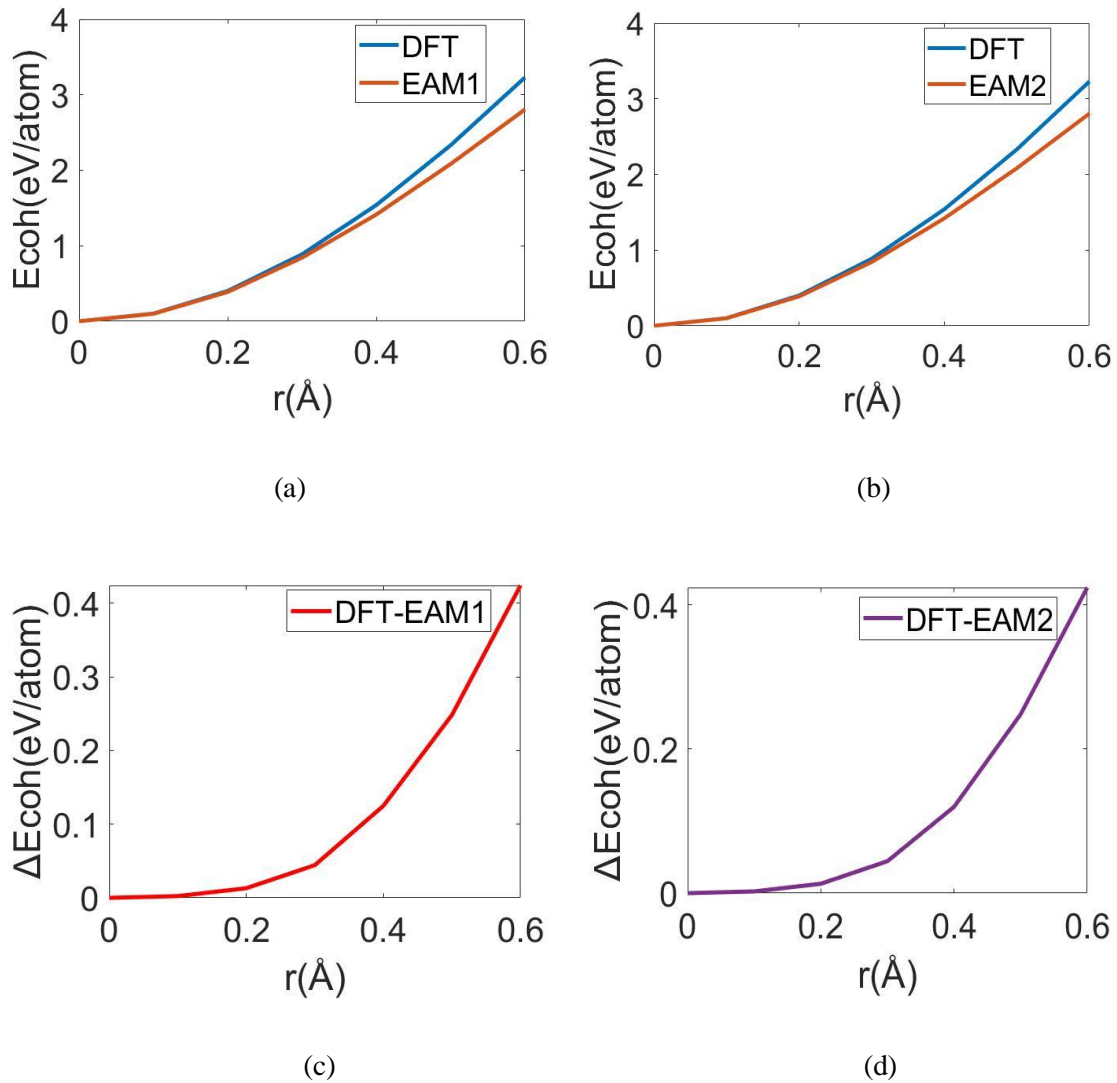


Figure 27 – (a, b):Plot of Change of Cohesive energy vs distance of Si atom from its lattice point for Free energy fitted EAM1, DFT and EAM2,DFT. (c, d) :Plot of difference in change of Cohesive energy in plot a and b with respective to distance in Angstrom

Here an FCC cubic structure of Silicon-Tin with 4 Silicon and 4 Tin atoms was created by quantum ATK as in Ge-Sn and Ge-Si study. The LAMMPS format EAM1 and EAM2

potentials were supplied in force field Calculator to calculate the Total energy of the given configuration when the atoms are at initial state and when one of the atoms was moved away by some distance from its initial equilibrium position. The total energy of the Si-Sn configuration by EAM1 potential when all atoms were at equilibrium was found to be -30.54899eV. Then one of the Si atoms, with initial Y-coordinate 2.03648Å, was moved by a distance of 0.1Å along Y-axis and the total energy of the configuration was calculated as -30.45018eV. Now taking the initial energy as reference, the energy of the configuration was calculated up to when the position of Silicon atom became 2.80537Å and the energies were -30.16131eV, -29.70678eV, -29.12968eV, -28.46582eV, -27.74362eV at positions 2.23648Å, 2.33648Å, 2.43648Å, 2.53648Å, 2.63648Å of Silicon atom respectively. Similarly by EAM2 potential, the energy of Si-Sn configuration was calculated to be -30.41894eV, -30.32013eV, -30.03122eV, -29.57659eV, -28.99939eV, -28.33553eV, -27.61338eV for the Y-coordinates 2.03648Å, 2.13648Å, 2.23648Å, 2.33648Å, 2.43648Å, 2.53648Å, 2.63648Å of a Silicon atom respectively. After calculating total energy by EAM1 and EAM2, the DFT calculation was performed on VASP by using the different POSCAR files for changed Y-coordinate of Silicon Atom. The energies calculated by DFT were -29.607210eV, -29.506011eV, -29.206451eV, -28.720509eV, -28.067887eV, -27.275631eV, -26.377664eV where the first energy was taken as reference. Now the reference energy for each EAM1, EAM2 and DFT were subtracted from the other energies when the positions of Silicon atoms were changed, and this energy is called Cohesive energy. The above plots (a, b) are the cohesive energy by EAM1, EAM2 and DFT against the interval by which the position of a single silicon atom was changed.

5.2.3.2 Stress fitted EAM1 and EAM2 potential

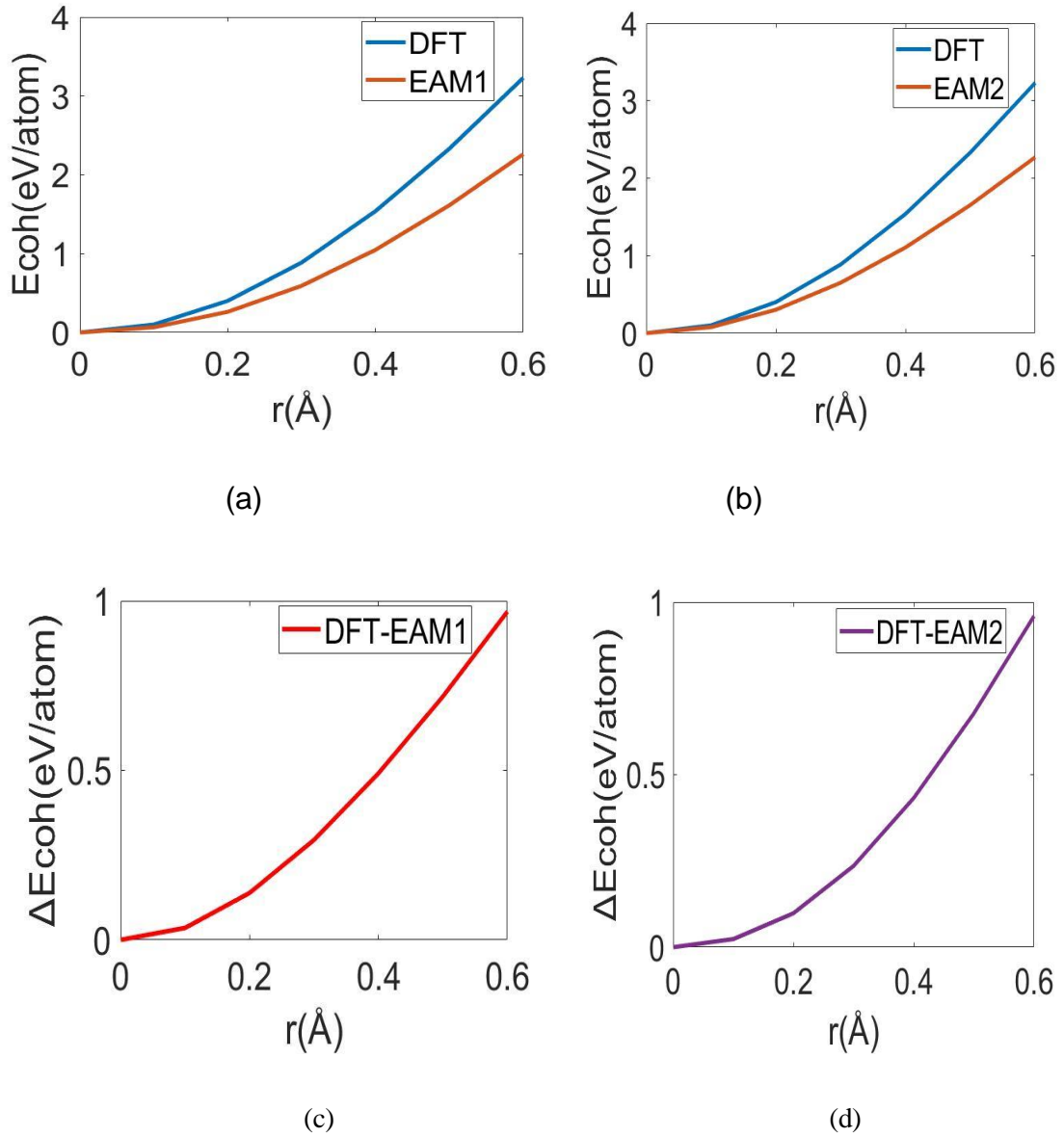


Figure 28 – **(a, b)**:Plot of Change of Cohesive energy vs distance of Si atom from its lattice point for Stress tensor fitted EAM1, DFT and EAM2,DFT. **(c, d)** :Plot of difference in change of Cohesive energy in plot a and b with respective to distance in Angstrom.

The plots 5.2.1.2 above are the cohesive energy plots of Si-Sn configuration by stress fitted EAM1 and EAM2 potentials and their comparison with DFT cohesive energies. By EAM1 the total energies were calculated to be 1.65631eV, 1.72214eV, 1.91854eV, 2.24808eV, 2.70427eV, 3.26988eV, 3.91775eV when the Y-coordinate of one of the Silicon atoms was changed from 2.03648Å to 2.63648Å, each time by 0.1Å. Similarly by EAM2 the total energies calculated were -0.54028eV, -0.46266eV, -0.23811eV, +0.11078eV, +0.56653eV, +1.11369eV, +1.72961eV. The DFT energies were the same as before that was done above.

After finding total energies, each of these energies were subtracted from the first reference energy which is called cohesive energy. The plots (a) and (b) are the Cohesive energies by EAM1, EAM2 and DFT along the Y-axis and in the X-axis are the interval by which a selected Silicon atom was changed each time by 0.1Å.

Plots 5.2.1.2 c and d are the plots of change in cohesive energies of DFT-EAM1 and DFT-EAM2 respectively along Y-axis whereas the X-axis is again the interval by which the position of Silicon atom was changed starting from the initial equilibrium structure.

In comparing the plots 'c' and 'd' of Free-energy fitted and Stress fitted EAM potentials' change in cohesive energy the Stress fitted EAM potential's Cohesive energy deviate more away from DFT Cohesive energy than the Free-energy Fitted EAM potentials. So, it can be said that Free energy fitted EAM potential are performing comparable performance as that of DFT.

5.2.4 Free-Energy Fitted EAM Parameters

Table 15 –: Embedding function parameters for free energy fitted EAM1 and EAM2 potentials

	<i>EAM1</i>		<i>EAM2</i>	
	E_{Si}^{emb}	E_{Sn}^{emb}	E_{Si}^{emb}	E_{Sn}^{emb}
$a(ev)$	$1.6284 \cdot 10^{-6}$	3.6598	$1.6322 \cdot 10^{-6}$	2.9384
$b(ev)$	$3.0362 \cdot 10^{-4}$	$-1.5234 \cdot 10^{-3}$	$1.2803 \cdot 10^{-4}$	$-6.3884 \cdot 10^{-7}$
$c(ev)$	$-8.3668 \cdot 10^{-7}$	$3.5530 \cdot 10^{-6}$	$-2.2904 \cdot 10^{-7}$	$9.6656 \cdot 10^{-7}$

Table 16 –: Electron density parameters for free energy fitted EAM1 and EAM2 potentials

	<i>EAM1</i>		<i>EAM2</i>	
	f_{Si}^0	f_{Sn}^0	f_{Si}^0	f_{Sn}^0
$a^1(ev)$	1.6264	12.6522	2.4971	19.402
$r^1(\text{\AA})$	4.28901	3.7783	4.2906	3.7789
$a^2(ev)$	426.1971	0.7751	680.45	1.2152
$r^2(\text{\AA})$	1.9937	4.4430	1.9958	4.4409

Table 17 –: Pairwise interaction potential parameters for free energy fitted EAM1 and EAM2 potentials

	<i>EAM1</i>			<i>EAM2</i>		
	ϕ_{Si-Si}	ϕ_{Si-Sn}	ϕ_{Sn-Sn}	ϕ_{Si-Si}	ϕ_{Si-Sn}	ϕ_{Sn-Sn}
$b^1(ev)$	-0.4957	11.919	7.0499	-0.4951	11.9046	6.9968
$s^1(\text{\AA})$	3.4348	2.5587	3.4390	3.4348	2.5589	3.4368
$b^2(ev)$	6.1675	0.4230	5.6740	6.1655	0.4191	5.6598
$s^2(\text{\AA})$	2.6138	4.4589	4.0273	2.6138	4.4615	4.0283

5.2.5 Stress-Tensor fitted EAM parameters

Table 18 –: Embedding function parameters for free energy fitted EAM1 and EAM2 potentials

	<i>EAM1</i>		<i>EAM2</i>	
	E_{Si}^{emb}	E_{Sn}^{emb}	E_{Si}^{emb}	E_{Sn}^{emb}
$a(ev)$	0.7584	$9.753 \cdot 10^{-5}$	0.6815	$3.666 \cdot 10^{-5}$
$b(ev)$	$1.2820 \cdot 10^{-3}$	$6.294 \cdot 10^{-3}$	$7.851 \cdot 10^{-5}$	$1.232 \cdot 10^{-3}$
$c(ev)$	$5.4079 \cdot 10^{-9}$	$7.779 \cdot 10^{-8}$	$2.0477 \cdot 10^{-9}$	$5.504 \cdot 10^{-7}$

Table 19 –: Electron density parameters for free energy fitted EAM1 and EAM2 potentials

	<i>EAM1</i>		<i>EAM2</i>	
	f_{Si}^0	f_{Sn}^0	f_{Si}^0	f_{Sn}^0
$a^1(eV)$	47.620	2.5638	47.6200	1.9783
$r^1(\text{\AA})$	1.5999	1.6507	1.6009	3.9539
$a^2(eV)$	0.5402	1.0188	1.1942	1.8749
$r^2(\text{\AA})$	4.2631	3.8919	4.3005	2.0190

Table 20 –: Pairwise interaction potential parameters for free energy fitted EAM1 and EAM2 potentials

	<i>EAM1</i>			<i>EAM2</i>		
	ϕ_{Si-Si}	ϕ_{Si-Sn}	ϕ_{Sn-Sn}	ϕ_{Si-Si}	ϕ_{Si-Sn}	ϕ_{Sn-Sn}
$b^1(eV)$	10.253	11.290	6.7487	10.3913	9.4623	6.2400
$s^1(\text{\AA})$	2.4092	2.4002	2.8099	2.4001	2.4925	2.8409
$b^2(eV)$	0.1353	2.6888	-5.5774	0.2059	1.4312	-5.5774
$s^2(\text{\AA})$	3.8516	2.8864	1.6665	3.9826	3.0642	1.6665

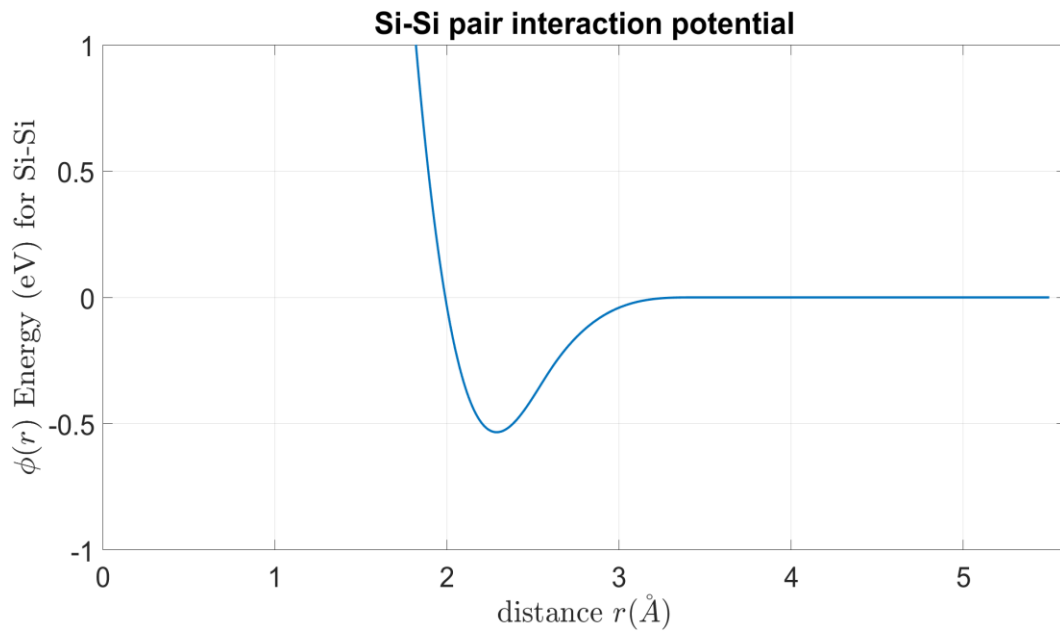


Figure 29 – Plot of Si-Si interatomic distance versus pair-interaction energy by Free energy fitted EAM2 potential.

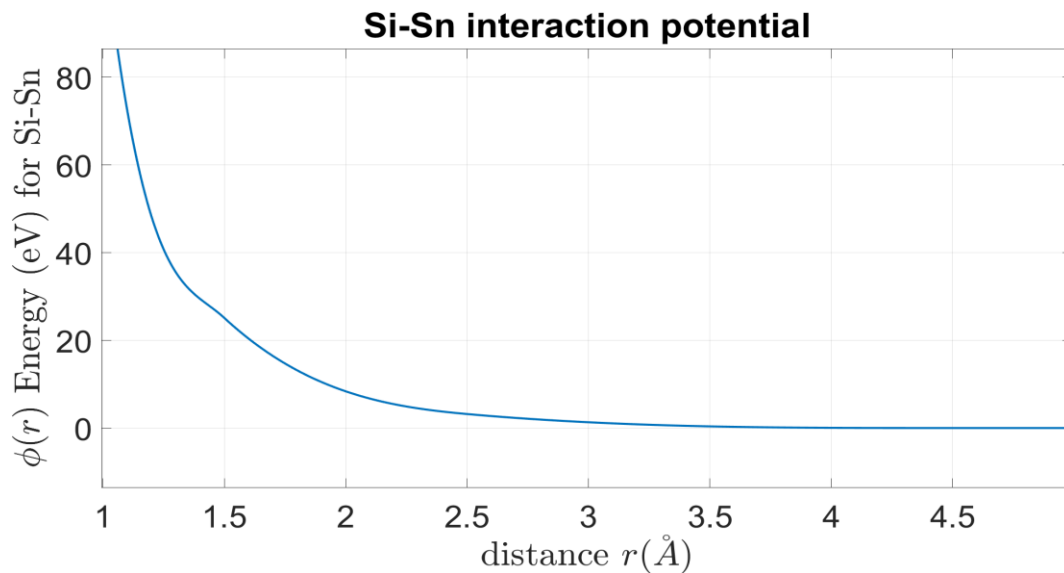


Figure 30 – Plot of Si-Sn interatomic distance versus pair-interaction energy by Free energy fitted EAM1 potential.

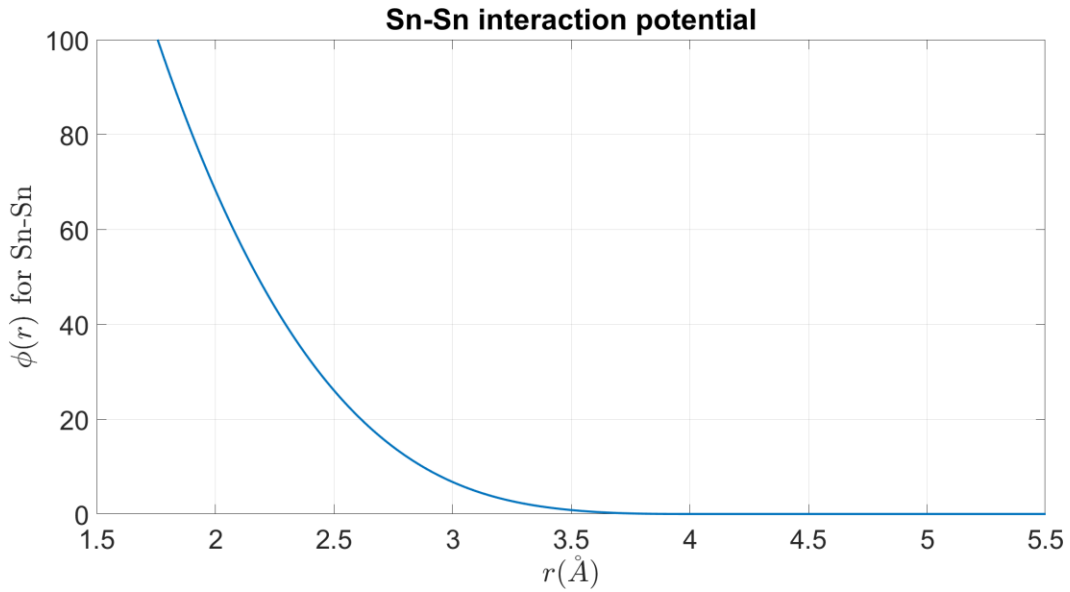
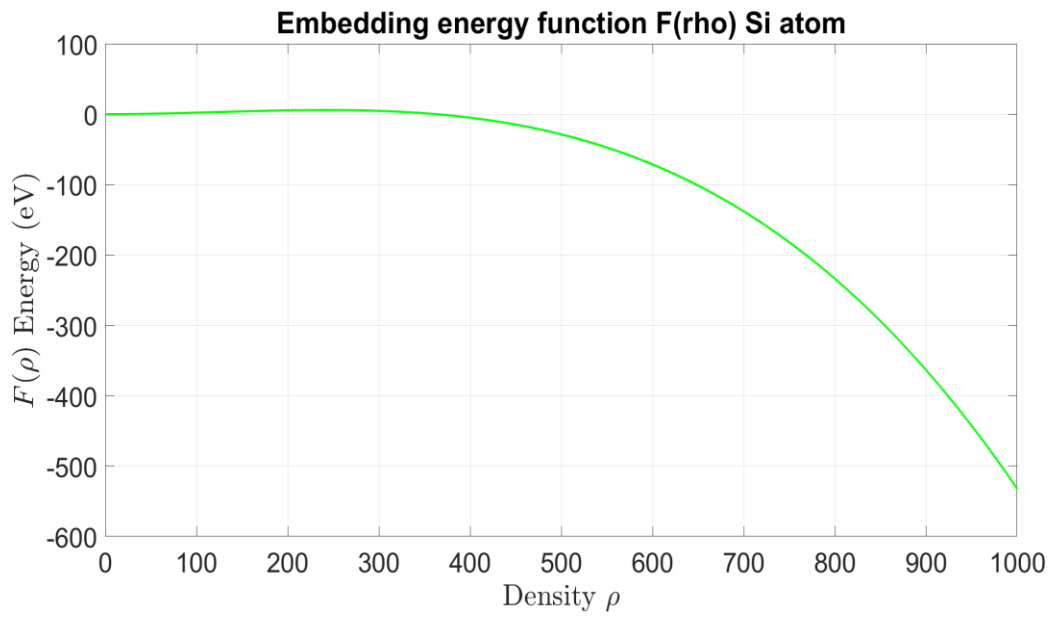
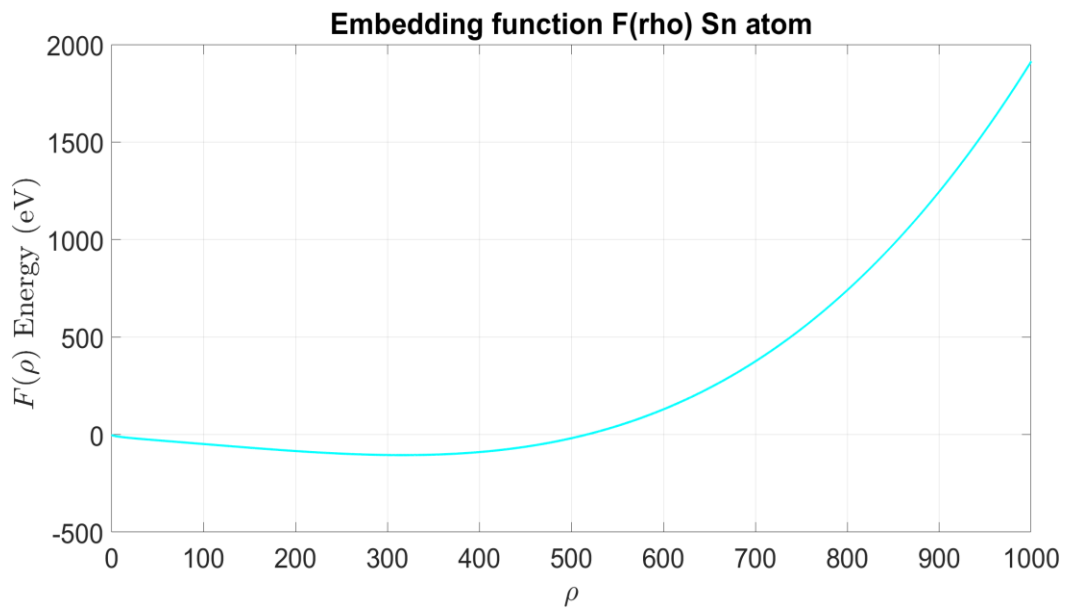


Figure 31 – Plot of Sn-Sn interatomic distance versus pair-interaction energy by Free energy fitted EAM1 potential

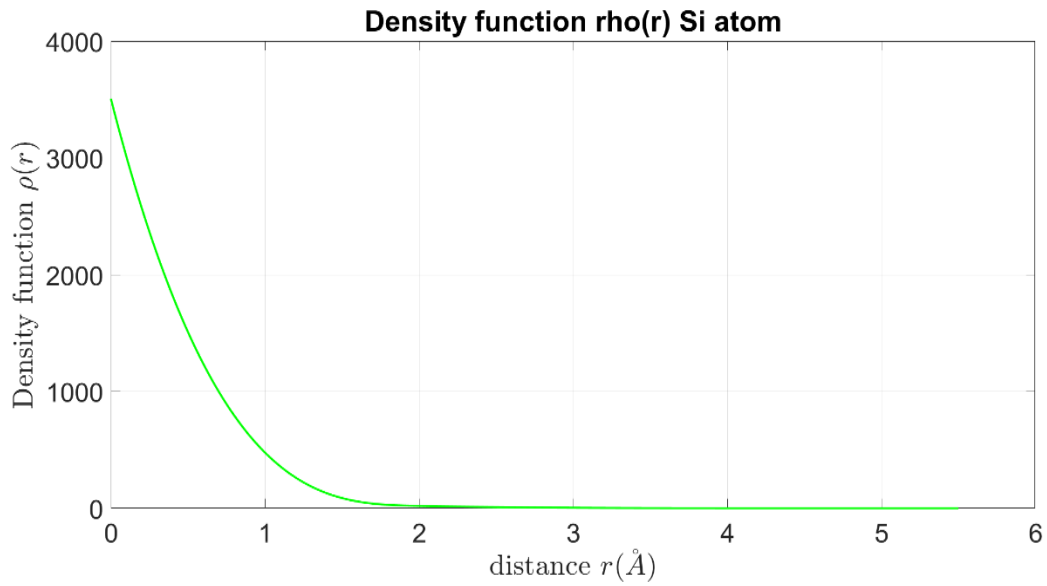
The above three plots are the interatomic potential energy of Si-Si, Si-Sn, Sn-Sn pairs with respect to their interatomic distance. For Si-Si pair the attractive potential energy has been observed in attractive interaction of the atoms but for Si-Sn and Sn-Sn no attractive potential energy has been observed. The reason why we did not see the attractive interaction is that sometime the attractive interaction is captured in embedding function but not in Pair-wise function. Si in this case we can expect that the attractive interaction is captured in embedding function while in all other the pair-wise term captured the attractive interaction. There are many combinations of embedding function and pair-potential that give the same result. The embedding function and electron density function of mono atoms Silicon and Tin are shown in figure 32.



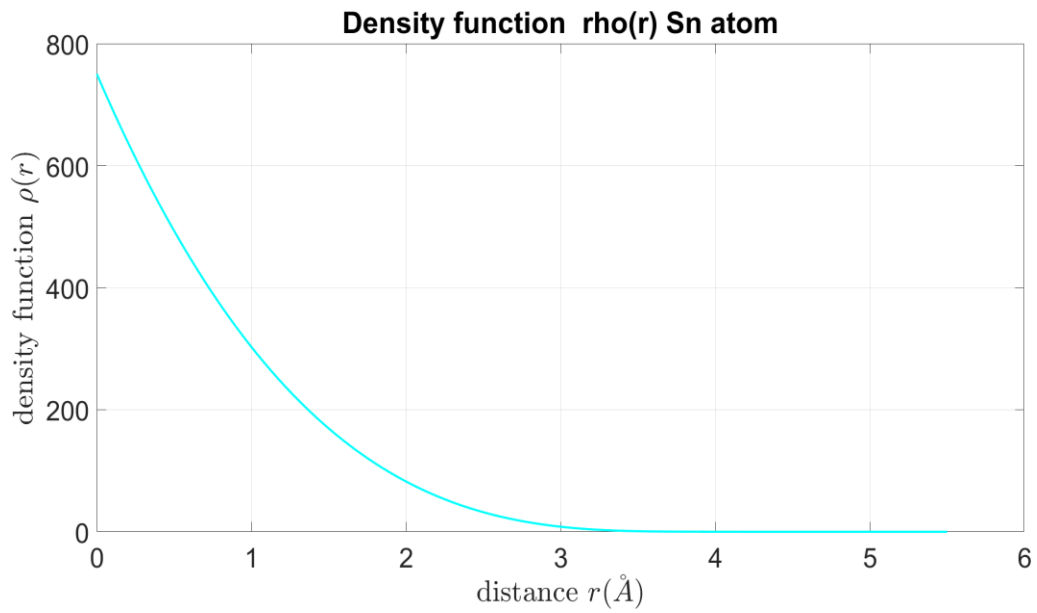
(a)



(b)

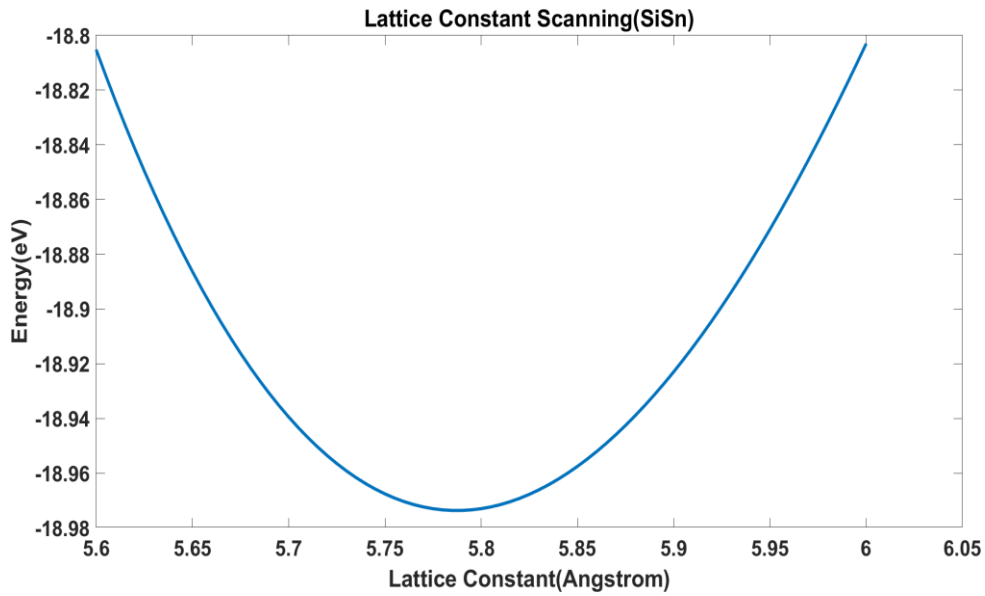


(c)

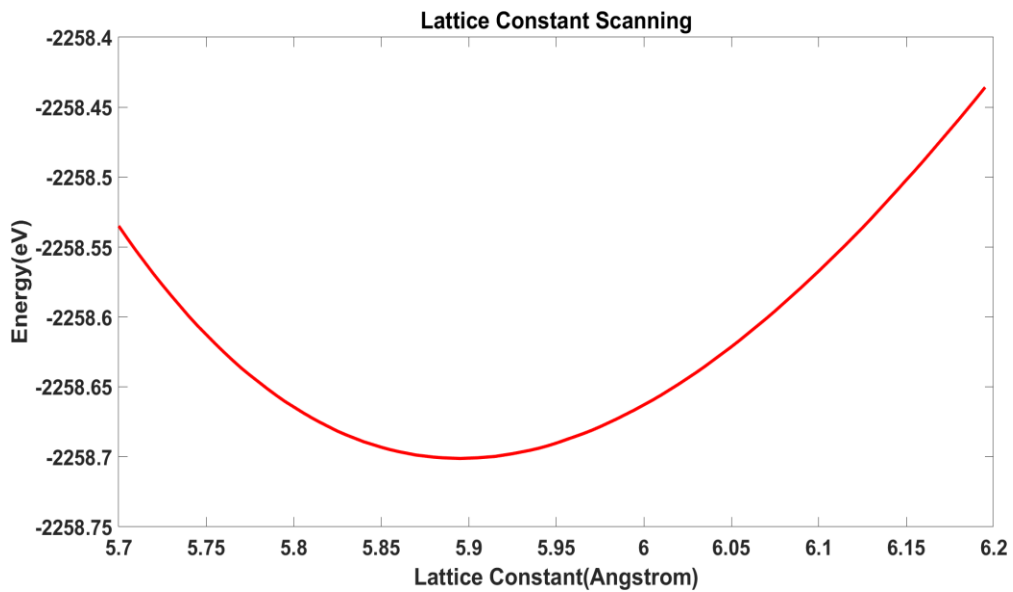


(d)

Figure 32 – (a, b) plot of Embedding energy function of Si and Sn respectively by free energy fitted EAM1. (c, d) plot of Density function versus distance of Si and Sn using free energy fitted EAM1.



(a)



(b)

Figure 33 –(a)The variation of Total energy with lattice constant for Ge-Si by free energy fitted EAM1 potential . (b) The Variation of Total energy with lattice constant in for Ge-Si by DFT(LDA).

The lattice constant scanning was done by both methods, using DFT and developed EAM potential. The similar procedure as before was followed here. The LAMMPS format potential was provided to quantum ATK and by writing the code on ATK, the equilibrium lattice constant was calculated. By DFT the lattice constant was found to be 5.86 and by EAM potential it was found to be 5.76. The energy corresponding to the equilibrium lattice constants were -18.97eV and -2258.73eV for EAM potential and DFT respectively.

Table 21 – Calculated Elastic properties of Si-Sn alloy by EAM potentials

	LDA	GGA	EAM1	EAM2
Lattice constant(a)	5.91	5.88	5.87	5.90
Bulk modulus(B)	198.25	172.06	269.75	269.84
Young's modulus	110.57	99.87	194.25	194.27
Shear Modulus	37.59	29.7	85.63	85.64
Poisson ratio	0.4070	0.4033	0.3800	0.3800
C ₁₁	250.63	219.50	363.60	363.69
C ₁₂	172.05	148.33	222.83	222.92
C ₄₄	36.53	26.75	100.07	100.10

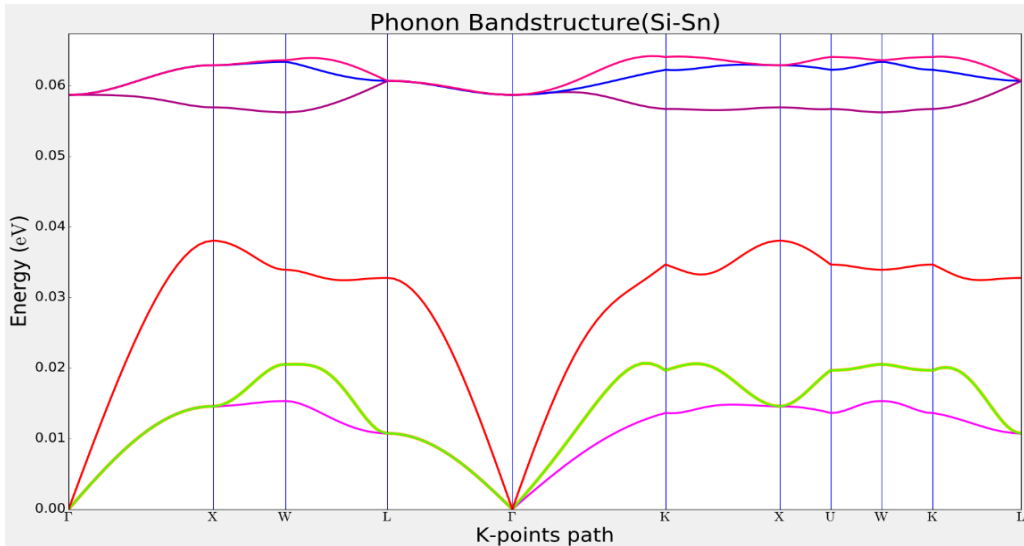


Figure 34 – Plot of phonon Band structure of Si-Sn using Free-energy fitted EAM1

The Band structure of Si-Sn binary system by free energy fitted EAM potential is shown above. The red line is the valence band whereas the lowest upper band (purple color) is the conduction band. The band gap for Ge-Si as shown above is nearly 0.02 eV.

The phonon density of States of Si-Sn alloy is shown in figure 35

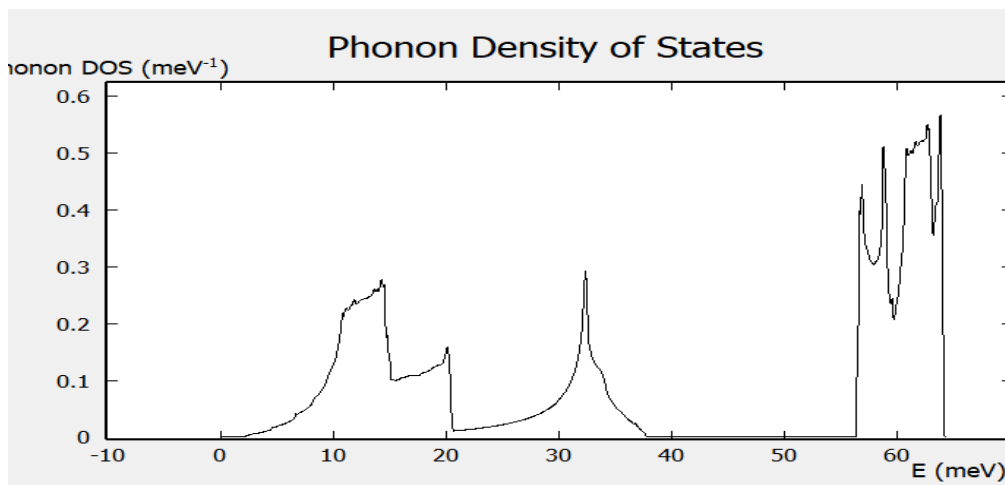


Figure 35 – Plot of Total Phonon density of States of Si-Sn using Free energy -fitted EAM1

CHAPTER 6. STUDY OF GERMANIUM-TIN SILICON

After developing the potential of Ge-Sn, Ge-Si and Si-Sn binary alloys, this chapter now provides a detail work on Ge-Sn-Si ternary system. As before, here the simulation method of Ge-Sn-Si ternary alloy using VASP and fitting the VASP generated Free-energy and stress tensor data using EAM fitting code to develop the EAM potentials will be discussed in detail.

This chapter is completely focused on detail about the simulation method of Silicon-Tin binary alloy system using VASP and fitting of VASP output Free-energy and Stress tensor using EAM fitting code to develop the EAM potential. This chapter has detail output EAM parameters of developed EAM potentials, both free fitted potential and Stress-tensor fitted potential. After developing the potential lie before three tests are performed, testing using data sets which were not used in fitting, reproduction of Free energy, Force and Tensor, and change in cohesive energy when a single atom id moved away from its lattice point and its comparison with DFT output. Detail explanation about the testing process is explained in this chapter. Similarly, after confirming that the potential is working well, it is tried to plot interatomic pair interaction with respective to distance compared.

6.1 Simulation method

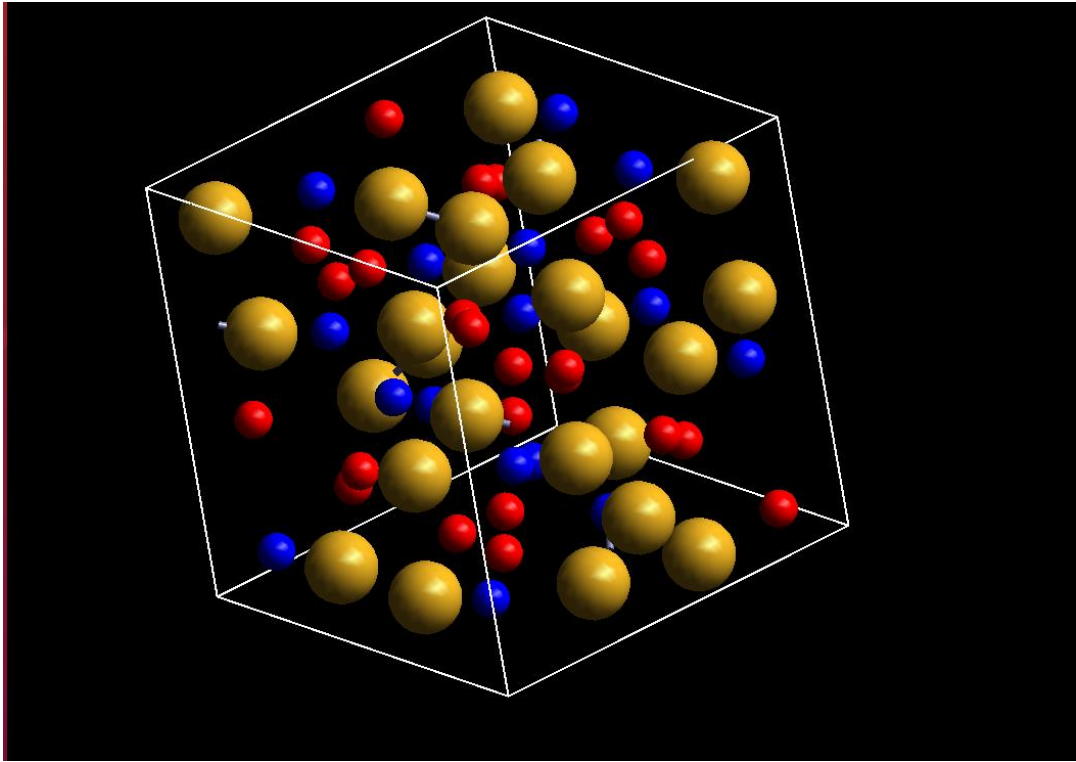


Figure 36 – Snapshot of movement of 64 atoms of Germanium, Silicon, and Tin in the box of dimension 11.3148 Å * 11.3148 Å * 11.3148 Å at temperature 1200K.

For MD DFT simulation of ternary Ge-Sn-Si, a crystalline configuration of 64 atoms in which 24 atoms are Silicon, 24 are Tin, and 16 are Germanium atoms was created in quantum ATK. This created configuration along with all other input files were taken to VASP and MD simulation was run. The simulation was run at temperatures in the range 800K-1200K. During simulation due to the high temperature the crystalline structure changes to Amorphous in each 3-4 iteration of MD the output were Energy, Force and Stress-tensors. These energies and Stress-tensor data were then fitted to Embedded atom method potential equations to obtain potential parameters.

6.2 Result and Discussion

In this section we outline the testing method of developed EAM potential of Ge-Sn-Si ternary alloy, potential parameters, plotting and elastic properties.

6.2.1 Testing using testing sets

6.2.1.1 Free energy fitted EAM1 and EAM2

One of the methods used in this work to test whether the developed potential performs well or not is to test the potential by using the testing sets of data and reproduce the Energy. For this, the testing set which were not used in fitting were taken and EAM fit was run without optimization. The optimization function obtained by optimized fitting of data for EAM1 and EAM2 potentials were 0.2316 and 0.2448 respectively. The optimization function obtained without optimization of data sets were 0.2868 and 0.2964 respectively. Here it can be seen that there is error of approximately 30% in the energy produced by fitting sets of data and testing set of data (using potential) which shows that EAM1 and EAM2 potentials are performing good.

6.2.1.2 Stress fitted EAM1 and EAM2

For Stress fitted EAM1 and EAM2 potentials, the optimization functions were obtained as 0.1155 and 0.1338 respectively. Then by the testing sets the optimized functions were calculated to be 0.1627 and 0.1896 respectively. Hence the error between the energy calculated by the fitted data sets and testing sets using developed potential is about 25% suggesting the potentials are working well.

6.2.2 Reproduction of Force by the developed potential

6.2.2.1 Free energy fitted EAM1 and EAM2

As a second method to test whether the developed potential is performing well or not, it was tried to reproduce the force using developed potentials and testing sets which is comparable to the force produced by fitted data sets. As written above the optimization function by fitting sets were 0.2316 and 0.2448 for EAM1 and EAM2 respectively. The optimization function without optimization of testing sets of data and developed potential were obtained to be 0.3073 and 0.3157 respectively suggesting that the developed potentials EAM1 and EAM2 did reproduce forces.

6.2.2.2 Stress fitted EAM1 and EAM2

The optimization function obtained by fitting data set were 0.1155 and 0.1338 respectively as written above. Then by changing the weighting factor for Force to 1 in setting file of EAM fit, the fitting was performed without optimization using testing data and developed potentials. Thus, obtained optimization functions were 0.1710 and 0.1579 respectively for EAM1 and EAM2 suggesting that both the best potentials did reproduce the force as by fitting set.

6.2.3 Cohesive energy test

6.2.3.1 Free energy fitted EAM1 and EAM2 potential

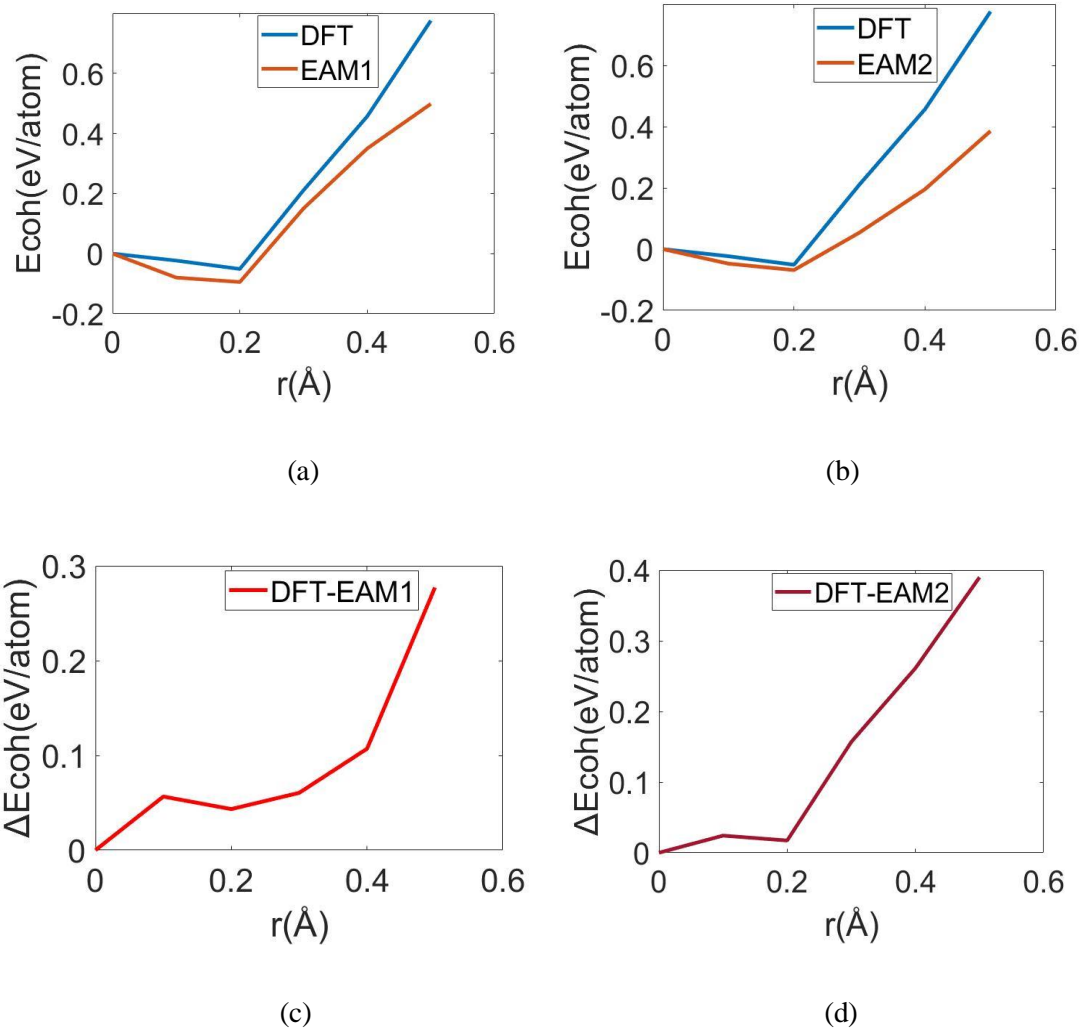
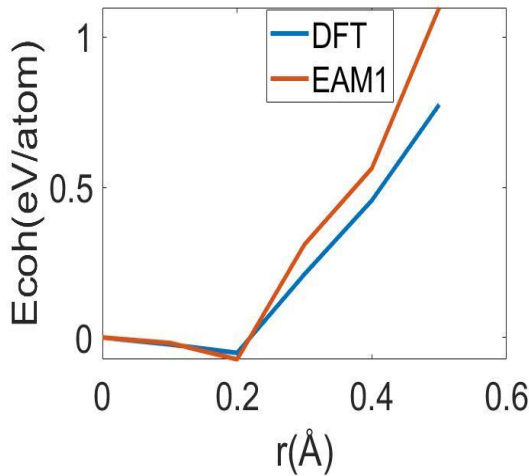


Figure 37 – Plot of Change of Cohesive energy vs distance of Ge atom from its lattice point for Free energy fitted EAM1, DFT and EAM2,DFT. (c, d) :Plot of difference in change of Cohesive energy in plot a and b with respective to distance in Angstrom

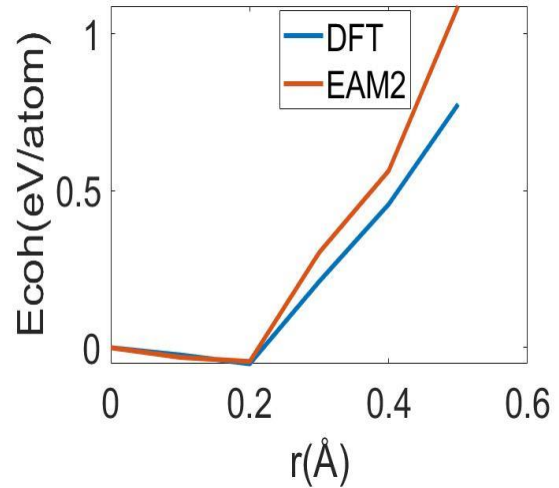
By following the procedure as in binary alloys, a configuration of Germanium, Silicon and Tin was created, and energy was calculated for each configuration in which one of the Ge atoms was moved along Z- axis each time by 0.1Å. Initially, before moving the Ge atom

from its initial position, the energy calculated was -166.78304eV at position 2.19715\AA . Then as before the Ge atom was moved each time by 0.1\AA and the energies calculated were as -166.86280eV , -166.87752eV , -166.63269eV , -166.43339eV , -166.28466eV . Similarly by creating the Input files using different POSCAR as above, DFT calculation was done and the energy was calculated to be -285.23409eV , -285.25728eV , -285.28519eV , -285.02325eV , -284.77741eV , -284.45857eV . Now again by providing the LAMMPS format free energy fitted EAM2 potential, the energy of initial configuration was calculated to be -118.12147eV . Again, the energies of configurations in which Ge atom was moved each time by 0.1\AA are -118.16891eV , -118.14989eV , -118.06750eV , -117.92605eV , and -117.73588eV .

6.2.3.2 Stress fitted EAM1 and EAM2 potential



(a)



(b)

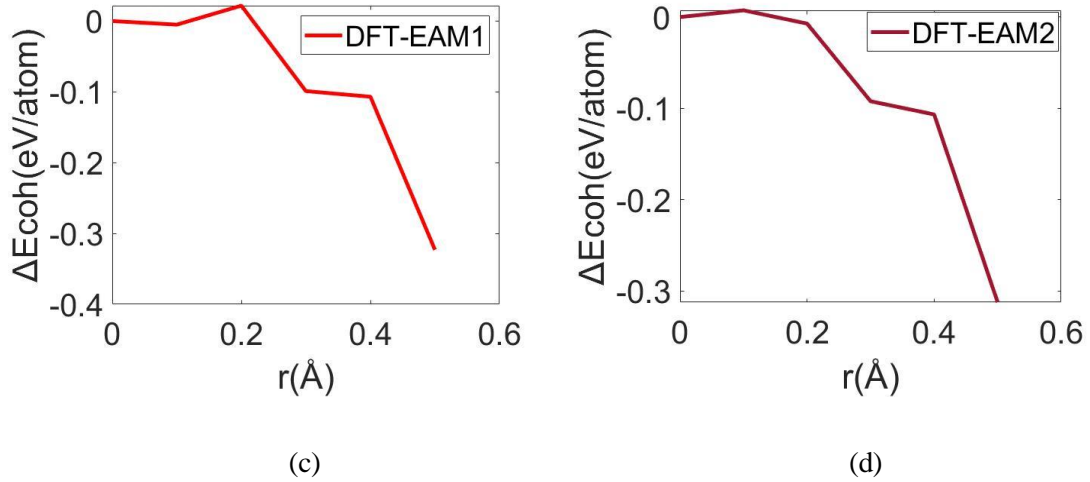


Figure 38 – Plot of Change of Cohesive energy vs distance of Ge atom from its lattice point for Free energy fitted EAM1, DFT and EAM2,DFT. **(c, d)** :Plot of difference in change of Cohesive energy in plot a and b with respective to distance in Angstrom

Cohesive energy plots for Changing the position of a Ge atom along Z-axis on the configuration of Ge, Si, and Sn atoms by the EAM1 and EAM2 potentials developed by fitting Stress-tensor data points are shown above in figure 6.2.1.2 and compared with the DFT cohesive energies. For EAM1, the total energy, when all the atoms were in equilibrium state was -63.08538eV which is taken as reference energy here. Now following the similar trend as in Energy fitted potential above, one of the Germanium atoms was moved by distance 0.1Å along Z-axis and for each configurations energies were calculated as -63.1035eV, -63.15821eV, -62.775eV, -62.5218eV, -61.9868eV. The reference energy was then subtracted from other energies and plotted along Y-axis with respect to changed position by 0.1Å each time along X-axis. Similarly, for EAM2, the energies were calculated as -104.0963eV, -104.1269eV, -104.1402eV, -103.7932eV, -103.5329eV, -103.0083eV, first energy being the initial reference energy.

6.2.4 Free-Energy Fitted EAM Parameters

Table 22 –: Embedding function parameters for free energy fitted EAM1 and EAM2 potentials

	<i>EAM1</i>			<i>EAM2</i>		
	E_{Ge}^{emb}	E_{Si}^{emb}	E_{Sn}^{emb}	E_{Ge}^{emb}	E_{Si}^{emb}	E_{Sn}^{emb}
$a(ev)$	2.370	2.588	17.88	0.598	0.608	2.484
$b(ev)$	$2.19 \cdot 10^{-5}$	$1.58 \cdot 10^{-3}$	$3.24 \cdot 10^{-9}$	$3.11 \cdot 10^{-5}$	$2.58 \cdot 10^{-3}$	$3.31 \cdot 10^{-5}$
$c(ev)$	$1.01 \cdot 10^{-9}$	$8.34 \cdot 10^{-9}$	$5.91 \cdot 10^{-9}$	$2.40 \cdot 10^{-9}$	$2.90 \cdot 10^{-9}$	$1.24 \cdot 10^{-7}$

Table 23 –: Electron density parameters for free energy fitted EAM1 and EAM2 potentials

	<i>EAM1</i>			<i>EAM2</i>		
	f_{Ge}^0	f_{Si}^0	f_{Sn}^0	f_{Ge}^0	f_{Si}^0	f_{Sn}^0
$a^1(ev)$	$5.82 \cdot 10^{-2}$	0.217	2.062	4.676	0.735	1.823
$r^1(\text{Å})$	5.700	2.526	2.497	2.244	3.973	2.217
$a^2(ev)$	0.161	-5.121	-5.495	-7.359	9.801	0.269
$r^2(\text{Å})$	5.306	2.764	2.338	3.360	2.151	3.877

Table 24 –: Pairwise interaction potential parameters for free energy fitted EAM1 and EAM2 potentials

	<i>EAM1</i>					
	ϕ_{Ge-Ge}	ϕ_{Ge-Si}	ϕ_{Ge-Sn}	ϕ_{Si-Si}	ϕ_{Si-Sn}	ϕ_{Sn-Sn}
$b^1(eV)$	3.543	1.253	-4.783	2.293	3.399	-43.28
$s^1(\text{\AA})$	2.759	4.236	4.516	2.091	1.607	3.350
$b^2(eV)$	-4.308	1.058	3.734	27.168	14.237	-59.893
$s^2(\text{\AA})$	2.017	4.358	2.964	2.788	2.636	3.243

	<i>EAM2</i>					
	ϕ_{Ge-Ge}	ϕ_{Ge-Si}	ϕ_{Ge-Sn}	ϕ_{Si-Si}	ϕ_{Si-Sn}	ϕ_{Sn-Sn}
$b^1(eV)$	1.371	4.108	4.754	4.777	-1.569	-7.157
$s^1(\text{\AA})$	2.040	1.655	2.920	2.607	2.147	1.682
$b^2(eV)$	-7.817	4.389	-3.278	-0.958	0.1346	3.301
$s^2(\text{\AA})$	1.936	2.675	3.447	2.031	4.662	3.199

6.2.5 Stress-Tensor fitted EAM parameters

Table 25 –: Embedding function parameters for free energy fitted EAM1 and EAM2 potentials

	<i>EAM1</i>			<i>EAM2</i>		
	E_{Ge}^{emb}	E_{Si}^{emb}	E_{Sn}^{emb}	E_{Ge}^{emb}	E_{Si}^{emb}	E_{Sn}^{emb}
$a(ev)$	0.3098	1.290	3.066	$1.82*10^{-2}$	0.718	1.053
$b(ev)$	$-1.01*10^{-2}$	$3.88*10^{-5}$	$1.67*10^{-5}$	$1.069*10^{-4}$	$1.32*10^{-4}$	$3.09*10^{-4}$
$c(ev)$	$2.11*10^{-7}$	$1.70*10^{-9}$	$5.07*10^{-9}$	$2.11*10^{-9}$	$3.13*10^{-8}$	$2.03*10^{-7}$

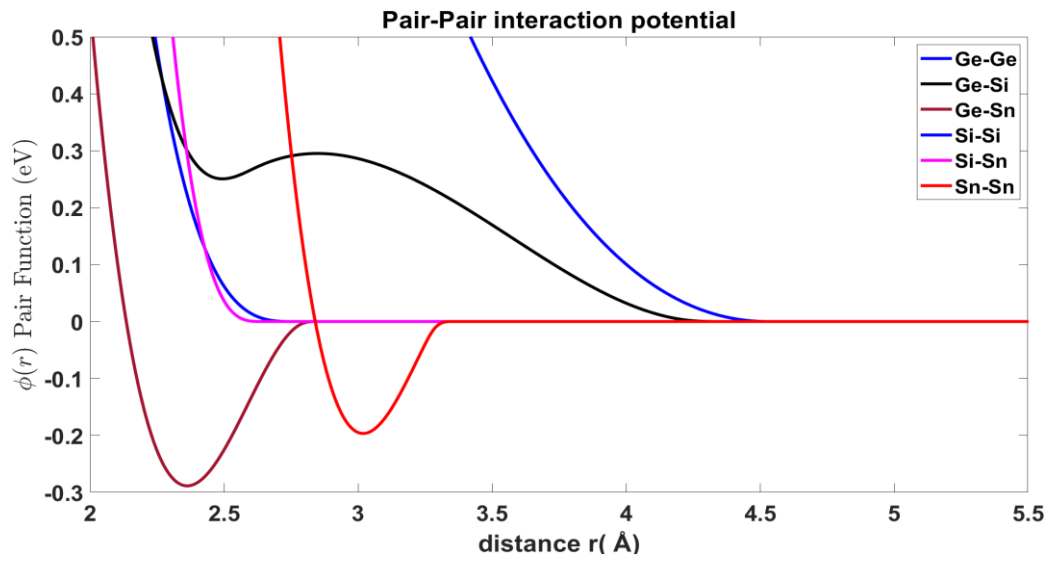
Table 26 –: Electron density parameters for free energy fitted EAM1 and EAM2 potentials

	<i>EAM1</i>			<i>EAM2</i>		
	f_{Ge}^0	f_{Si}^0	f_{Sn}^0	f_{Ge}^0	f_{Si}^0	f_{Sn}^0
$a^1(ev)$	-1.126	-3.159	2.065	6.228	-1.557	6.343
$r^1(\text{Å})$	3.255	2.796	2.341	1.701	5.313	3.445
$a^2(ev)$	15.839	0.170	$9.10*10^{-2}$	5.273	1.103	3.730
$r^2(\text{Å})$	2.594	3.749	5.331	1.862	5.702	1.612

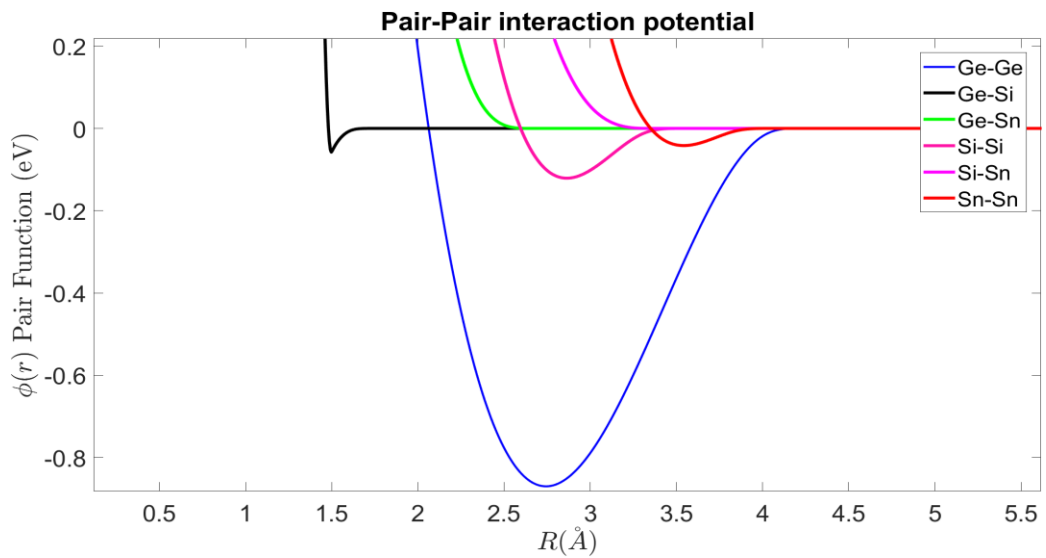
Table 27 –: Pairwise interaction potential parameters for free energy fitted EAM1 and EAM2 potentials

	<i>EAM1</i>					
	ϕ_{Ge-Ge}	ϕ_{Ge-Si}	ϕ_{Ge-Sn}	ϕ_{Si-Si}	ϕ_{Si-Sn}	ϕ_{Sn-Sn}
$b^1(ev)$	17.351	-2.720	1.112	8.726	0.596	-13.822
$s^1(\text{Å})$	2.516	2.110	1.723	2.174	3.576	2.446
$b^2(ev)$	5.649	5.577	15.861	3.592	-2.022	0.328
$s^2(\text{Å})$	1.947	2.629	2.634	2.513	2.309	4.839

	<i>EAM2</i>					
	ϕ_{Ge-Ge}	ϕ_{Ge-Si}	ϕ_{Ge-Sn}	ϕ_{Si-Si}	ϕ_{Si-Sn}	ϕ_{Sn-Sn}
$b^1(ev)$	2.658	-1.930	2.952	2.464	2.698	2.454
$s^1(\text{Å})$	4.007	1.728	3.310	2.649	2.747	3.848
$b^2(ev)$	-1.967	-5.706	-1.361	1.105	1.235	-0.960
$s^2(\text{Å})$	4.212	1.681	3.516	2.537	3.352	4.031



(a)



(b)

Figure 39 – Plot of interatomic distance versus pair-interaction energy by (a) Free energy fitted EAM1 potential and (b) Stress fitted EAM2 potential for each pair of atoms

The above plots 6.2.2.1 a and b are the pair interaction potential energy versus the distance between the binary atoms. It can be seen in the above plots that for some pairs the attractive energy is captured in pairwise potential while in some pairs there is no attractive energy. The reason for this might be that in some cases the attractive potential is captured either in Embedding energy function or electron density function. Also in plot 'a', Ge-Sn pair has more deeper well depth compared to Sn-Sn pair which suggests that the attractive energy between Ge and Sn is greater than that of Sn and Sn. Similarly from plot 'b' Ge-Ge pair has most deeper curve indicating the most attractive potential energy between Ge and Ge.

CHAPTER 7. DISCUSSION AND CONCLUSION

In this work the Embedded atom method potential for classical particles like atoms is developed which can be used for Molecular dynamics simulation in future. Though the developed potentials are doing comparable performance as DFT but there are still some limitations and there are many things that need to be improved in the future. It can be seen above in testing part that the Stress fitted potentials are not performing as good as Free energy fitted potential. The possible reason for this might be ignorance of angular contribution in electron density in EAM fit. The more developed way of fitting modified embedded atom potential, MEAM can be used in the future so that angular contribution can be taken into consideration, which could improve the developed potential to some extent. In this work also it was tried to develop the potential by MEAM approach, and it was done as well, but it was unknown about how to create the readable format of MEAM potential parameters so that the developed potential could be tested and different properties could be calculated. So, this whole work was done by the EAM approach, which gave LAMMPS format file as output, which was easy to read, and Quantum ATK, which was used in this thesis to calculate different properties, can easily read the LAMMPS format potential parameters.

REFERENCES

- [1] Duff, Andrew Ian, et al. "MEAMfit: A reference-free modified embedded atom method (RF-MEAM) energy and force-fitting code." *Computer Physics Communications* 196 (2015): 439-445.
- [2] Hospital, Adam, et al. "Molecular dynamics simulations: advances and applications." *Advances and applications in bioinformatics and chemistry: AABC 8* (2015): 37.
- [3] Büyükoztürk, Oral, et al. "Structural solution using molecular dynamics: Fundamentals and a case study of epoxy-silica interface." *International Journal of Solids and Structures* 48.14-15 (2011): 2131-2140.
- [4] Chistyakova, Nadezhda, and Thi My Hue Tran. "A study of the applicability of different types of interatomic potentials to compute elastic properties of metals with molecular dynamics methods." *AIP Conference Proceedings*. Vol. 1772. No. 1. AIP Publishing LLC, 2016.

- [5] Zhang, Xudong, et al. "First-principles calculations of structural stability, elastic, dynamical and thermodynamic properties of SiGe, SiSn, GeSn." *Superlattices and Microstructures* 52.3 (2012): 459-469.
- [6] Oehme, Michael, et al. "Epitaxial growth of strained and unstrained GeSn alloys up to 25% Sn." *Thin Solid Films* 557 (2014): 169-172.
- [7] Kasper, E., et al. "Growth of silicon-based germanium tin alloys." *Thin Solid Films* 520.8 (2012): 3195-3200.
- [8] Aubin, Joris, et al. "Very low temperature epitaxy of Ge and Ge rich SiGe alloys with Ge₂H₆ in a Reduced Pressure–Chemical Vapor Deposition tool." *Journal of Crystal Growth* 445 (2016): 65-72.
- [9] Ye, Kaiheng, et al. "Absorption coefficients of GeSn extracted from PIN photodetector response." *Solid-State Electronics* 110 (2015): 71-75.
- [10] Zheng, Jun, et al. "Growth of high-Sn content (28%) GeSn alloy films by sputtering epitaxy." *Journal of Crystal Growth* 492 (2018): 29-34.
- [11] Tersoff, J. J. P. R. B. "Modeling solid-state chemistry: Interatomic potentials for multicomponent systems." *Physical review B* 39.8 (1989): 5566.

- [12] Ko, Won-Seok, et al. "Atomistic simulations of pure tin based on a new modified embedded-atom method interatomic potential." *Metals* 8.11 (2018): 900.
- [13] Oehme, M., et al. "Germanium waveguide photodetectors integrated on silicon with MBE." *Thin Solid Films* 517.1 (2008): 137-139.